Experimental and Modeling Investigation of Arsenate Adsorption on Synthetic Iron-Coated Sands

by

Gautham P Jeppu

A dissertation submitted to the Graduate Faculty of
Auburn University
in partial fulfillment of the
requirements for the Degree of
Doctor of Philosophy

Auburn, Alabama
May 9, 2011

Keywords: Arsenic, iron-coated sand, surface complexation, adsorption, unified isotherm

Approved by

T. Prabhakar Clement, Chair, Professor of Civil Engineering
Mark O. Barnett, Professor of Civil Engineering
Clifford R. Lange, Associate Professor of Civil Engineering
Ming-Kuo Lee, Professor of Geology and Geography

Abstract

Arsenic is an environmental contaminant of worldwide concern due its high toxicity and presence in groundwater aquifers. Adsorption of arsenic onto metal-oxides is an important phenomenon that locally controls the transport of arsenic in groundwater systems. In this study, we have investigated adsorption of arsenic(V) onto iron (goethite) coated sands. We also developed novel methods to scale the adsorption models. The study is divided into three phases:

(i) In the first phase, we developed a scalable surface complexation modeling framework for predicting arsenic(V) adsorption onto various types of iron (goethite) coated sands. We first synthesized four different types of goethite-coated sands with iron content varying by nearly an order of magnitude and generated adsorption isotherms and pH edges for these four sands. We then used experimental data from one of the sands to develop a surface complexation model for the sand. We then scaled the surface complexation model developed for the sand, based on measured surface site density values, to predict adsorption onto the three other sands using the scaling procedure we developed. In addition, we also scaled the model to make predictions for several other arsenate-goethite adsorption datasets available in literature. The scaled models gave successful

predictions for all datasets, with an average error of less than 5%, as quantified using RMSE values.

(ii) Currently there are no suitable experimental setups available for studying equilibrium-controlled geochemical reactive transport. In the second phase of the study, we developed a new experimental setup to study equilibrium- reactive transport of arsenate on goethite-coated sands. The proposed experimental setup, identified as the sequential equilibration reactor (SER) system, consists of several equilibrium batch reactors that are linked in series. The reactors are operated in a sequential manner analogous to the operations performed in a one-dimensional numerical model. Arsenic(V) solution is introduced into the first reactor and is allowed to react until equilibrium is reached in the first reactor. The solution phase is then transferred to the second reactor. This process is repeated until the solution reaches the last reactor. The effluent from the last reactor is analyzed. We conducted several SER experiments to study equilibrium arsenic transport under a wide range of pH, solid/solution ratio, and concentration conditions. The experimental datasets generated were also used to test whether the surface complexation models developed in the first phase were able to model the equilibrium reactive transport observed in the sequential equilibration reactor system.

(iii) In the third phase of the study, we developed a novel Unified Langmuir-Freundlich (ULF) model, to describe pH-dependent arsenate adsorption on goethite-coated sands. The ULF model was integrated within a semi-analytical solution to predict arsenate transport observed in SER experiments. The semi-analytical solution was then validated by using experimental datasets from SER experiments completed at various pH, solid/solution ratio, and concentration conditions. The predictions form the ULF isotherm based semi-analytical model matched with surface complexation model predictions. The approach was further tested by recreating a well-known benchmark problem (Cederberg *et al.*, 1985). The ULF isotherm-based transport codes were more than 10 times faster than surface-complexation-coupled transport codes.

Overall, the study has made the following three contributions to the field:

1) Development of scalable surface complexation modeling framework for arsenic-goethite system
2) A new experimental system to study equilibrium-controlled reactive transport problems
3) A unified pH-dependent isotherm model and a semi-analytical modeling framework to predict equilibrium-controlled reactive transport at different pH values.

Acknowledgements

I would like to infinitely thank my advisor Dr. T. Prabhakar Clement for his continuous support and guidance. I am grateful for his scientific expertise, insightful advice, and outstanding mentorship during all phases of this Ph.D. degree. Dr. Clement is a wonderful advisor and brilliant researcher on all levels. I would not have made it through this process without his guidance.

I am immensely thankful to Dr. Mark. O. Barnett for his valuable guidance and for his laboratory and office facilities. His ideas and support greatly helped shape up this research project. I also thank Dr. Clifford Lange and Dr Ming-Kuo Lee for their valuable suggestions, timely cooperation and guidance. Special thanks to Dr. James Saunders for being a continuous source of enthusiasm and for agreeing to the external reader. I thank the following mentors who helped this research at various stages: Drs. Suvasis Dixit, Chetin Kantar, Daniel Giammer, Henning Prommer, Dongye Zhao, David Dzombak, David Pharkhurst, Kang-Kun Lee, Anke Richter, Tao Cheng and Sabine Goldberg. I thank my seniors, Tanja Radu and Anjani, for providing a framework for carrying out my work.

I thank Jinling for laboratory assistance. I thank post-doctoral fellows Dr. Sushil Kanel and Dr. Zayed Ali for their guidance. I thank Dr. Tanja Radu and Anjani Kumar

for laying the foundation for my work. I thank to all my present and past colleagues including Rohit, Linzy, Venkat, Vijay, Feng, Carrie, Jagadish, Wes, Matt, Vivek, Gerald, Sunwu, Katie, Zhong, Fang for their companionship. I thank Auburn University for providing facilities for research and course work.

I thank my friends and family for their continuous support. I thank my friend Sachin Jambovane for his valuable suggestions. I thank my mother for her endless care and support without which this degree would not have been possible. I thank my father and sister for their support and encouragement. I thank all my friends who helped me in times of need. I thank all the people/ objects which have helped make this project successful.

This research was, in part, supported by, the office of science (BER), U.S.D.O.E. Grant No. DE-FG02-06ER64213, Auburn University teaching assistantship and by the Sustainable Water Resources Research Center of Korea's 21st Century Frontier Research Program via Seoul National University.

Table of Contents

List of Tables

List of Figures

List of Abbreviations

SCM	Surface complexation model
LF	Langmuir-Freundlich
ULF	Unified Langmuir-Freundlich
SER	Sequential equilibration reactor
SSER	Single sequential equilibration reactor
MSER	Multiple sequential equilibration reactor
EDL	Electrical double layer
IOCS	Iron-oxide coated sand
GCS	Goethite-coated sand
ICS	Iron-coated sand
HFO	Hydrous ferric oxide

CHAPTER 1

GENERAL INTRODUCTION

1.1 Background

Adsorption plays an important role in reducing the mobility of metals and colloids in natural systems. Batch experiments have been extensively used to understand various adsorption reactions in laboratory-scale systems. However, there have been only a few studies that have attempted to scale the models developed for batch-scale systems to other large-scale natural systems.

Surface complexation models are commonly used to simulate batch adsorption experiments (Goldberg, 1986; Dzombak and Morel, 1990; Goldberg, 1992). However, these models are system dependent since the model parameters derived for one adsorbent may not work for another similar adsorbent. Therefore, there is an urgent need to develop adsorption models, which can be easily modified to model adsorption at different scales for use in common groundwater transport codes. In this study we aim to develop such modeling methods for describing arsenic (a representative contaminant) interactions with iron-coated sand (a representative adsorbent).

In natural environments, arsenic is known to strongly interact with metal-oxide coatings found on sediment particle surfaces (Smedley and Kinniburgh, 2002; Nath *et al.*, 2009). Goethite is one of the most common metal-oxyhydroxide coatings present abundantly on natural sediments (Wang *et al.*, 1993; Fuller *et al.*, 1996). Developing a fundamental understanding of arsenic adsorption processes onto goethite (iron) coated sands would help better predict arsenic transport in natural subsurface environments and could provide valuable insights into the fate of arsenic (and similar contaminants) in groundwater aquifers. In this study we have focused on As(V) (arsenate), the most common form of arsenic under aerobic conditions, since As(V) adsorption can be easily studied in laboratory without oxidation effects, unlike As(III), which may get oxidized to As(V).

1.2 Objectives

The overall goal of this dissertation is to investigate arsenic(V) transport in experimental subsurface systems and develop novel experimental and modeling methods to scale adsorption reactions. The specific objectives are:

I. To develop a scalable surface complexation modelling framework for arsenate adsorption onto goethite and goethite-coated sands.

II. To develop and demonstrate a novel experimental setup to generate equilibrium-reactive transport datasets for arsenate adsorption on iron-coated sands under a wide range of pH, solid/solution ratio and concentration conditions.

III. To develop and test a new isotherm to describe pH-influenced adsorption, and to integrate the new isotherm within an analytical modeling framework to simulate pH influenced reactive transport processes.

1.3 Organization

This dissertation is organized into six Chapters including this general introduction Chapter (Chapter 1). In Chapter 2, we present a brief literature review of arsenic adsorption.

Chapter 3 describes the development of a method to scale surface complexation models using arsenate as a representative adsorbate and iron-coated sand as a representative adsorbent. A summary of the work was published in journal article titled "A scalable surface complexation modeling framework for predicting arsenate adsorption on goethite-coated sands" (Journal of Environmental Engineering and Science, 2010, 27 147-158).

Chapter 4 describes a novel experimental setup to generate equilibrium-transport datasets for arsenate adsorption on iron-coated sand. A summary of the work has been submitted as another journal article titled "A novel experimental system to study equilibrium-reactive transport problems" (Applied Geochemistry, submitted).

In Chapter 5, we develop a semi-analytical formulation for modelling the experimental setup from Chapter 4 using a pH dependent unified Langmuir-Freundlich isotherm. We plan on submitting this work as a journal article titled "A semi-analytical

solution for reactive transport in sequential equilibration reactors using a novel unified Langmuir-Freundlich isotherm" (Journal of Contaminant Hydrology, to be submitted).

Chapter 6 provides a short summary of the key contributions of this study and suggests some ideas for future work.

CHAPTER 2

LITERATURE REVIEW

2.1 Introduction

Arsenic is classified as a metalloid in the periodic table. It has an atomic number of 33 and atomic weight of 74.92. Its minerals are ubiquitously found in nature and it ranks 20^{th} in earth's crust, 14^{th} in seawater and 12^{th} in human body (Mandal and Suzuki, 2002) in terms of abundance. When in the elemental form, arsenic is a silvery-grey, brittle, crystalline solid with a specific gravity of 5.73, melting point of 817^0C (at 28 atm), boiling point of 613^0C, and vapor pressure of 1 mm Hg at 372^0C (Mohan and Pittman, 2007). Arsenic was first isolated in 1250 A.D. by Albertus Magnus, a German scientist, and has since then been notorious for its poisonous effects. Some of the common arsenic minerals are arsenopyrite (FeAsS), realgar (AsS), orpiment (As_2S_3), loellingite ($FeAsS_2$) and arsenolite (Azcue *et al.*, 1994). Arsenic compounds have been used in various medicines, insecticides, wood preservatives, dye, and industrial chemicals. Human exposure to arsenic and its compounds may occur through air, water, seafood, tobacco smoking, beverages, medicinal preparations, and industrial chemicals.

2.2 Toxicity of arsenic

The most common pathway for human exposure to arsenic is via drinking water contaminated with arsenic. Due to its toxic effects at low concentration, the US Environmental Protection Agency (EPA) has recently reduced the maximum contaminant limit (MCL) standard for arsenic from 50 μg/l to 10 μg/ L (EPA, 2001), which is also the WHO drinking water quality guideline for arsenic.

Inorganic As species are more toxic than organic. Among the inorganic species, As(III) is estimated to be two to ten times more toxic than As(V) (Kosnett, 1994). The toxicity of arsenic is mostly due to its ability to interact with sulfhydryl groups of proteins and enzymes and its ability to substitute for phosphorous in a variety of biochemical reactions (Goyer, 1996). Arsenic can be commonly detected in hair, nails and urine of people consuming arsenic contaminated water (Ahamed *et al.*, 2006). Most of inorganic arsenic is metabolized to monomethylarsonic acid and dimethylarsenic acid in the human body. Arsenic-contaminated water is known to cause skin lesions, neurological problems, heart diseases, hypertension, cardiovascular disease, and internal cancers such as bladder, kidney and lung cancer (Smith *et al.*, 2000; Mead, 2005; Walvekar *et al.*, 2007). The most notable effect of arsenic is known as blackfoot disease, which is characterized by peripheral atheroscelrosis, resulting in dry gangrene causing spontaneous amputation of feet, arm and other organs (Tchounwou *et al.*, 2003). Arsenic consumption in drinking water may also cause diabetes mellitus (Tsai *et al.*, 1999) and hypertension (Rahman *et al.*, 1999) . The US EPA has concluded that arsenic is a Group A carcinogen, which is known to trigger skin, bladder and lung cancers.

2.3 Speciation of arsenic

An Eh-pH diagram of arsenic is given at Figure 2-1. Arsenic is present in arsenate [As(V)] or arsenite [As(III)] oxidizing states in most natural groundwater systems. As(V) is stable in oxidizing conditions and As(III) is stable in moderately reducing conditions. A speciation diagram of As(III) and As(V) is given below in Figure 2-2. Under typical EH values found in natural groundwater systems, the predominant As(V) specie is $H_2AsO_4^-$ when pH is between 2.2 and 6.9, and $HAsO_4^-$ when pH is between 6.9 and 11.5 (Ferguson and Gavis, 1972). For As(III) oxidation state, $H_3AsO_3^0$ is predominant below pH 9.2, and $H_2AsO_3^-$ is predominant between pH 9.2 and 12 (Ferguson and Gavis, 1972). Therefore, the major As(III) species found in natural groundwater systems are $H_3AsO_3^0$ and H_3AsO_4(aq). These species are neutral in charge and do not adsorb to charged surface, hence As(III) is highly mobile in groundwater systems. At very low Eh, arsine (AsH_3) might be formed. Various methylated species such as monomethylarsonic (MMAA) [$CH_3AsO(OH)_2^0$] and dimethylarsinic acid (DMAA [$(CH_3)_2AsO(OH)^0$] may also be formed if conditions are favorable for biomethylation to occur. However, inorganic As species are the ones of the greatest environmental concern. Because of their high solubility, abundance and toxicity, As(V) and As(III) are the most important inorganic states of arsenic.

Reducing conditions such as flooding enhance arsenic mobilization due to reduction of As(V) to more mobile As(III) species, or through dissolution of iron-oxides and iron-oxyhydroxides which then release adsorbed arsenic (Beauchemin and Kwong, 2006; Wang *et al.*, 2007). Dry periods can cause oxidizing conditions, which could

decrease arsenic concentration by precipitation of dissolved minerals of Fe, Mn, and As (La Force *et al.*, 2000).

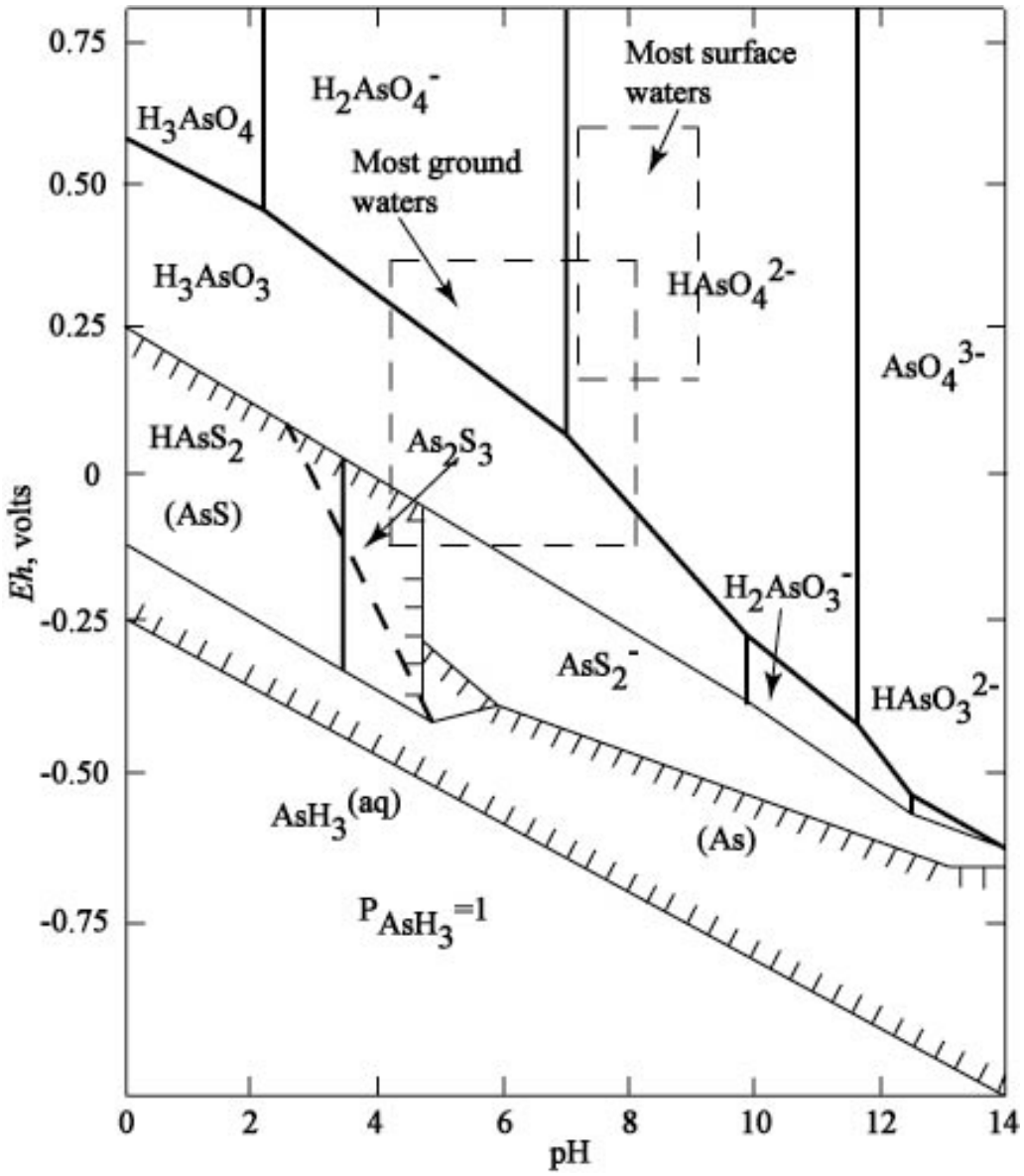

Figure 2-1: Eh-pH diagram for As at 25°C and 1 atm with total As 10^{-5} M and total sulfur at 10^{-3} M (Schnoor, 1996)

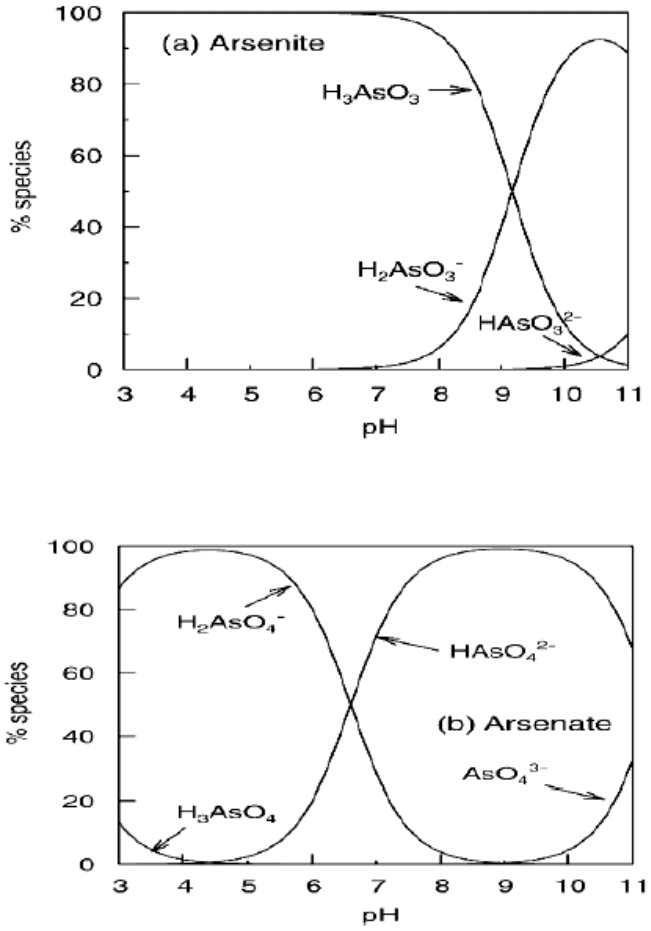

Figure 2-2: As(III) and As(V) speciation as a function of pH (I=0.01M) (Smedley and Kinniburgh, 2002). Redox conditions were chosen so that the specified redox state As(V) or As(III) is dominant.

2.4 Arsenic problem in Bangladesh

Countries affected by severe arsenic contamination are: Bangladesh, India, Argentina, Vietnam, Hungary, Romania, and Chile (WHO, 2003). Among these countries, Bangladesh has attracted worldwide attention since it has the highest number of people impacted by arsenic poisoning (Dhar *et al.*, 1997). A British geological survey study found that at least 22 million people drank water with arsenic levels more than 50 µg/L in Bangladesh (British Geological Survey and Mott MacDonald Ltd, 1999). Groundwater pollution of Bangladeshi aquifers with arsenic was noticed first during the 1970s, when the government of Bangladesh started to encourage drilling tube wells to solve drinking water problem as suggested by British Geological survey.

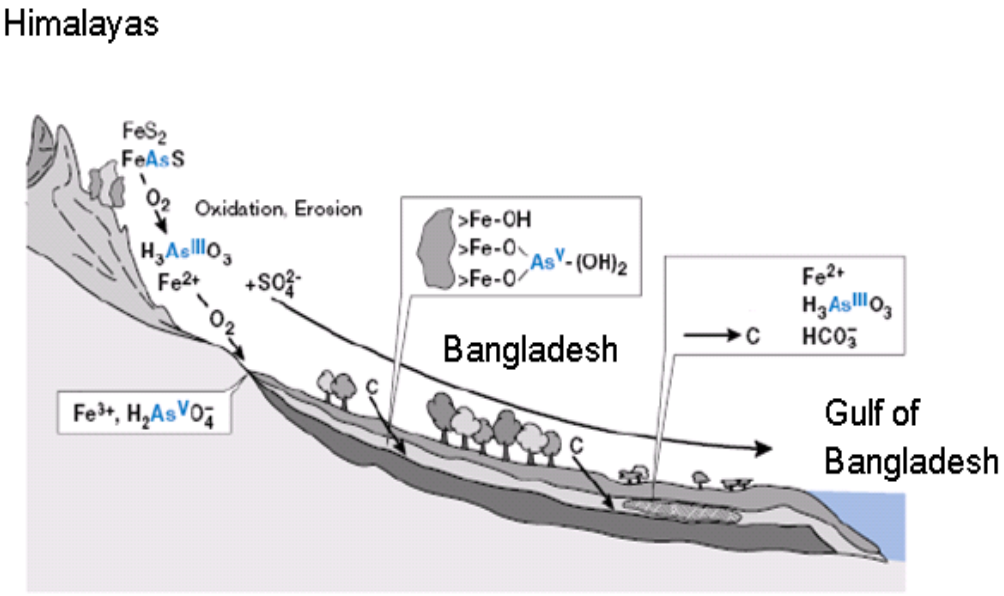

Figure 2-3: Conceptual representation of arsenic problem in Bangladesh (Boreysza *et al.*, 2006)

It is thought that the main non-point source of high arsenic concentration in ground water is natural (Smedley and Kinniburgh, 2002). However, there are many localized point sources due to mining, pesticides, wood-treatment, agriculture etc which may have small secondary influence. As shown in the conceptual diagram, the currently accepted theory is that the high As concentrations is mainly due the microbially mediated reductive dissolution of arsenic containing metal oxyhydroxides (Nickson *et al.*, 2000; Macur *et al.*, 2001). Under aerobic conditions arsenic is strongly bound to metal oxides found in the sediments.

As illustrated in Figure 2-3, it is thought that the source of arsenic is upstream and arsenic is carried downstream by the Ganga and Brahmaputra rivers. Arsenic minerals in sediments in Himalaya mountains, Bihar plateau and Rajmahal-Chotonagpur plateau areas in India were dissolved by rainwater. The dissolved arsenic was adsorbed by iron oxides and suspended sediments in water and was transported towards Bangladesh by the rivers. These arsenic-loaded dissolved oxyhydroxides were deposited in the aquifer sediments in low lying regions over the thousands of years. If organic matter is available, anaerobic conditions are created, dissolving the minerals and releasing high levels of arsenic (Nickson *et al.*, 2000). Saunders et al. (2008) showed that iron-reducing conditions caused by addition of organic carbon (sucrose, methanol) can favor release of arsenic. Shamsudduha et al. (2009) used digital elevation data to suggest that low hydraulic gradients in low lying deltaic regions cause slow groundwater velocities and slow flushing rates, wherein reducing conditions can cause arsenic release due to microbial reduction.

Low hydraulic gradient and reducing conditions favor formation of highly mobile $H_3AsO_3^0$, causing high arsenic in groundwater.

2.5 Arsenic adsorption on metal-oxides

Arsenic transport is influenced by a number of complex parameters such pH, redox potential, alkalinity, and the presence of metal-oxides and organic matter (Smedley and Kinniburgh, 2002; Nath *et al.*, 2009). One of the important mechanisms by which transport of arsenic is retarded is by adsorption onto metal-oxides and metal-oxyhydroxides (Anawar *et al.*, 2003; Davis *et al.*, 2005). Metal-oxides are ubiquitously present in the subsurface as coatings on soil grains (Wang *et al.*, 1993; Coston *et al.*, 1995), and have a high affinity for adsorbing arsenic in water.

2.5.1 Arsenic adsorption on metal-oxides: Surface reaction mechanism

The adsorption of arsenic on metal oxides occurs by inner-sphere adsorption mechanism. Surface metal oxide groups exist in their hydroxylated form in aqueous solutions. Arsenic is adsorbed by ligand exchange with surface functional groups of metal-oxides containing OH^- or OH_2^+ ions as shown in the following surface reactions:

As(V) adsorption:

$$>FeOOH + H_3AsO_4^0 \leftrightarrow \ >FeOH_2AsO_4^0 + H_2O$$

$$>FeOOH + H_2AsO_4^- \leftrightarrow \ >FeOHAsO_4^- + H_2O$$

$$>FeOOH + HAsO_4^{2-} \leftrightarrow \ >FeOAsO_4^{2-} + H_2O$$

As(III) adsorption:

$$> FeOOH + H_3AsO_3^0 \leftrightarrow \ > FeOH_2AsO_3^0 + H_2O$$

$$> FeOOH + H_2AsO_3^- \leftrightarrow \ > FeOHAsO_3^- + H_2O$$

$$> FeOOH + HAsO_3^{2-} \leftrightarrow \ > FeOAsO_3^{2-} + H_2O$$

Where, >FeOH represents the hydroxylated surface iron-oxide group. Since adsorption of arsenic on metal-oxides is independent of ionic strength, it is thought that inner-sphere surface complexes could be formed (Hsia *et al.*, 1992; Grossl and Sparks, 1995). Asenic adsorption on iron-oxides and iron-oxyhydroxides was found to reduce the isoelectric point (Manning and Goldberg, 1996; Jain *et al.*, 1999; Goldberg and Johnston, 2001) , which also indicates that inner-sphere complexes are formed. Formation of inner-sphere complexes is further confirmed by X-ray absorption fine structure (EXAFS) spectroscopy (Waychunas *et al.*, 1993).

Mechanism of surface adsorption can be classified as monodentate or bidentate depending on the number of surface groups sharing a single ligand. Monodentate adsorption occurs when a single surface group complexes with a single ligand. Bidentate adsorption occurs when two surface groups complex with a single ligand, by sharing the ligand. Both bidentate and monodentate adsorption are thought to occur during arsenic adsorption on metal-oxides spectroscopy (Waychunas *et al.*, 1993; Goldberg and Johnston, 2001). Monodentate complexes are predominant at low surface coverages, whereas bidentate complexes are predominant at high surface coverages (Fendorf *et al.*, 1997). However, monodentate models are commonly assumed in published literature (Dzombak and Morel, 1990; Dixit and Hering, 2003). Arsenic adsorption on metal-oxides

can be modeled either using empirical models or using mechanistic surface complexation models.

2.6 Arsenic adsorption modeling using isotherm models

Empirical adsorption models correlate a relationship between the aqueous concentration and solid phase concentration at equilibrium without mathematically modeling the actual surface reaction mechanisms. Empirical adsorption models that are commonly used for modeling arsenic adsorption on metal-oxides are linear model, Langmuir model, Freundlich model and Langmuir-Freundlich model.

The Linear adsorption model assumes that adsorption linearly increases with concentration and that solid phase has infinite adsorption capacity. The Linear adsorption isotherm is given by:

$$q = K_d C$$

where, q is amount sorbed per weight of solid, C is amount in solution per unit volume of solution and K_d is the partition coefficient usually expressed in ml/g.

The Langmuir adsorption isotherm is a commonly used function to model arsenic adsorption on metal-oxides (Hingston, 1970; Raven *et al.*, 1998; Thirunavukkarasu *et al.*, 2001; Thirunavukkarasu *et al.*, 2003; Kundu and Gupta, 2006). The Langmuir adsorption isotherm can be represented as:

$$q = K_{max} \frac{C}{K_S + C} \tag{2-1}$$

Where, K_{max} is the maximum adsorption capacity per unit weight of solid (mg/ kg), k_s is the Langmuir constant (mg/L), and C is the aqueous concentration (mg/L).

The Freundlich isotherm is a common empirical model used to model arsenic adsorption on metal oxides (Raven *et al.*, 1998; Lin and Wu, 2001; Badruzzaman *et al.*, 2004). The Freundlich isotherm equation is given by the relation:

$$q = KC^n \tag{2-2}$$

Where, q represents the total amount of adsorption per unit weight of solid (mg/kg), K is the distribution or partition coefficient (mg kg^{-1} (mg $l^{-1})^{-n}$), C is the aqueous concentration (mg/L), and n is the dimensionless reactor order, which is typically less than 1.

The Langmuir-Freundlich isotherm (Sips, 1948) is a combined form of Langmuir and Freundlich isotherms. Rau et al. (2003) studied arsenic adsorption on metal-oxides using different types of adsorption isotherms and concluded that the Langmuir-Freundlich isotherm best described the data. The Langmuir-Freundlich isotherm is given by the expression:

$$q = K_{max} \frac{(K_1 C)^n}{(K_1 C)^n + 1} \tag{2-3}$$

Where, K_1 is the affinity constant (L/mg), K_{max} is the maximum adsorption capacity (mg/ kg).

2.7 Adsorption modeling using surface complexation approach

Surface complexation models provide a mechanistic description of the reactions occurring on metal-oxide surfaces. Chemical reactions occurring at metal-oxide surfaces

cause charge development on surfaces. The sorption of metal ions on metal oxides occurs by the attraction of opposite charges. The electrical-double layer (EDL) theory (Gouy, 1910; Chapman, 1913) can be used to describe the charge development.

2.7.1 Background of surface complexation modeling

The following is a summary of history of surface complexation modeling from the comprehensive book by Dzombak and Morel (1990). The science of surface complexation modeling has evolved since the 1960's, due to the interest in chemistry of adsorption in aqueous solutions (Dzombak and Morel, 1990) . Early research involved the use of electrical double layer (EDL) theory of Guoy and Chapman to explain physical adsorption. However, surface reactions were not considered. Later, several researchers used surface reactions and mass law equations to describe reactions at individual surface sites (Kurbatov *et al.*, 1951; Stanton and Maatman, 1963; Dugger *et al.*, 1964). However, they did not consider surface charge and electrostatic factors. The importance of surface charge was first recognized by Parks and Debruyn (1962). A significant ideological breakthrough came when the mass law approach was combined with the EDL theory by Schindler's group, who proposed the constant capacitance model (Schindler and Kamber, 1968; Schindler and Gamsjager, 1972). At the same time Stumm and co-workers proposed the diffuse layer model (Stumm *et al.*, 1970; Huang and Stumm, 1973). The triple layer model was later proposed by Davis et al. (1978a). Westall and coworkers devised a method to incorporate surface complexation reactions into chemical speciation models using electrostatic correction factor as a component (Westall, 1979a) . This

helped to incorporate the SCM models into computer-based geochemical speciation models, thus making the SCM models available for use within geochemical speciation models.

In a surface complexation model, the adsorption on a surface is calculated as a function of the surface charge σ. Surface is assumed to be at a potential Ψ with respect to the bulk of the solution. The potential Ψ has a representative component exp (-ΔZFΨ/RT) and the equivalent total mass of this component is represented by the charge on the surface. The potential Ψ also has a direct relation to the charge σ via the mass action equation. The term ΔZ is the change in surface charge due to the surface reaction. Consider the following surface reactions:

$$XOH + H^+ \leftrightarrow XOH_2^+$$

$$XOH - H^+ \leftrightarrow XO^-$$

The equilibrium constants describing the surface complexation reactions are:

$$K_1 = \frac{(XOH_2^+)}{(XOH)\{H^+\}} \exp\left[+\frac{F\Psi}{RT}\right] \quad (2\text{-}4)$$

and,

$$K_2 = \frac{(XO^-)}{(XOH)\{H^+\}^{-1}} \exp\left[-\frac{F\Psi}{RT}\right] \quad (2\text{-}5)$$

Where, ( ) denotes concentration and {} denotes activity.

Several expressions have been proposed to relate Ψ to σ, and based on these expressions, following four types of surface-complexation models have been proposed: constant capacitance model, triple layer model, diffuse double layer model and the generalized diffuse double layer model.

2.7.2 Constant capacitance model

The constant capacitance model was developed by Schindler and coworkers (Schindler and Kamber, 1968; Schindler and Gamsjager, 1972). The constant capacitance model assumes a high ionic strength, which implies a constant capacitance condition. It also assumes that all the surface complexes are inner-sphere complexes. The relationship between surface charge density (σ_0) and surface potential (Ψ_0), (where $_0$ indicates the surface plane) in the constant capacitance model is given by the relationship:

$$\sigma_0 = \frac{\mathrm{CAS}}{\mathrm{F}}\Psi_0 \qquad (2\text{-}6)$$

Where, C is the capacitance density (F/m^2), A is the surface area ($m^2\ g^{-1}$), S is the suspension density ($g\ L^{-1}$), *F* is the Faraday constant ($Coulombs\ mol^{-1}$), σ_0 is the surface charge density ($Volt\ L^{-1}$), and Ψ_0, is the surface potential (volts). A diagram of the structure of the surface-solution interface for the constant capacitance model is shown in Figure 2-4

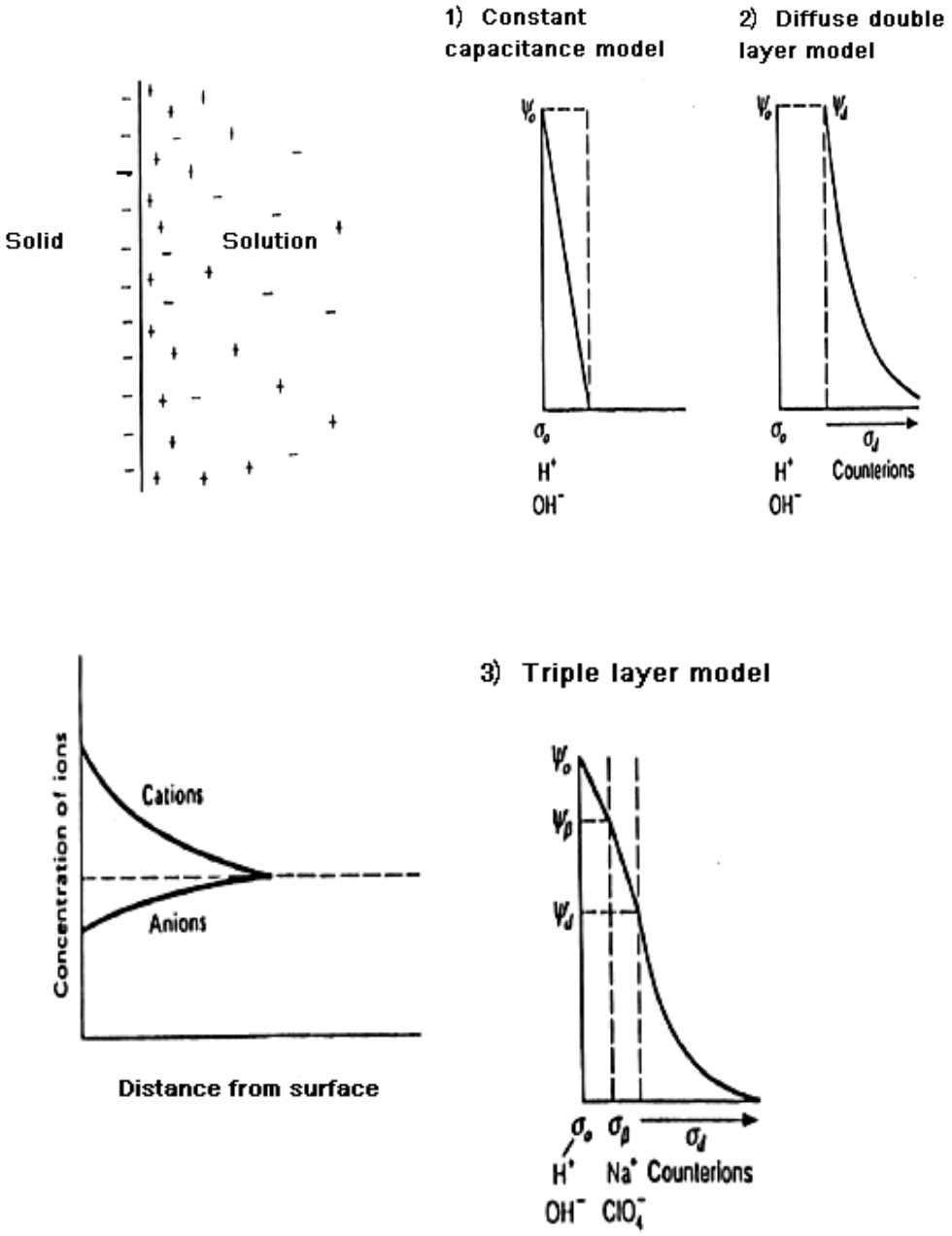

Figure 2-4: Conceptual representation of surface charge development in: 1) constant capacitance model 2) diffuse double layer model and 3) triple layer model (Drever, 1982)

2.7.3 Diffuse double layer model

The diffuse double layer model was developed by Stumm and his co-workers (Stumm *et al.*, 1970). The diffuse double layer model assumes two planes for surface charge: a surface layer (plane 0) and diffuse layer of counter ions (plane d). All the reactions are assumed to be inner-sphere complexation reactions. The relationship between surface charge and surface potential is described with the Gouy-Chapman theory. The relationship between surface charge and surface potential can be expressed as follows:

$$\sigma_d = -0.1174\ \mathrm{I}^{1/2} \sinh\left[\frac{\mathrm{ZF}\Psi_\mathrm{d}}{2\mathrm{RT}}\right] \qquad (2\text{-}7)$$

Where σ_d is the surface charge density (volt L^{-1}), Ψ_d is the surface potential (volts), *I* is the ionic strength (M), Z is the valence of the symmetrical electrolyte, T is the temperature (K), and R is the gas constant.

2.7.4 Triple layer model

The triple layer model was developed by Leckie and his co-workers (Davis and Leckie, 1978a). The triple layer model assumes three planes of charge (plane 0, plane d, and plane β) for surface charge. The reactions can either be outer-sphere or inner-sphere surface complexation reactions. Outer-sphere surface complexes are formed with ions from the background electrolyte. The relationships between surface charges and surface potentials in the triple layer model are given by:

$$\sigma_0 = \frac{C_1 A}{F}\left[\Psi_0 - \Psi_\beta\right] \quad (2\text{-}8)$$

$$\sigma_d = \frac{C_2 A}{F}\left[\Psi_d - \Psi_\beta\right] \quad (2\text{-}9)$$

Where, C_1 and C_2 are capacitance densities, A is the surface area ($m^2\ g^{-1}$), σ_0 and σ_d are surface charge densities (Volt L^{-1}), Ψ_0 , Ψ_β and Ψ_d are the surface potential (Volts) of the plane 0, plane β and plane d. A diagram of the structure of the triple layer model is shown in Fig. 2-4.

2.7.5 Generalized diffuse double layer model and work of Dzombak and Morel

Dzombak and Morel modified the diffuse double layer model of Stumm and co-workers (Stumm *et al.*, 1970; Huang and Stumm, 1973) and developed the well known generalized diffuse double layer model or the Dzombak and Morel model (Dzombak and Morel, 1987; Dzombak and Morel, 1990). The generalized diffuse double layer model is similar to the diffuse double layer model, but contains two types of sites (Type I and Type II sites, or weak sites and strong sites) for cation adsorption. Only Type-I sites (weak sites) are available for anion adsorption.

Dzombak and Morel compiled a list of measured site densities from literature. The site densities in literature varied from 0.001 to 0.01 mole sites/mole Fe for Type-I sites. So they fixed the site density for Type-I sites as 0.05 mole sites/ mole Fe, which is

an approximate arithmetic mean of the site densities in literature. Similarly, the site density of Type-II sites was fixed as 0.2 mole sites/ mole Fe, from the approximate arithmetic mean of literature site densities, which ranged from 0.1 to 0.3 mole sites/ mole Fe. Similarly, they also compiled a list of surface areas of hydrous ferric oxide (HFO) from N_2 BET measurements and suggested an average surface area of 600 m^2/g, which was also recommended by Davis (1977)), Davis and Leckie (1978b), and Luoma and Davis (1983). They used these fixed surface area and site density values for HFO and developed a list of consistent set of equilibrium constants for sorption of inorganic cations and anions on HFO. Their efforts helped standardize the model development and parameter extraction procedure using FITEQL, thus providing a framework for further work.

They noted that if the site density changes by a factor of 2, the sorption constants associated with the type-I sites may change systematically by 0.3 to 0.7 log units, and the log K values associated with type II sites may be systematically off by 0.15 to 0.3 log units (Dzombak and Morel, 1990). They also noted that errors in surface site densities could lead to poor results, especially when surface is close to saturation with adsorbate molecules. They also suggested that variations in site densities are to be expected among various samples of HFO and that sometimes different site densities may have to be used (Dzombak and Morel, 1990)

The work of Dzombak and Morel (1990) was the first comprehensive attempt to develop a consistent and unified database in the field of surface complexation modeling. They developed a standard model for HFO which was later adopted by several

geochemistry modeling codes such as MINTEQA2 and PHREEQC. They also standardized the parameter estimation procedures to be used for developing surface complexation models using the FITEQL code.

The limitation of the Dzombak and Morel model (generalized diffuse double layer model) is that site density is fixed. Whereas, site density and adsorption capacity and of a metal-oxide may vary widely. Natural systems contain complex mixtures of minerals and it is difficult to quantity the concentration of surface sites for individual minerals. Stollenwork (1995) measured the site density of 51 core samples from a sand and gravel aquifer and found that the site density varied widely from 1.6 μmoles/ m^2 to 4.1 μmoles/ m^2. Therefore, it is difficult to satisfactorily model experimental adsorption results for different kinds of adsorbents using a single site density and use of a single site density may lead to significant modeling errors. Hence, several later studies used experimentally measured site densities for HFO, which differed from the value suggested by Dzombak and Morel (Stollenwerk, 1995; Dixit and Hering, 2003; Giammar *et al.*, 2004).

2.8 Equilibrium geochemical speciation codes

Several computer codes have been developed to solve the geochemical speciation problems. Some of the initial developments include REDEQL2 (McDuff and Morel, 1972) ,WATEQ (Truesdell and Jones, 1974), MINEQL (Westall J. C. *et al.*, 1976), MICROQL-I (Westall, 1979b) and MICROQL-II (Westall, 1979a). MINEQL was later developed into MINTEQA2 (Allison *et al.*, 1990), MINEQL+ (Schecher and McAvoy, 1998), MINTEQA2 for windows (Allison, 2003) and Visual MINTEQ (Gustafsson,

2006). The code PHREEQE (Parkhurst *et al.*, 1980) was developed by USGS and has been updated into PHREEQC (Parkhurst, 1995), PHREEQC2 (Parkhurst, 1999) and PHREEQCI (Clarlton and Parkhurst, 2002). The speciation code SOILCHEM (Sposito and Mattigod, 1980) was derived from GEOCHEM (Sposito and Mattigod, 1980) and REDEQL (McDuff and Morel, 1972).

MINTEQA2 for windows is a user friendly chemical speciation code, which is used widely used by EPA, and contains a specialized sub-model for calculations involving dissolved organic matter. The original MINTEQ (Felmy *et al.*, 1983) was developed at Battelle Pacific Northwest Laboratory (PNL) by incorporating the U.S. Geological Survey's WATEQ3 database (Ball *et al.*, 1981) into MINEQL (Westall J. C. *et al.*, 1976). Recently the Fortran code of MINTEQA2 was converted to Visual Basic to create the program called Visual MINTEQ (Gustafsson, 2006), which has an easy to use Windows based interface. The PHREEQC family of codes is developed and maintained by USGS. The latest version called PHREEQCI (Clarlton and Parkhurst, 2002), has diverse capabilities including one-dimensional transport, inverse modeling and kinetic reaction routines.

2.9 Coupling geochemical speciation codes to transport codes

To model contaminant transport in groundwater, which involves both transport (advection, dispersion) and geochemistry, a number of reactive transport codes have coupled the equilibrium speciation models such as PHREEQC and MINTEQ to transport codes. For example, Cederberg et al. (1985) developed TRANQL by coupling the

geochemical code MICROQL-II (Westall, 1979a) to a transport routine. Noorishad et al. (1987) developed CHMTRNS using PHREEQE as the equilibrium module. Engesgaard and Kipp (1992) used CHMTRNS to develop benchmark problems for geochemical transport codes. Narasimhan et al. (1986) coupled the transport code TRUMP with PHREEQE to create a reactive transport model DYNAMIX. Walter et al. (1994) developed MINTRAN by coupling the finite-element transport module PLUME2D to MINTEQA2. Phanikumar and McGuire (2004) coupled PHREEQC-2 with RT3D (Clement, 1997) to create a biogeochemical, kinetic, reactive transport code BGTK. The widely used code PHAST (Parkhurst *et al.*, 2004) couples PHREEQC with HST3D (Kenneth, 1997). Another popular reactive transport model PHT3D (Prommer *et al.*, 2003a) couples the transport code MT3DMS (Zheng and Wang, 1999) with PHREEQC-2 (Parkhurst, 1999).

2.10 Scaling of reactive transport processes

When modeling contaminant transport using geochemical coupled transport codes, it is often necessary to predict the sorption parameters for a new chemical system by scaling the parameters obtained for a similar experimental systems (Ochs *et al.*, 2006). Radu et al. (2007) scaled kinetic and Langmuir parameters obtained from batch experiments to predict arsenic adsorption and oxidation by pyrolusite (MnO_2) in column experiments. A few studies have used extractable iron content or surface area to scale the adsorption parameters (Davis *et al.*, 2005; Hartzog *et al.*, 2009; Loganathan *et al.*, 2009).

However, scaling methods have not been well established for predicting surface

complexation model parameters. The surface complexation stability constants (log K values of surface complexation reactions) strongly depend on the value of the surface site density (Davis and Kent, 1990; Goldberg, 1991). Davis and Kent (1990) pointed out that the stability constants derived using a known surface site density value for a given system may not be directly used for predicting adsorption in another system that has a different surface site density value. Hence, it will be useful to develop systematic scaling procedures for predicting such surface complexation model stability constants.

CHAPTER 3

DEVELOPMENT OF A SCALABLE SURFACE COMPLEXATION MODELING FRAMEWORK

3.1 Introduction

Analysis of natural sediments shows that one of the commonly found metal-oxide coatings present on sediments is goethite (Wang *et al.*, 1993), which is also one of the most thermodynamically stable iron-oxyhydroxides. Hence, several researchers have used goethite-coated sands as a test media to study the interaction of various types of inorganic contaminants with natural sediments (Cheng *et al.*, 2004; Giammar *et al.*, 2004 ; Cheng *et al.*, 2006; Romero-Gonzalez *et al.*, 2007). Arsenic is a representative contaminant of worldwide concern, and goethite-coated sand resembles metal-oxide coated sediments in subsurface. Understanding the scaling of arsenic adsorption on goethite-coated sands can also help us understand scaling of other similar inorganic groundwater contaminants and adsorbents.

In natural sediments, with a low organic content, inorganic adsorption is primarily controlled by metal-oxide/oxyhydroxide (Fe, Mn and Al) content of sediments (Lion *et al.*, 1982; Davis and Kent, 1990; Fuller *et al.*, 1996). Inch and Killey (1987) suggested that adsorption is proportional to the available surface area. The adsorption capacity

(maximum adsorption per gram of soil) appears to correlate well with the amount of metal-oxides present on soil per unit surface area, suggesting that metal-oxide content per surface area could be one of the geochemical parameters that control the spatial variations in metal adsorption (Fuller *et al.*, 1996). The adsorption capacity per surface area is quantified by surface-site density parameter in surface complexation models. Therefore, surface-site density can be a useful scaling parameter for surface complexation models. The use of surface complexation models for predicting arsenic adsorption on pure iron-oxide minerals, such as hydrous ferric oxide (HFO), has been extensively studied (Dzombak and Morel, 1990; Manning and Goldberg, 1996; Sun and Doner, 1996; Goldberg and Johnston, 2001; Dixit and Hering, 2003; Dixit and Hering, 2006). However, none of these studies have explored the scaling properties of surface complexation models for different types of iron oxide/oxyhydroxide coated sands.

The objective of this study is to develop a scalable surface complexation modeling framework for describing As(V) adsorption onto synthetic goethite-coated sands with different amount of iron content. We first generated multiple adsorption datasets (pH edges and isotherms) for four types of goethite-coated sands. A diffuse double layer surface complexation model was developed and the log K values for the system were estimated by fitting the model to an adsorption dataset for one of the synthetic test sands. This model was then scaled to make predictions for the other three sands. In addition, we compiled three literature datasets to further test the validity of the scaling approach.

3.2 Materials and methods

3.2.1 Experimental methods

Goethite-coated sands (GCS) were synthesized in our laboratory as outlined in Cheng et al (2004). Pure goethite was synthesized from ferrous chloride using the recipe from Schwertmann and Cornell (2000) and was then coated onto white quartz sand (0.210-0.297 mm) purchased from Sigma-Aldrich using the homogeneous suspension method (Scheidegger *et al.*, 1993). The preparation of the goethite-coated sands is reported by the same group in an earlier study by Loganathan et al. (2009). Four types of goethite-coated sands with their iron content and surface area varying by nearly an order of magnitude were prepared for this study. Figure 3-1 shows the four goethite-coated sands, which are identified as Sand-A, Sand-B, Sand-C and Sand-D. The iron contents of these sands were modified by varying the number of goethite coating cycles during synthesis. The iron contents of the four sands were estimated using the dithionite-citrate-bicarbonate buffer (DCB) extraction method. The data indicated that Sand-B had the lowest iron content (0.40 mg Fe/g), followed by Sand-C (1.82 mg Fe/g), Sand-D (3.15 mg Fe/g) and Sand-A (3.48 mg Fe/g). The surface areas of the sands were determined by five-point BET measurements using N_2 gas. The measured values of surface area are: 1.08 m^2/g, 0.18 m^2/g, 0.43 m^2/g, and 0.57 m^2/g, for Sand-A, Sand-B, Sand-C and Sand-D, respectively. SEM and XRD studies were done and the results indicated that the coatings mainly consisted of goethite (Loganathan *et al.*, 2009). Table 3-1 provides a detailed summary of these sand characteristics.

Table 3-1: Characteristics of the various goethite-coated sands

Sorbent Type	Sand-A	Sand-B	Sand-C	Sand-D
Iron content (mg Fe/ g sand)	3.48 ±0.1	0.40 ±0.01	1.82 ±0.05	3.15±0.07
Surface area (m^2/ g sand)	1.08	0.18	0.43	0.57
Maximum adsorption (mg As(V)/g sand)	0.140	0.028	0.070	0.097
Maximum adsorption (mmoles As(V)/ mole Fe)	30.10	52.45	28.72	23.03
Surface site density (μmoles/m^2)	1.73	2.11	2.18	2.29
Surface site density (sites/nm^2)	1.04	1.27	1.32	1.38

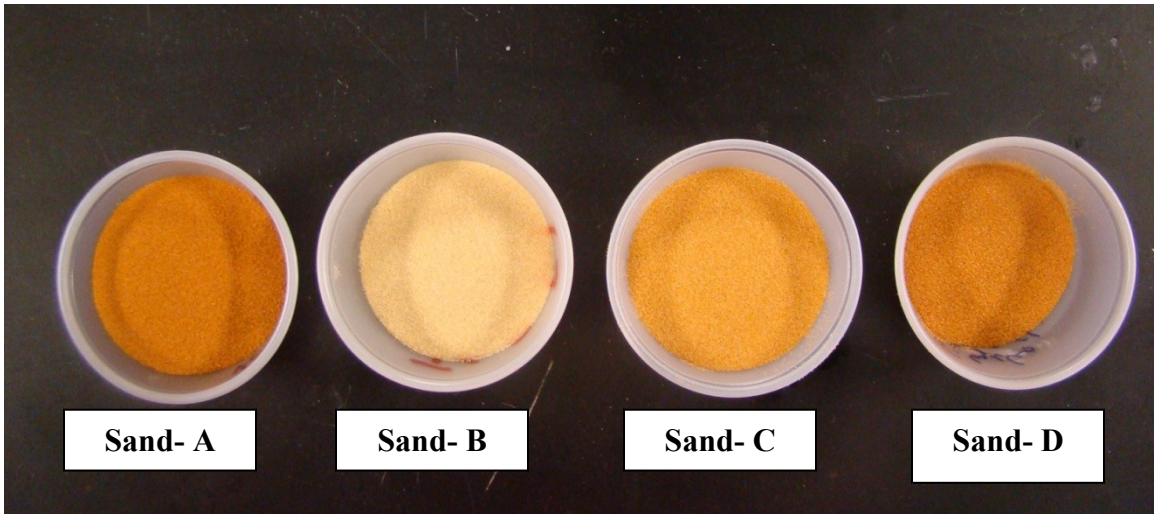

Figure 3-1 : Samples of the four synthetic goethite-coated sands

As (V) solutions were prepared by diluting 100 ppm As(V) stock solution, which was made by dissolving 0.416 grams of reagent grade $Na_2HAsO_4.7H_2O$ in 1 liter of deionized water. All the experiments were completed in triplicates. Unless otherwise mentioned, the ionic strength of all the solutions in this study were adjusted to 0.01 M ionic strength using sodium nitrate (Harter and Naidu, 2001). The room temperature was set at $25^0C \pm 2^0C$ for all experiments. The pH of the solution was adjusted using either NaOH or HNO_3 and was measured using an Orion (model 250A) pH meter. The pH

meter was calibrated using commercial pH 4.0, 7.0, and 10.0 buffers. All reported pH values are the final pH values of solutions at equilibrium. The batch experiments were equilibrated for 24 hours in a shaker and the supernatant solution was centrifuged and filtered through a 0.45 μm membrane filter (Millipore) using a disposable syringe. Our initial kinetic experiments (data not shown) indicated that the reactions attained close to equilibrium conditions within twenty four hours. The solutions were analyzed using a Graphite Furnace Atomic Absorption Spectrophotometer (GFAAS; Perkin-Elmer 5100 PC). The amounts of GCS used in the pH adsorption edge experiments were 10, 50, 5 and 2.5 g/liter for the systems having Sand-A, Sand-B, Sand-C and Sand-D, respectively. The experiments were conducted in tightly capped centrifuge tubes, thus minimizing interferences with atmospheric carbon dioxide. Also, earlier research studies have shown that carbonate has very little influence on arsenate adsorption at atmospheric CO_2 partial pressures (Meng *et al.*, 2000; Radu *et al.*, 2005b). Furthermore, we also completed several control experiments which verified that pure silica sand without goethite coating did not adsorb arsenate.

3.2.2 Modeling methods

3.3.2.1Surface complexation modeling tools

The stability constants for surface complexation of As(V) onto goethite for Sand-A were determined using FITEQL 4.0 software (Herbelin and Westall, 1999). The "goodness of fit" was quantified by the FITEQL's WSOS/DF (weighted sum of squares of residuals divided by degrees of freedom) parameter. The stability constants obtained

from FITEQL were incorporated into MINTEQA2 For Windows software (Allison, 2003) and the subsequent model simulation runs were completed using MINTEQA2. As(V) adsorption onto goethite was modeled using a single-site, monodentate diffuse double layer model.

The difference between model predictions and experimental data was quantified by the root mean square error (RMSE) of the normalized concentrations (Cheng *et al.*, 2004):

$$\text{RMSE} = \left[\frac{1}{(n_d)} \sum_{i=1}^{nd} \left(\frac{C - \hat{C}}{C_0} \right)^2 \right]^{1/2} \quad (3\text{-}1)$$

Where, n_d is the numbers of data points, i is an index, C is the measured aqueous concentration, $\hat{C}$ is the predicted aqueous concentration, and C_0 is the initial aqueous concentration (all in moles/L). The RMSE is a measure of the average difference between predicted and experimental data as a fraction of the initial concentration; thus smaller RMSE values indicate a better fit.

3.3.2.2 Method for correcting stability constants

Kulik (2002) derived an equation to normalize the log K values estimated for a system to a standard reference surface site density level. The reference site density, standard states, and surface activity were defined and used to construct an uniform, internally consistent thermodynamic dataset. The equation is given by the relationship (Kulik, 2002; Richter *et al.*, 2005b) :

$$\text{Log } K_0 = \log K_C + \log(\Gamma_C / \Gamma_0) \quad (3\text{-}2)$$

Where,

Γ_0 is the reference surface site density expressed as sites/m^2 of surface area

K_0 is the stability constant value at a reference surface site density Γ_0

K_C is the stability constant value at a surface site density value of Γ_C

The standard surface site density level is fixed at Γ_0 =20 μmole/m^2 or 12.05 sites/nm^2, which approximately corresponds to the maximum density of H_2O molecules in a surface monolayer (Kulik, 2002). The above equation can be used to approximately convert the log K values estimated for a given system to another system with a different value of surface site density and the method has an uncertainty of less than 0.2 pK units (Kulik, 2002).

The Kulik equation was found to be useful for predicting log K values when experimental data is not available (Brendler *et al.*, 2004; Richter *et al.*, 2005b). This equation has been successfully used in RES^3T database, which is a mineral-specific surface complexation database (Brendler *et al.*, 2002; Richter *et al.*, 2003). A similar type of normalization approach has also been proposed by Sverjensky (2003). We employed the Kulik equation in our scaling approach since it gave good predictions for our data; furthermore, it has been used in several other published studies (Brendler *et al.*, 2002; Kulik *et al.*, 2003; Brendler *et al.*, 2004; Kersten and Kulik, 2005; Richter *et al.*, 2005b; Richter *et al.*, 2005a; Kulik, 2006; Richter and Brendler, 2006).

3.3.2.3 Surface complexation reactions

The surface complexation reactions used in this study are summarized in Table 3-2. The equilibrium constants for the aqueous protonation reactions (Reactions 1, 2 and 3 in Table 3-2) were obtained from the MINTEQA2 for Windows database (Allison, 2003). The equilibrium constants, pKa_1 and pKa_2, for surface hydrolysis reactions (reactions 4 and 5) for goethite are available in the literature. Richter et al. (2005b) compiled the surface hydrolysis equilibrium constants for goethite in the RES^{3}T database for a surface site density value of 12.05 sites/nm^2 at zero ionic strength to be: $pKa_1 = 6.38$ and $pKa_2 = -10.36$. We used the Kulik equation to scale these values for our system. For our Sand-A, which had a surface site density of 1.04 sites/nm^2, the scaled values are: $pKa_1=7.44$ and $pKa_2 = -9.30$, at zero ionic strength. The reaction equations 6, 7 and 8 in Table 3-2 were used to describe surface complexation reactions of As(V) species with goethite, as done in earlier studies (Goldberg, 1985; Manning and Goldberg, 1996; Dixit and Hering, 2003). The equilibrium constants (pK_1, pK_2 and pK_3) for the above reactions were evaluated for Sand-A by fitting the model to one of the adsorption data (25.3 μmoles/L data) using FITEQL and the results are given in Table 3-2.

Reactions			**Log K** (I=0, Γ=1.04 sites/	
Protonation reactions for As(V) [A]				
H_3AsO_4		= $H_2AsO_4^- + H^+$	-2.24	(1)
H_3AsO_4		= $HAsO_4^{2-} + 2H^+$	-9.20	(2)
H_3AsO_4		= $AsO_4^{3-} + 3H^+$	-20.70	(3)
Surface hydrolysis reactions of goethite-coated sand [B]				
>FeOH	$+ H^+$	= $> FeOH^{2+}$	7.44	(4)
>FeOH		= $> FeO^- + H^+$	-9.30	(5)
Surface complexation reactions [C]				
>FeOH	$+ H_3AsO_4$	= $>FeH_2AsO_4 + H_2O$	11.37	(6)
>FeOH	$+ H_3AsO_4$	= $>FeHAsO_4^- + H_2O + H^+$	5.98	(7)
>FeOH	$+ H_3AsO_4$	= $>FeAsO_4^{2-} + H_2O + 2H^+$	-0.33	(8)

Surface site density =1.04 sites/nm^2 for sand A, Surface area=1.08 m^2/ g GCS.

Total sites =18.6 μ moles/L for solid concentration of 10g/L of Sand-A

[A] – From MINTEQA2 for Windows thermodynamic database

[B] –From Richter et al.(2005) normalized to surface site density of Sand A

[C] – Values from FITEQL fitting of data collected in this study

Table 3-2: Aqueous protonation constants and intrinsic surface complexation constants for Sand-A at a surface site density of 1.04 sites/nm^2 and at zero ionic-strength

3.3.2.4 Scaling approach used in this study

The methodology used for scaling models in this study is summarized in Figure 3-2. We first developed adsorption isotherms to evaluate the maximum adsorption capacity for one of the goethite-coated sands, Sand-A. The surface site density value for Sand-A was calculated based on the maximum adsorption capacity and the measured surface area (from BET analysis). Next, a diffuse double layer surface complexation model was developed for Sand-A by fitting the model results to the site density and pH edge data to derive the optimized log K values for the three surface complexation reactions using FITEQL.

To apply the model to a new sand, we first determined the value of the maximum adsorption capacity of the new sand from the measured adsorption isotherm. We used the maximum adsorption capacity value and the measured surface area to calculate the surface site density value for the new sand. This was used in the Kulik equation to correct the log K values estimated for Sand-A. The values of new log Ks and the measured surface site densities for the sands were incorporated into MINTEQA2 to make predictions to validate the model.

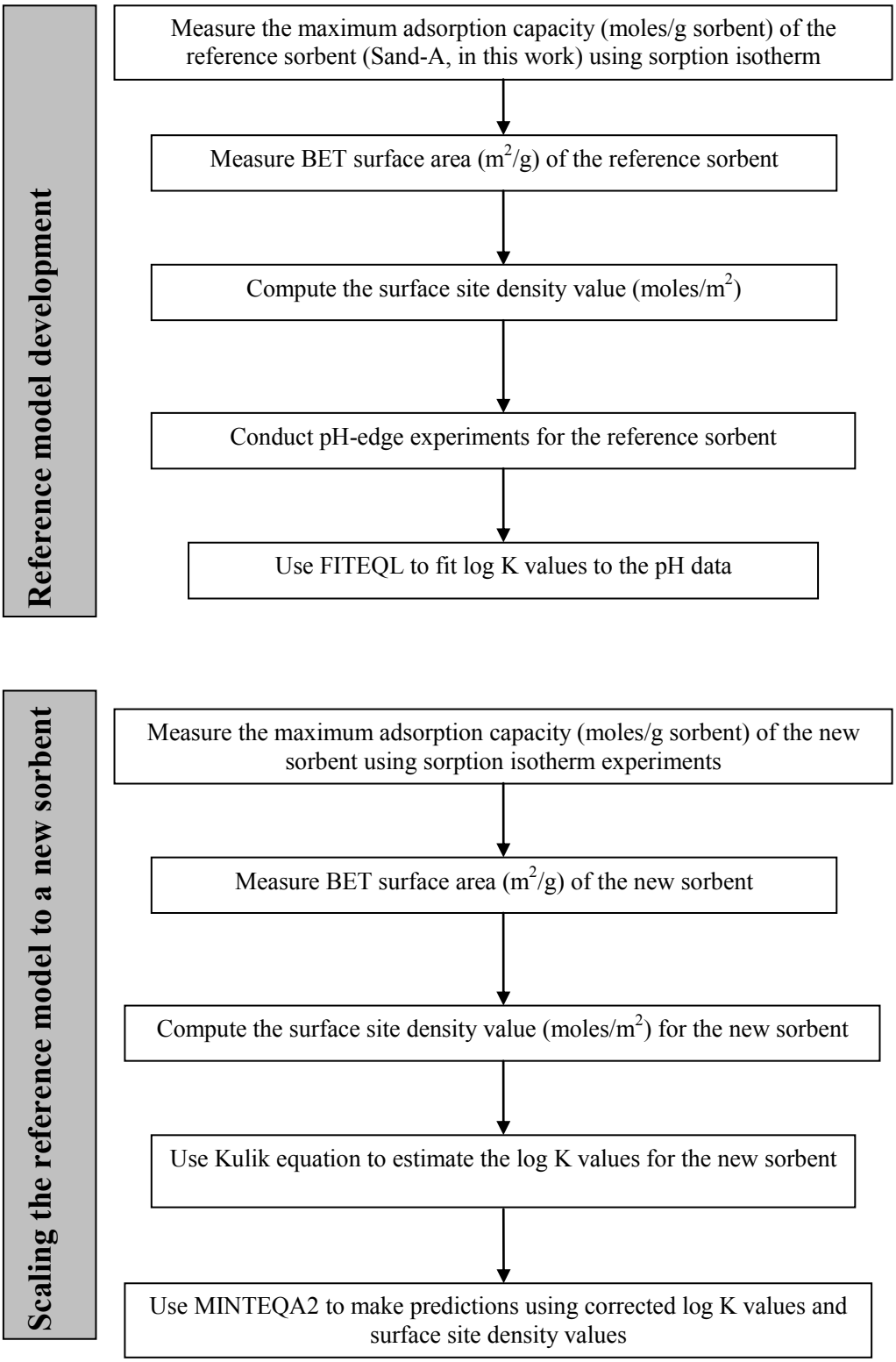

Figure 3-2 : Flow chart of the modeling approach used in this study

3.4 Results and discussions

3.4.1 Evaluation of surface site density values from adsorption isotherms

Our preliminary experiments showed that the maximum adsorption occurred near pH = ~ 4, and this value is consistent with other studies (Goldberg, 1985; Dixit and Hering, 2003). Therefore, pH 4 was used as the operating pH for determining the maximum adsorption capacity values. We also conducted multiple screening experiments (results not shown) and found that the maximum sorption capacity was similar at different solid solution ratios.

Adsorption isotherm experiments were completed by equilibrating a known amount of sand with solutions of different As(V) concentrations at pH 4 for 24 hours. The solid to solution ratio used were: 10, 100, 25 and 12.5 g/liter for Sand-A, Sand-B, Sand-C and Sand-D, respectively. Figure 3-3 shows the adsorption isotherms for all four sands. The shape of the isotherms suggests that the goethite-coated sands have a strong affinity for adsorbing As(V). We fitted the following Langmuir model to these datasets:

$$q_e = K_{max} * C_e / (K_s + C_e) \quad (3\text{-}3)$$

where,

q_e is the amount of As(V) adsorbed onto the sand at equilibrium (mg As(V)/ g sand)

K_{max} is the maximum adsorption capacity of the sand (mg As(V)/ g sand)

C_e is the aqueous phase equilibrium concentration (μM)

K_s is the Langmuir constant (μM)

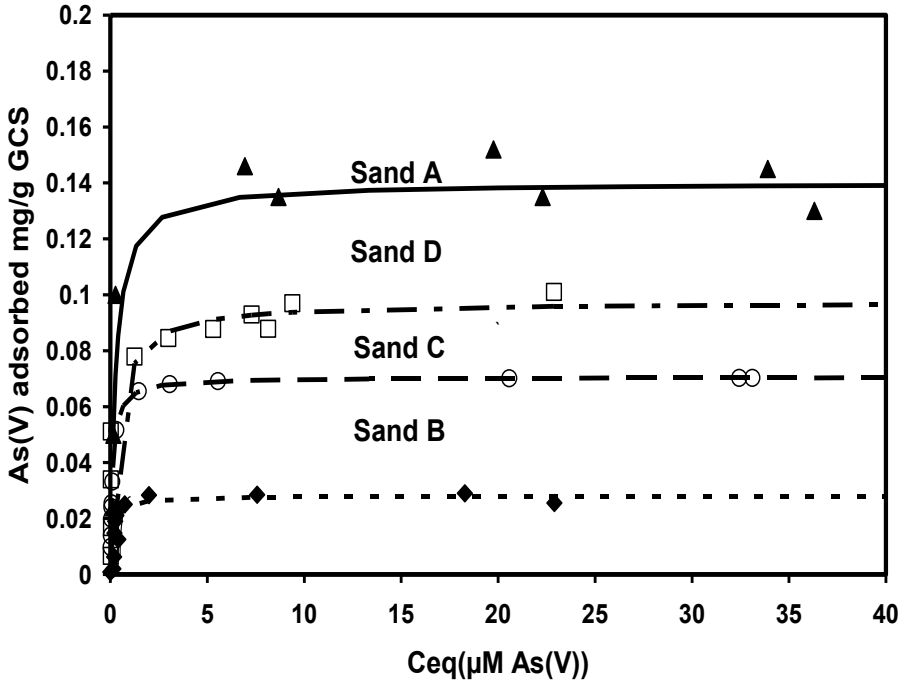

Figure 3-3 : As(V) adsorption isotherm at pH 4 for Sand A, B, C and D (I=0.01M)

Sand type	K_{max}(mg/g)	K_s (μM)	R^2
Sand-A	0.14	0.019	0.90
Sand-B	0.028	0.01	0.67
Sand-C	0.07	0.008	0.89
Sand-D	0.097	0.364	0.75

Table 3-3: Values of the fitted Langmuir model for various sands

We used the generalized reduced gradient algorithm, available within EXCEL solver and solved the equations to minimize the sum of square errors to evaluate the Langmuir parameters. The maximum adsorption capacity (K_{max}), Langmuir constant (K_s) and the corresponding R^2 values are given in Table 3- 3.

We computed the surface site density values using the maximum adsorption capacity and the measured surface area (given in Table 3- 1). The computed values of surface site density are: 1.04, 1.27, 1.32 and 1.38 sites/nm^2 for Sand-A, Sand-B, Sand-C, and Sand-D, respectively.

3.4.2 Calibration results for Sand-A pH edge data

The first set of adsorption edge data was compiled by reacting 10 g/L of Sand-A with 25.3 μM initial As(V) solution at different equilibrium pH values ranging from pH= 4 to pH= 12. This data was used to fit the three surface complexation stability constants (log K values of reactions 6, 7 and 8 shown in Table 3- 2) using FITEQL. The surface site density value was set to 1.04 sites/nm^2, a value determined above for Sand-A. The estimated surface complexation stability constants were then incorporated into MINTEQA2 for windows software to generate the model simulated pH edges. Figure 3-4 compares the calibrated model simulation results with experimental data. The goodness of fit (WSOF/DF) value estimated for the FITEQL fit was 0.243, for an estimated 3% experimental error in As(V) concentration measurements and 0.02 units of error in pH measurements. This value of goodness of fit estimate indicates a good fit (Dzombak and Morel, 1990; Herbelin and Westall, 1999). We completed additional FITEQL test

simulations using artificially higher experimental error (of 5%) and the log K values were similar to the third decimal place. The root mean square error (RMSE) value for the fit was 0.022 (i.e., average error is 2.2% of initial concentration), which indicates a good correspondence between model simulated results and experimental data. The fitted values of log Ks are summarized in Table 3- 2 and these values are used as base-line parameters in this study.

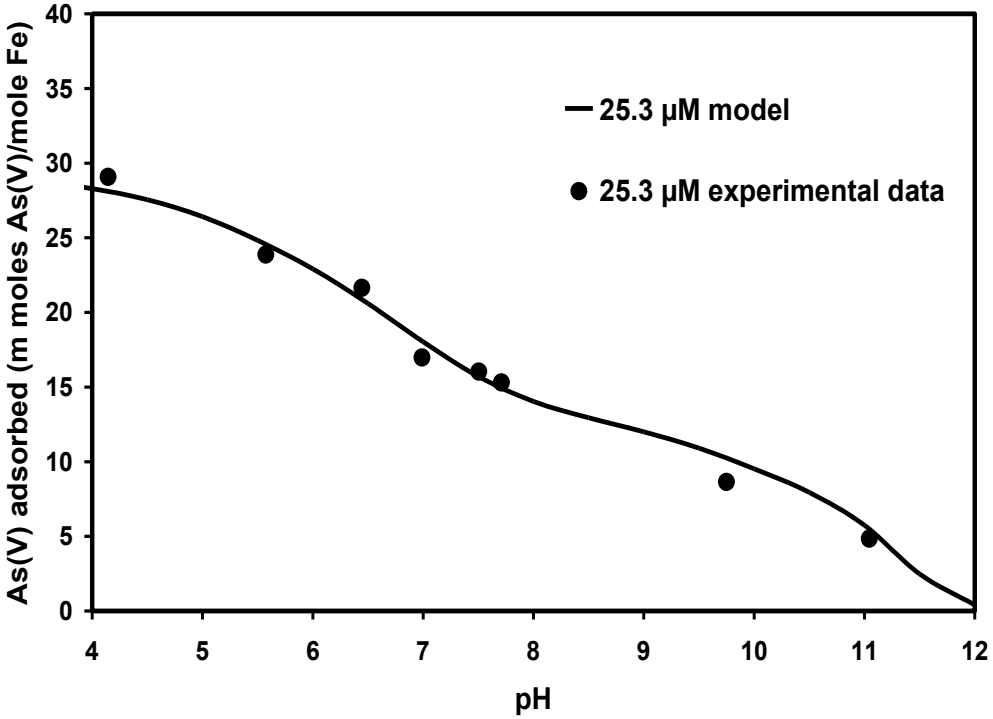

Figure 3-4: Comparison of calibrated model results against adsorption data for Sand-A for an initial As(V) concentration =25.3 µM (10g/ L of Sand-A, I=0.01M)

3.4.3 Validating the model using different initial As(V) concentration datasets

To test the predictive capability of the calibrated model at a different initial As(V) concentration, we conducted additional pH edge experiments for Sand-A at two different initial As(V) concentrations: 5.82 µM and 11.5 µM. We used the calibrated model to make independent predictions using MINTEQA2 for windows software for these new arsenate concentrations. Figure 3-5 compares the model-predicted pH edges with experimental data. The results show that the model was able to successfully predict the adsorption for the two different initial As(V) concentrations. The root mean square error was 0.076 for the 11.5 µM dataset, and 0.18 for the 5.82 µM dataset (i.e., 7.6% and 18% of respective initial concentrations).

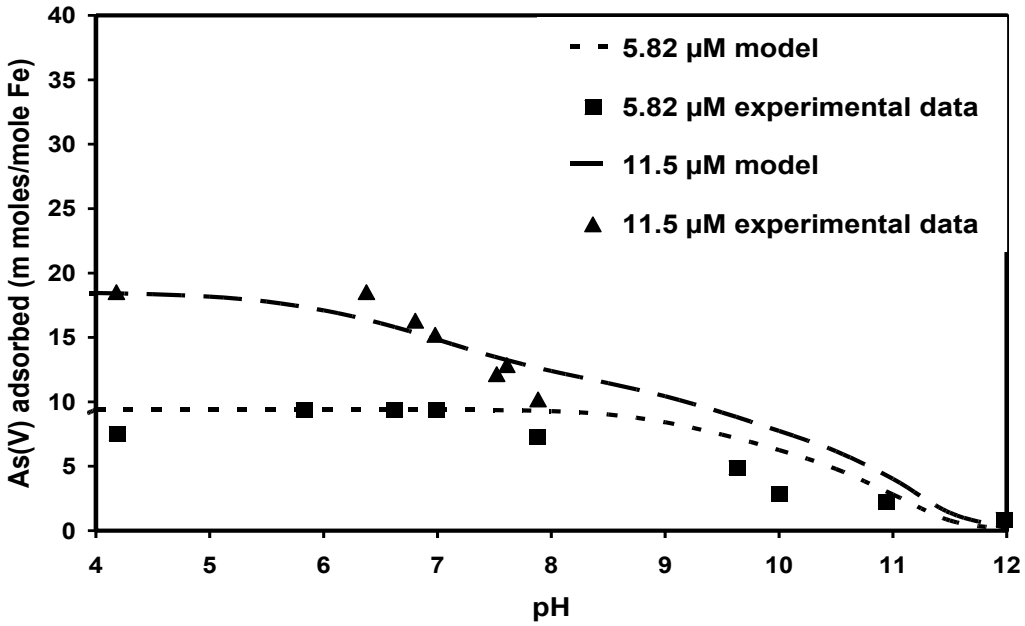

Figure 3-5: Comparison of model predictions against adsorption data for Sand-A using 5.82 and 11.5 µM As(V) solutions (10g/ L of Sand-A, I=0.01M)

3.4.4 Validating the model using a different solid to solution ratio data for Sand-A

To test the predictive capability of the model at a different solid to solution ratio, we conducted a pH edge experiment for Sand-A at a lower solid-to-solution ratio of 4.25g/L using 12.1 μM of initial As(V). We then used the model to predict the pH edge data for this solid to solution ratio. Figure 3-6 compares experimental data with model-predicted pH edges for this simulation. The results show that the model was able to successfully predict the experimental data. The root mean square error was 0.033 (i.e., 3.3% of initial concentration).

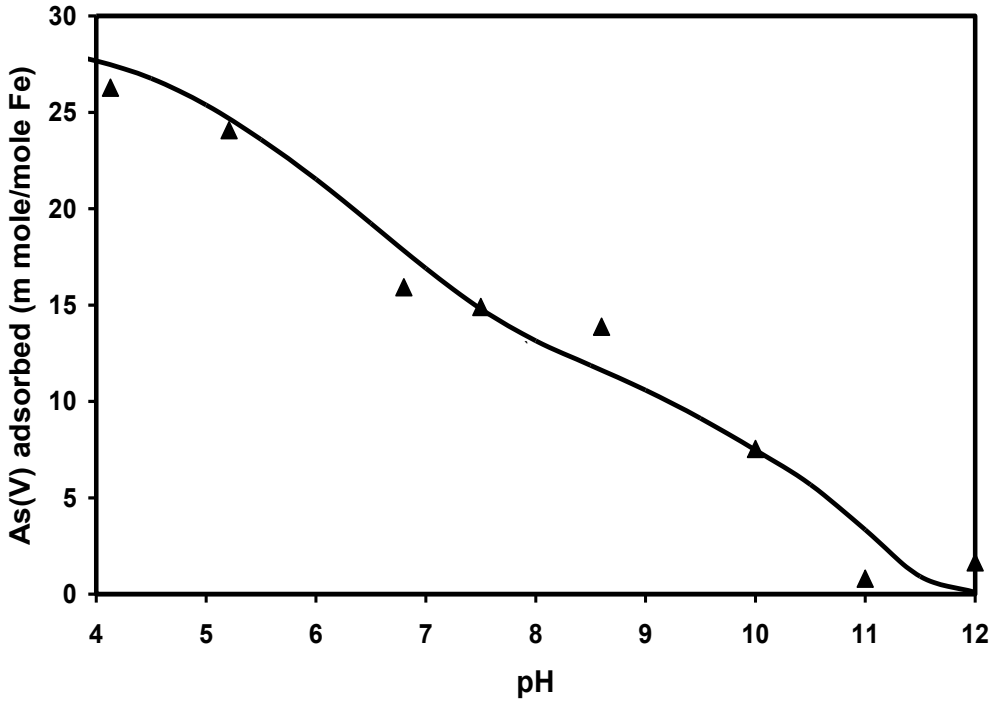

Figure 3-6 : Arsenic(V) adsorption Vs pH for Sand-A at an initial concentration of 12.1μM and a lower solid to solution ratio of 4.25 g/L (I =0.01M)

3.4.5 Testing the scaling approach using Sand-B, Sand-C and Sand-D datasets

In order to test whether the model developed for Sand-A can be scaled, using the approach described in Figure 3-1, we used the model to make independent predictions for Sand-B, Sand-C and Sand-D. All the simulations were completed by running the model in a predictive mode after completing the scaling steps shown in the figure. We computed the log K values for Sand-B, Sand-C and Sand-D by scaling the log K values of Sand-A using the Kulik equation and these values are summarized in Table 3- 4. The parameters given in Table 3- 4 were used to make predictions using MINTEQA2. Figure 3-7 shows the measured pH edge data for Sand-B, Sand-C and Sand-D along with the model predictions. The results show that the model described the experimental data well. The RMSE values for Sand-B, Sand-C and Sand-D datasets were 0.09, 0.014 and 0.013, respectively (i.e., 9%, 1.4% and 1.3% of respective initial concentration levels), which indicate a good fit. The scaled model made good predictions for all the three sands (Sand-B, Sand-C and Sand-D) though the iron content and surface area varied by nearly an order of magnitude.

Table 3-4: Scaled surface complexation parameters for Sands-B ,C and D, I=0

Sorbent Type	Sand-A	Sand-B	Sand-C	Sand-D
Surface site density(Sites/nm^2)	1.04	1.27	1.32	1.38
pK_{a1}	7.44	7.35	7.34	7.32
pK_{a2}	-9.30	-9.39	-9.40	-9.42
pK_1	11.37	11.28	11.27	11.25
pK_2	5.98	5.89	5.88	5.86
pK_3	-0.33	-0.42	-0.43	-0.45
Surface area(m^2/g)	1.08	0.18	0.43	0.57
Amount of Sand (g/L)	10.00	50.00	5.00	2.50

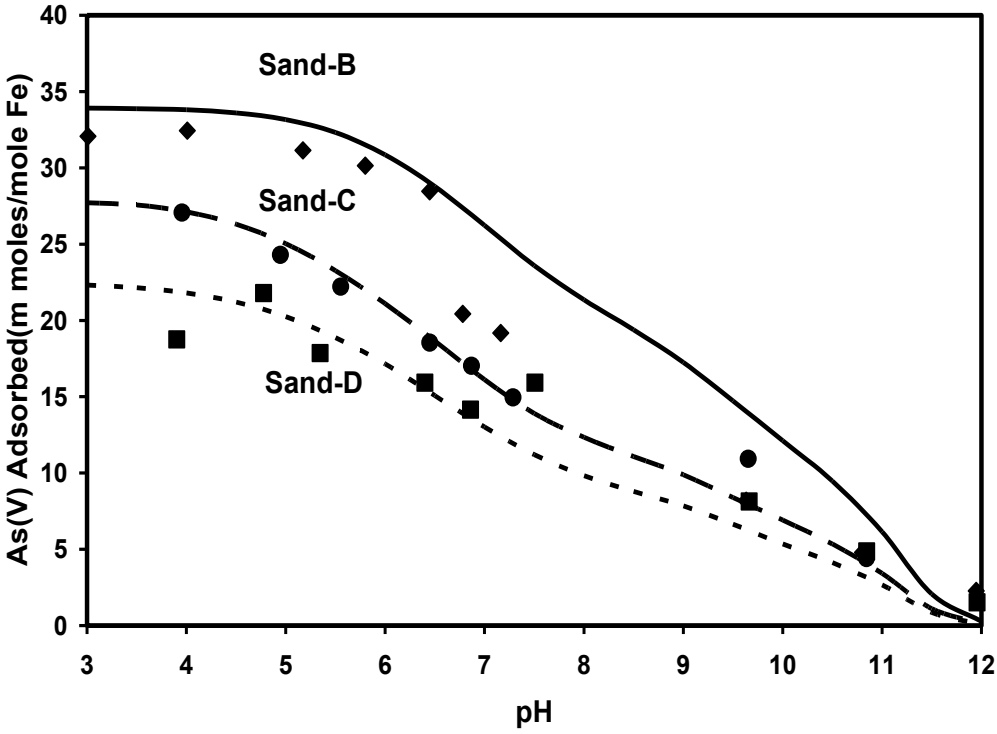

Figure 3-7 : Comparison of scaled-model predictions against pH edge data using an initial As(V) concentration of 12.1 μM (50, 5, 2.5 g/L of Sand-B, Sand-C and Sand-D, respectively, I=0.01M)

We then tested the model performance by comparing model-predicted isotherms for the four sands against measured isotherm data. The model simulation results (predictions) and the experimental data are compared in Figure 3-8. The figure shows that the scaled model was able to predict the isotherm patterns very well. These results show that the scaling approach can yield good predictions for a wide range of arsenate concentrations.

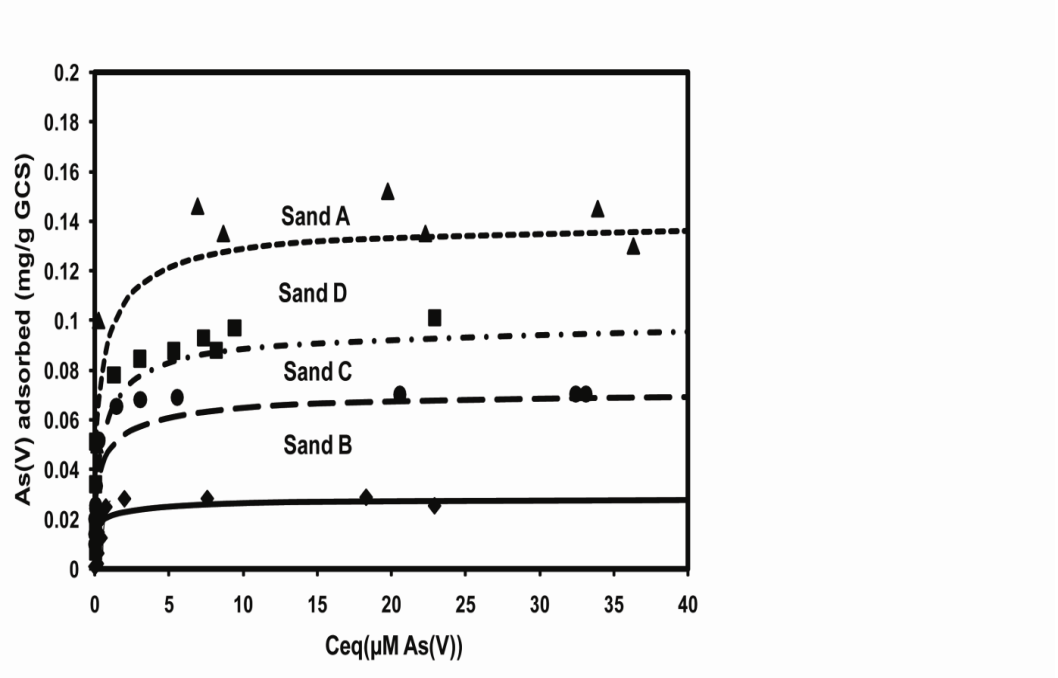

Figure 3-8 : Prediction of As(V) adsorption isotherms at pH 4 for Sand A, B, C and D (I=0.01M)

3.4.6 Testing the scaling approach using literature datasets

We further tested the predictive capacity of the proposed modeling approach using three independent pure goethite datasets derived from the published literature (Hingston, 1970; Hingston *et al.*, 1971; Manning and Goldberg, 1996; Dixit and Hering, 2003). The estimated surface site density values and surface complexation reaction constants (log K values), which were computed using the Kulik equation, are summarized in Table 3- 5 for all three datasets. The literature data was normalized to have a consistent solid-phase concentration unit of mole As(V) per mole Fe in the Y-axis to allow inter-comparison of different published datasets. The model parameters summarized in Table 3- 5 were used in MINTEQA2 to make predictions.

Table 3-5: Surface complexation parameters for published adsorption datasets for arsenate adsorption onto goethite at zero ionic-strength. Abbreviations: DH: Dixit and Hering (2003), MG: Manning and Goldberg (1996), H71: Hingston et al. (1971), H70: Hingston (1970)

Sorbant type	Sand-A	DH	MG	H71	H70
Surface site density (sites/nm^2)	1.04	1.56	1.26	1.59	1.76
pKa_1	7.44	7.26	7.36	7.26	7.21
pKa_2	-9.30	-9.48	-9.38	-9.48	-9.53
pK_1	11.37	11.19	11.29	11.19	11.14
pK_2	5.98	5.80	5.90	5.80	5.75
pK_3	-0.33	-0.51	-0.41	-0.51	-0.56
Surface area (m^2/g)	1.08	54.00	43.10	60.00	32.00

The first dataset was compiled from Manning and Goldberg's (1996) study, which investigated competitive adsorption of arsenate onto pure goethite. They developed a constant capacitance model using FITEQL and used the model to predict adsorption. The surface area was 43.2 m^2/g and the maximum adsorption capacity of their goethite were estimated to be 90 mmol As(V)/kg from their pH edge data (Manning and Goldberg, 1996). The log K values were evaluated by us for diffuse layer model using the surface site density and the Kulik equation and the results are summarized in Table 3- 5. Figure 3-9 compares their published data against our scaled model predictions. The RMSE values were 0.031 for the 133 μM data, and 0.059 for the 266 μM data (i.e., 3.1% and 5.9% of respective initial concentration levels), which indicate a good fit.

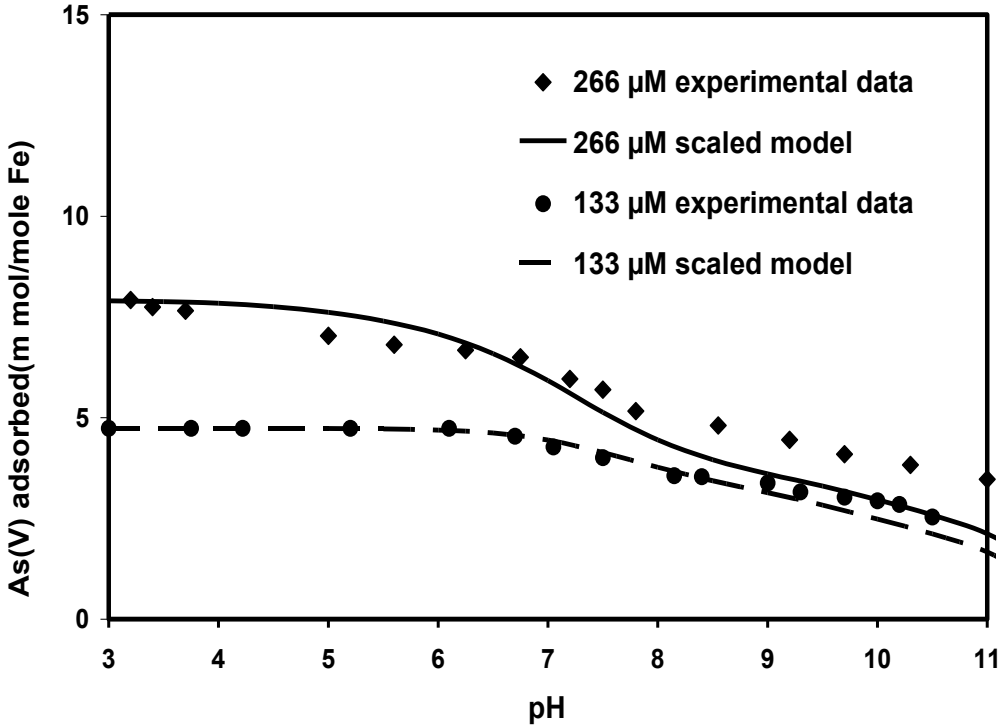

Figure 3-9 : Comparison of scaled-model predictions against published data from Manning and Goldberg (1996) (2.5 g/L goethite, I=0.01M)

The second dataset was compiled from Dixit and Hering (2003). They investigated adsorption of arsenate onto pure goethite and HFO and used the diffuse double layer model to predict the experimental data. We first refitted their adsorption isotherm to estimate the value of the maximum adsorption capacity without using high As(V) data (> 500 µM) since surface precipitation could occur at high As(V) concentrations (Dzombak and Morel, 1990). The estimated value of maximum adsorption capacity was 140 µmoles As(V)/g goethite. We used the reported values of surface area (54 m^2/g) and evaluated the value of surface site density for the system as 1.56 sites/nm^2. These values were then used to evaluate the log K values (summarized in Table 3- 5)

using the scaling approach. The scaled model predictions are compared against Dixit and Hering (2003) data in Figure 3-10. The Figure shows that the scaled model was able to make excellent predictions at various arsenate concentration levels. The RMSE values are 0.040, 0.024, 0.034 and 0.020 for 100 μM, 50 μM, 25 μM and 10 μM As(V) data, respectively (i.e., 4%, 2.4%, 3.4% and 2% of respective initial concentration levels).

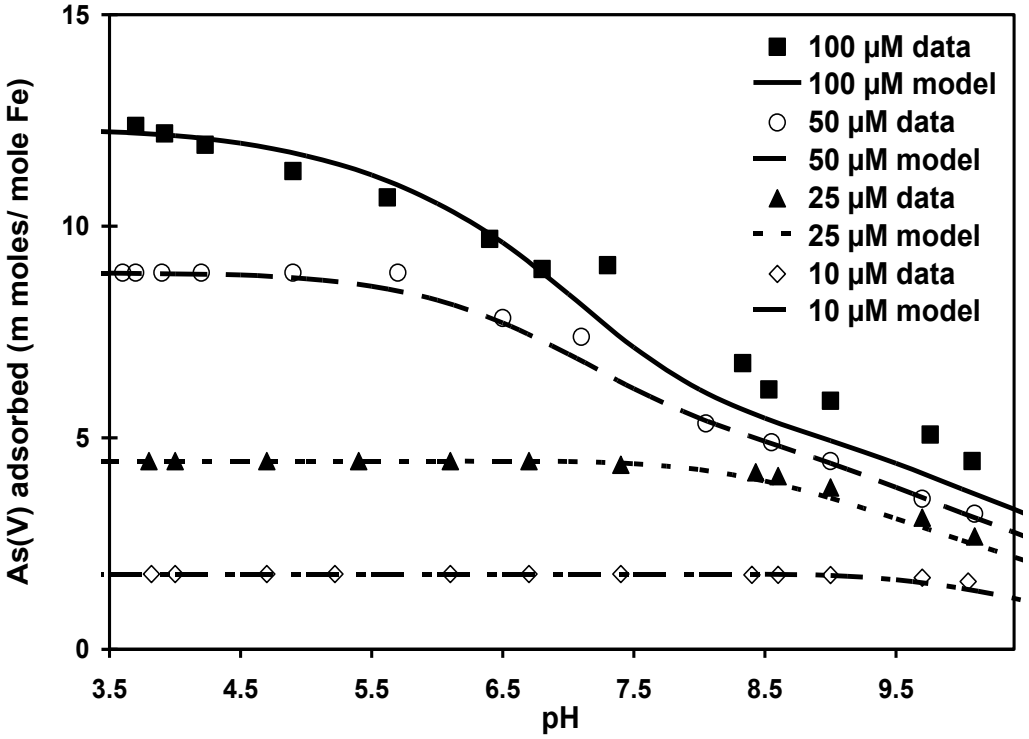

Figure 3-10 : Comparison of scaled-model predictions against published data from Dixit and Hering (2003) (0.5 g/L goethite, I=0.01M)

The third sorption dataset was assembled from two different studies that analyzed As(V) sorption onto pure goethite using the standard Langmuir isotherm model (Hingston, 1970; Hingston *et al.*, 1971; Goldberg, 1986). The maximum adsorption capacity and surface area for the system were reported to be 0.588 moles of As(V)/m^2

and 60 m^2/g, respectively, for the Hingston at al. (1971) data and 0.433 mole/m^2 and 32 m^2/g, respectively, for the Hingston (1970) data. These values were used in the Kulik equation to compute the log K values and the results are given in Table 3- 5. Figure 3-11a compares the experimental data and scaled model predictions. The RMSE values are 0.046 for the 1070 μM dataset, and 0.086 for the 534 μM dataset (i.e., 4.6 % and 8.6% of respective initial concentration levels).

Finally, in order assess the relative importance of the proposed scaling approach, we used the model derived for Sand-A to directly (without scaling) predict the Hingston (1970) and Hingston at al. (1971) datasets. This unscaled model utilized the site density and log-K estimated for Sand-A (see Table 3- 2) without any scaling. Figure 3-11b compares the model predictions against experimental data. The results show that the unscaled model severely under predicted both 1070 μM and 534 μM datasets. The differences are particularly high at lower pH and near surface saturation. This result is consistent with the observations made by Dzombak and Morel (1990), who suggested that the systematic errors in surface site densities could lead to poor predictions at near surface saturation. For the 1070 μM As(V) data the RSME value was 0.13 (13%) using the unscaled model; this was considerably higher than the RMSE value of 0.046 (4.6%) estimated for the scaled model predictions (see Figure 3-11a). For the 534 μM As(V) data, the RSME values was 0.220 (22%) using the unscaled model, which was much higher than the scaled model RMSE value of 0.086 (8.6%).

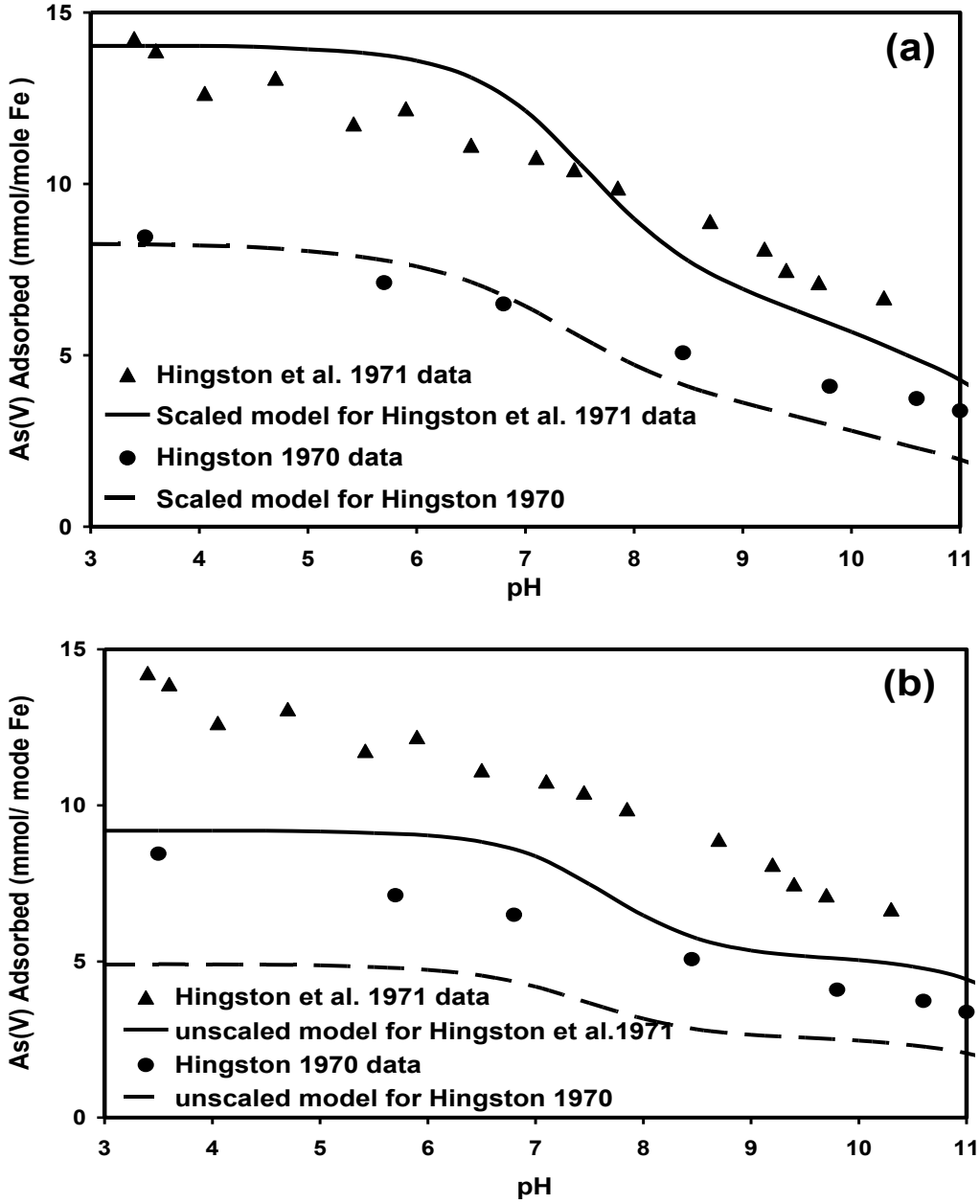

Figure 3-11 : Comparison of a) scaled-model b) unscaled model predictions against published data from Hingston (1970) and Hingston et al. (1971) for 534 μM (4.64 g/L of goethite) and 1070 μM (3.72 g/L of goethite) initial As(V) concentrations (I=0.01M)

3.4.7 Using existing published models for goethite to predict adsorption onto goethite-coated sands without using the scaling approach

Next, we investigated the ability of the literature based models to predict adsorption onto goethite-coated sands without using the scaling approach. We used the same surface complexation parameters as published by (Dixit and Hering, 2003) and we used it to model the data for Sand-A. The model predictions are compared with published experimental data in Figure 3-12. The root mean square error was 0.209 for the 25.3 μM, 0.247 for the 11.5 μM and 0.187 for the 5.82 μM data. Thus the model gave extremely poor predictions especially at high As(V) concentrations. This was expected because the measured site density for Sand-A (1.04 sites/nm^2) was much lower than the site density for their model for goethite. Since extra sites are available, the model for goethite over predicts adsorption when arsenic concentration is higher than the experimental maximum adsorption capacity. This is because the model can adsorb an amount of arsenate nearly up to the site density value used in the model. Thus when we used a model developed for pure goethite to model adsorption data for goethite-coated sands without scaling, the unscaled models give poor prediction due the differences in the site density.

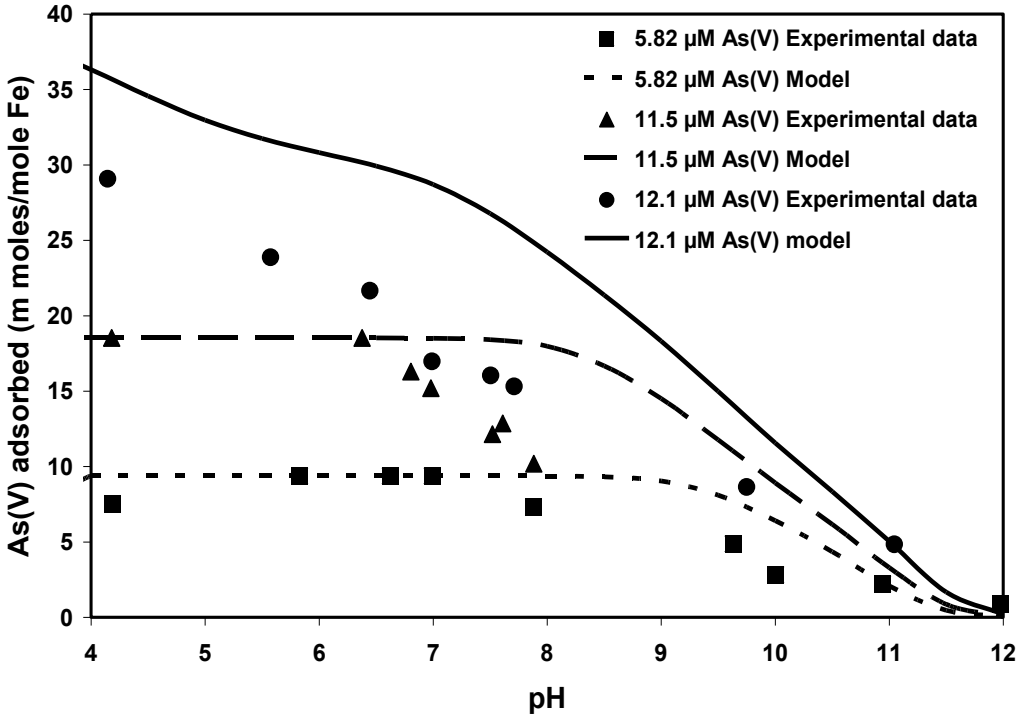

Figure 3-12 : Using model from (Dixit and Hering, 2003) for goethite to predict adsorption onto Sand-A without using the scaling method

Next we used a generic a model from (Mathur and Dzombak, 2006) for PO_4^{-3} adsorption by goethite and used it for arsenate since they have not studied arsenate adsorption and phosphate and arsenate exhibit similar surface complexation behavior. The generic model failed to capture the adsorption by the goethite coated sand especially when the concentrations are above surface saturation. This indicates that generic models may fail to predict adsorption by goethite coated sands. Our approach using the measured site density was able to predict the adsorption well for all goethite-coated sands and literature data for goethite, which suggests that our approach is better than the generic models especially when the sorbate concentrations are above surface saturation.

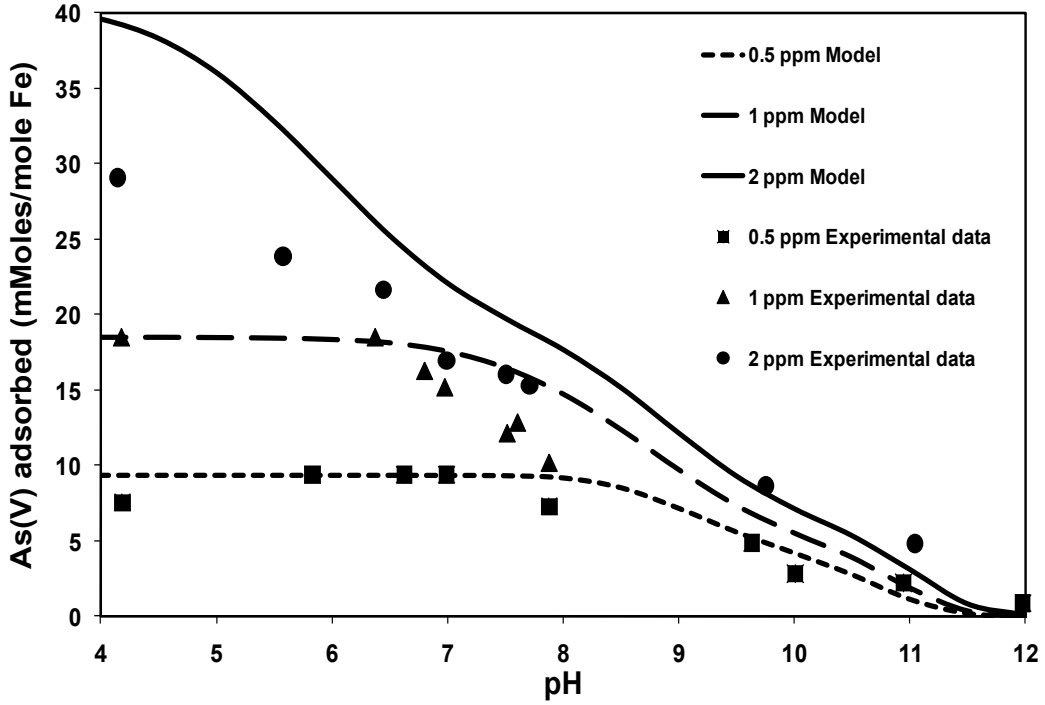

Figure 3-13 : Using model from (Mathur and Dzombak, 2006) for goethite to predict adsorption onto Sand-A without using the scaling method

3.4.8 Using models developed for goethite-coated sands to predict adsorption for pure goethite without scaling the logK values.

In this modeling runs we used the model developed for Sand-A in Table 3- 2 (log K values and site density determined for sand-A), to model the adsorption onto pure goethite by (Dixit and Hering, 2003) without using the scaling procedure. The model predictions are compared with published experimental data in Figure 3-14. The RMSE values are 0.168, 0.162, 0.134 and 0.0523 for 100 μM, 50 μM, 25 μM and 10 μM As(V) data, respectively. The unscaled model gave very poor predictions especially at high initial As(V) concentrations. The models under predicted the adsorption. This was

expected because the site density used in our model for Sand-A (1.04 sites/nm^2) is much lower than the actual site density for their study (Dixit and Hering, 2003). The model under predicts adsorption because, the number of sites available according to the model is much lower than the actual maximum adsorption capacity and the model can adsorb only up to the site density used in the model and no higher.

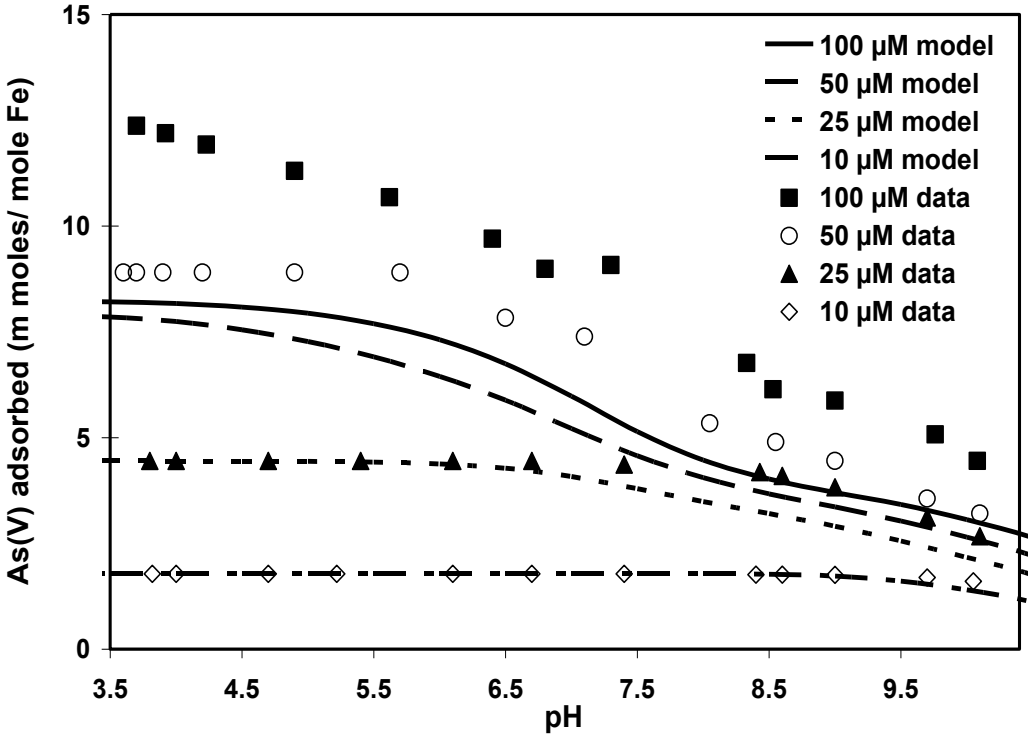

Figure 3-14 : Using models developed for Sand-A to predict adsorption for pure goethite from (Dixit and Hering, 2003) without using the scaling method

3.4.9 Development of a model for pure goethite and predicting adsorption onto goethite-coated sands by scaling

Finally, to test the robustness of the approach, we developed a surface complexation model for published data from (Dixit and Hering, 2003) for pure goethite and scaled it to make predictions for goethite-coated sand, Sand-A. We used the site density and surface area for Sand-A (Table 3- 5) and fitted the log K values for the above published data, using FITEQL 4.0 software. The log K values we estimated for the data are given in Table 3- 6. These surface complexation parameters were used to make predictions for the datasets. The plots of model predictions verses the experimental data is given in Figure 3-15a. The RMSE values are 0.0206, 0.049, 0.0231 and 0.0156 for 100 μM, 50 μM, 25 μM and 10 μM As(V) data, respectively. Thus the model developed was able to describe the adsorption for the experimental data from (Dixit and Hering, 2003).

Next we used the model from Table 3- 6 to predict the adsorption onto Sand-A by scaling. The values of surface complexation constants for Sand-A, got by scaling using Kulik equation are given in Table 3- 7. The surface complexation parameters from Table 3- 7 were used to make predictions for the literature datasets. Model predictions were made based on the scaled model in Table 3-7 for Sand-A. Figure 3-15b shows the predictions for Sand-A by the scaled model. The scaled model was able to predict the adsorption for Sand-A satisfactorily as shown in Figure 3-15b. The root mean square errors were 0.0484, 0.138, and 0.224 respectively for the 25.3 μM, 11.5 μM and 5.82 μM datasets. This shows the robustness of the approach which could be used for scaling models developed for pure goethite to predict adsorption onto goethite-coated sands.

Table 3-6: Aqueous protonation constants and intrinsic surface complexation constants for pure goethite from (Dixit and Hering, 2003) at surface site density of 1.56 sites/nm^2 and zero ionic-strength.

Reactions			**Log K** (I=0, Γ=1.56 sites/ nm^2)	
Protonation reactions for As(V) [A]				
H_3AsO_4		$= H_2AsO_4^- + H^+$	-2.24	(1)
H_3AsO_4		$= HAsO_4^{2-} + 2H^+$	-9.20	(2)
H_3AsO_4		$= AsO_4^{3-} + 3H^+$	-20.70	(3)
Surface hydrolysis reactions of goethite[B]				
>FeOH	$+ H^+$	$= > FeOH^{2+}$	7.26	(4)
>FeOH		$= > FeO^- + H^+$	-9.48	(5)
Surface complexation reactions [C]				
>FeOH	$+ H_3AsO_4$	$= >FeH_2AsO_4 + H_2O$	11.52	(6)
>FeOH	$+ H_3AsO_4$	$= >FeHAsO_4^- + H_2O + H^+$	6.74	(7)
>FeOH	$+ H_3AsO_4$	$= >FeAsO_4^{2-} + H_2O + 2H^+$	-0.05	(8)

Surface site density =1.56 sites/nm^2 for sand A, Surface area=54 m^2/ g GCS.

[A] – From MINTEQA2 for windows thermodynamic database

[B] –From Richter et al.(2005) normalized to surface site density of 1.56 sites/nm^2

[C] – Values from FITEQL optimization for the data from Dixit and Hering(2003)

Table 3-7: Scaled surface complexation parameters for Sand-A at zero ionic-strength

ite density	**Dixit and Hering**	**Sand A**
(Sites/nm^2	**1.56**	**1.04**
pK_{a1}	7.26	7.44
pK_{a2}	-9.48	-9.30
pK_1	11.52	11.70
pK_2	6.74	6.92
pK_3	0.05	0.23
Surface area(m^2/g)	54.00	1.08

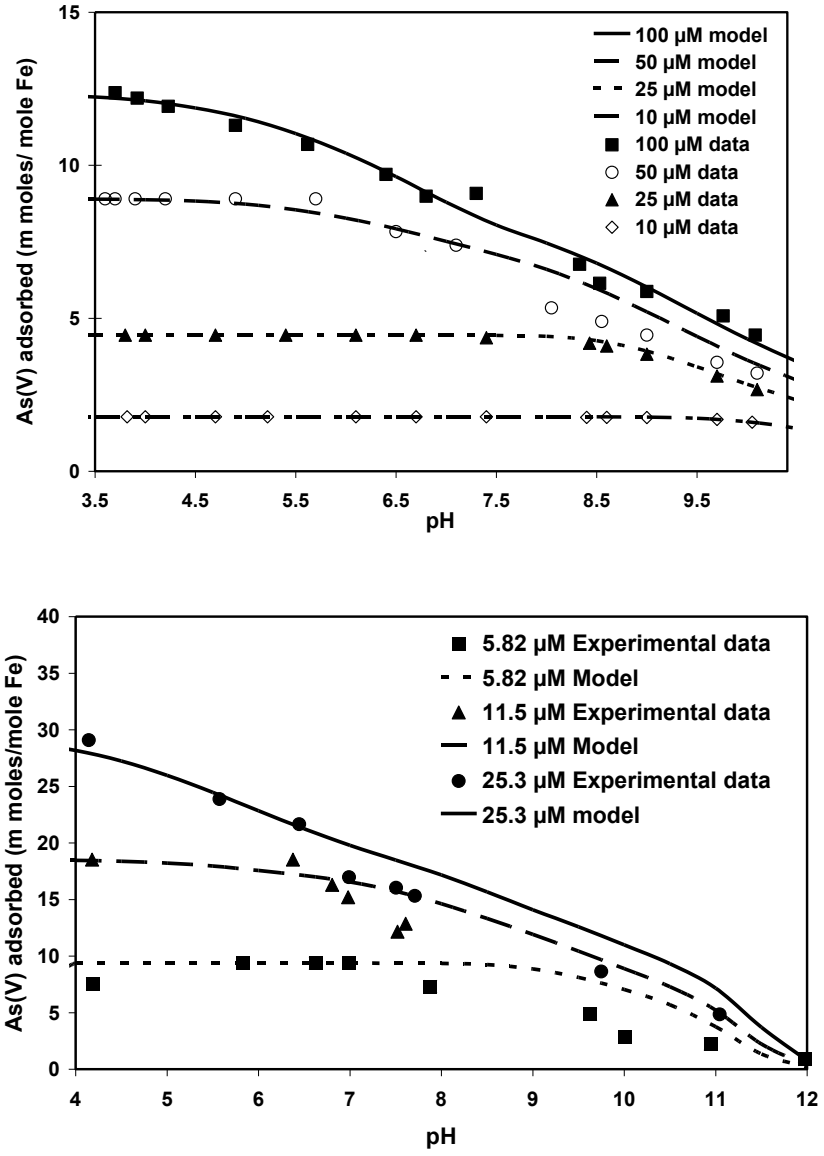

Figure 3-15 : a) Comparison of model predictions verses adsorption data for the model developed by using literature data (Dixit and Hering, 2003) b) Comparison of model predictions verses adsorption data for scaled model for the data for Sand-A using 12.1, 5.82 and 11.5 µM As(V) solutions (10g/ L of Sand-A).

3.5 Conclusions

A scalable surface complexation modeling framework for predicting As(V) adsorption onto various types of goethite-coated sands and goethite is presented. The approach was tested using a set of experimental data that characterized As(V) adsorption on four different goethite-coated sands with iron content and surface area values varying by nearly an order of magnitude. In addition, three sets of literature-derived data for As(V) adsorption on to pure goethite were used to further validate the modeling approach. The results indicate that surface site density was the most important scaling parameter. Also, the Kulik (2002) equation provides an approach for consistently correcting the log K constants for changes in site density values.

In this study, we first calibrated a diffuse double layer model to fit a pH edge data obtained for one of the four goethite-coated sands (Sand-A). The calibrated model was then validated by predicting the adsorption edges at different initial As(V) concentrations and solid-to-solution ratios. The model was then scaled for the other three goethite-coated sands using the measured values of surface site density and the log-K values were estimated using the Kulik equation. The scaled model was able to successfully predict arsenate adsorption data obtained for the three goethite-coated sands. In addition, the scaled model was also able to predict several literature-derived arsenate adsorption datasets for goethite. Whereas, unscaled models failed to satisfactorily predict the adsorption data.

The results also show that a model developed for a pure goethite may not be able directly to predict adsorption for goethite-coated sands due the differences in site density.

And a model developed for goethite-coated sand was not able to predict adsorption onto pure goethite for the same reason. This inability of the models becomes particularly obvious at arsenate concentrations higher than the number of sites available. However models developed for goethite gave good predictions for goethite-coated sands when scaled according to the measured site densities.

This study provides a practical surface complexation modeling framework that can be easily adapted from one system to another. The scaling approach yielded good predictions with minimum amount of experimental data. The average error in model predictions for the three goethite coated sands and the published datasets is less than 5%, as quantified using RMSE values. Also, the scaled models yielded predictions that were either comparable to or, in some cases, better than the original published model fits. These results are consistent with studies that have shown that scaling log K values based on surface site density can provide acceptable predictions (Richter *et al.*, 2005b; Richter *et al.*, 2005a; Kulik, 2006; Richter and Brendler, 2006). The limitation of the proposed scaling approach is that it requires measurement of site densities of the sorbent using adsorption isotherms. However, the approach is much easier than developing a whole new surface complexation model using FITEQL for every new adsorbent. Also, it is perhaps possible to develop empirical relationships between site density and iron content and/or surface area, and such relationships could be used to avoid direct measurement of site density for similar types of sorbents. Future studies should focus on testing this "scaling" procedure for systems involving other types of inorganic contaminants and/or other metal-oxide surfaces.

CHAPTER 4

A NOVEL EXPERIMENTAL SYSTEM TO STUDY EQUILIBRIUM-REACTIVE TRANSPORT PROBLEMS

4.1 Introduction

Geochemical equilibrium reactions are important processes that control the transport of inorganic contaminants in groundwater aquifers. Under natural groundwater flow conditions, equilibrium conditions are usually assumed for most common geochemical reactions such as cationic exchange, acid-base reactions, complexation reactions, and adsorption reactions (Huber and Garrels, 1953; Rubin, 1983; Coston *et al.*, 1995; Davis *et al.*, 1998; Wernberg, 1998; Friedly *et al.*, 2002). Therefore, studying geochemical reactions under equilibrium transport conditions, in laboratory setting, is useful for developing vital insights into the transport processes occurring in natural groundwater systems.

Different types of experimental reactor setups have been used for studying geochemical reactions in laboratory conditions. Single reactor experimental setups that are commonly used are batch reactors, column reactors (plug flow reactors) and continuous stirred tank reactors (Levenspiel, 1991). Multiple reactor setups that employ

several batch reactors in series or parallel or a combination are also sometimes used (Bale and Morris, 1981; García-Luque *et al.*, 2006). However, none of the above reactor setups is suitable for studying equilibrium reactive transport involving geochemical reactions. In this Chapter we propose a novel sequential equilibration reactor experimental setup for studying equilibrium geochemical transport problems. We demonstrate the use of this experimental setup by investigating arsenate adsorption by surface complexation reactions on a synthetic goethite-coated sand. Arsenic was chosen as a representative reactive species since it is a common groundwater contaminant of world-wide concern (Smedley and Kinniburgh, 2002); also, goethite is a ubiquitously present adsorbent in groundwater aquifers (Wang *et al.*, 1993; Fuller *et al.*, 1996).

Traditionally, batch reactors have been used for studying geochemical reactions since batch experiments are easy to conduct and parameterize. In a typical batch-reactor experiment, the reactants are initially charged into the reactor, mixed well and left to react until equilibrium is reached (Levenspiel, 1991). The resultant mixture is then analyzed for adsorbate concentration. Batch experiments have been extensively used for studying inorganic contaminant adsorption onto different types of metal oxides (Hingston, 1970; Manning and Goldberg, 1996; Dixit and Hering, 2003; Cheng *et al.*, 2004; Giammar *et al.*, 2004 ; Dixit and Hering, 2006). Although batch experiments are relatively easy to conduct, they are quite different from dynamic subsurface systems; they are usually conducted under no-flow conditions and hence they cannot be directly used to study subsurface transport problems.

Column experiments (which are conceptually similar to plug flow reactors) are commonly used to study geochemical transport under one-dimensional uniform flow conditions. Several researchers have studied arsenic transport in packed bed columns containing iron-coated sand or other adsorbents (Kuhlmeier, 1997; Williams *et al.*, 2003; Radu *et al.*, 2005a; Zhang and Selim, 2006; Dadwhal *et al.*, 2009). Residence times usually possible in column experiments is on the order of minutes, whereas it could take several hours or days to reach equilibrium for adsorption reactions such as arsenic adsorption on metal-oxides (Manning and Goldberg, 1996; Raven *et al.*, 1998; Khaodhiar *et al.*, 2000). Thus, one of the major disadvantages of studying geochemical equilibrium adsorption reactions in column reactors is that the experimental flow conditions might not allow sufficient contact time to attain equilibrium and hence the results could be influenced by kinetic effects (Williams *et al.*, 2003; Zhang and Selim, 2006). Besides, column experiments are influenced by various issues related to irregular mixing and preferential flow paths. Barnett et al. (2000) observed that column experimental results could not be predicted using batch equilibrium adsorption parameters, and that modeling of column-scale adsorption data could be significant problem due to the presence of non-linear kinetic effects.

Continuous flow stirred tank reactor (CSTR) is another type of reactor, which is used in geochemistry literature to study kinetic reactions. Kirby and Brady (1998) used a continuous stirred tank reactor to determine the Fe^{2+} oxidation rates for an acid mine drainage problem. The rate constants obtained were later used to model a field scale wetland treatment facility. Rimstidt and Dove (1986) used a CSTR to determine

mineral/solution reaction rates for wollastonite hydrolysis reaction. Some researchers have used a series of CSTRs, with continuous flow from one reactor to next, to study estuarine mixing dynamics (Bale and Morris, 1981; García-Luque *et al.*, 2006). However, since CSTRs are continuous flow through systems, they offer a limited amount of retention time, and are hence not suitable for studying equilibrium reactions that need longer residence time.

Geochemical equilibrium reactions in batch reactors can be mathematically simulated using batch computer codes such as PHREEQC (Parkhurst and Appelo, 1999) and MINTEQA2 (Allison *et al.*, 1990). More recently, researchers have coupled these codes with transport codes to simulate reactive transport problems involving geochemical reactions (Cederberg *et al.*, 1985; Noorishad *et al.*, 1987; Gao *et al.*, 2001; Prommer *et al.*, 2003b; Parkhurst *et al.*, 2004). Of these coupled codes, PHT3D (Prommer *et al.*, 2003b) and PHAST (Parkhurst *et al.*, 2004) are widely used for simulating three-dimensional reactive transport. The 2002 version of PHREEQC called as PHREEQCI (Clarlton and Parkhurst, 2002) also has the capability to simulate one-dimensional reactive geochemical transport. However, currently there are no suitable experimental setups available to conduct equilibrium geochemical transport experiments for validating these geochemical equilibrium coupled transport models. Therefore, theoretical problems (Cederberg *et al.*, 1985; Engesgaard and Kipp, 1992), analytical solutions (Parlange *et al.*, 1984; Sun *et al.*, 1999), simulations from already established models such as RT3D (Clement, 1997) or simplified field problems (Valocchi *et al.*, 1981) are commonly used as benchmarks for testing geochemistry-coupled reactive transport codes. However, such

validation approaches can only provide an indirect assessment and do not really test reactive transport of a specific contaminant of interest to the modeler. Besides, due to uncertainties in equilibrium constants (Schecher and Driscoll, 1987; Ekberg and Emrén, 2001), it is critical to validate geochemical-equilibrium transport models using actual experimental data.

The goal of this phase of the study is to develop an experimental methodology to conduct reactive transport experiments involving equilibrium geochemical reactions. The methodology was inspired by the conceptual ideas inherently assumed in geochemical transport codes such as PHREEQCI and PHT3D (Clarlton and Parkhurst, 2002; Prommer *et al.*, 2003b). These numerical codes conceptualize one-dimensional reactive transport as a system involving a series of sequential equilibration reactors, as shown in Figure 4-1. The numerical operations at a node or a grid cell (which can be conceptualized as a batch reactor) consist of: (i) transferring fresh influent solution (aqueous phase) into the cell, (ii) allowing the reactants in both aqueous and solids phases to react until equilibration is reached, and (iii) transferring the equilibrated aqueous phase to the next cell. The solid-phase components (immobile phase) are retained in the cell. We propose an experimental setup that mimics the conceptual numerical grid system using a series of batch reactors, and is identified in this study as the multiple sequential equilibration reactor (MSER) experimental setup. It is also possible to exclusively study just a single numerical grid cell using a single batch reactor; this setup is identified as the single sequential equilibration reactor (SSER) experimental setup. Both MSER and SSER systems are

illustrated in Figure 4-1. Both of these sequential equilibration reactor experimental setups can be used to study equilibrium geochemical transport problems.

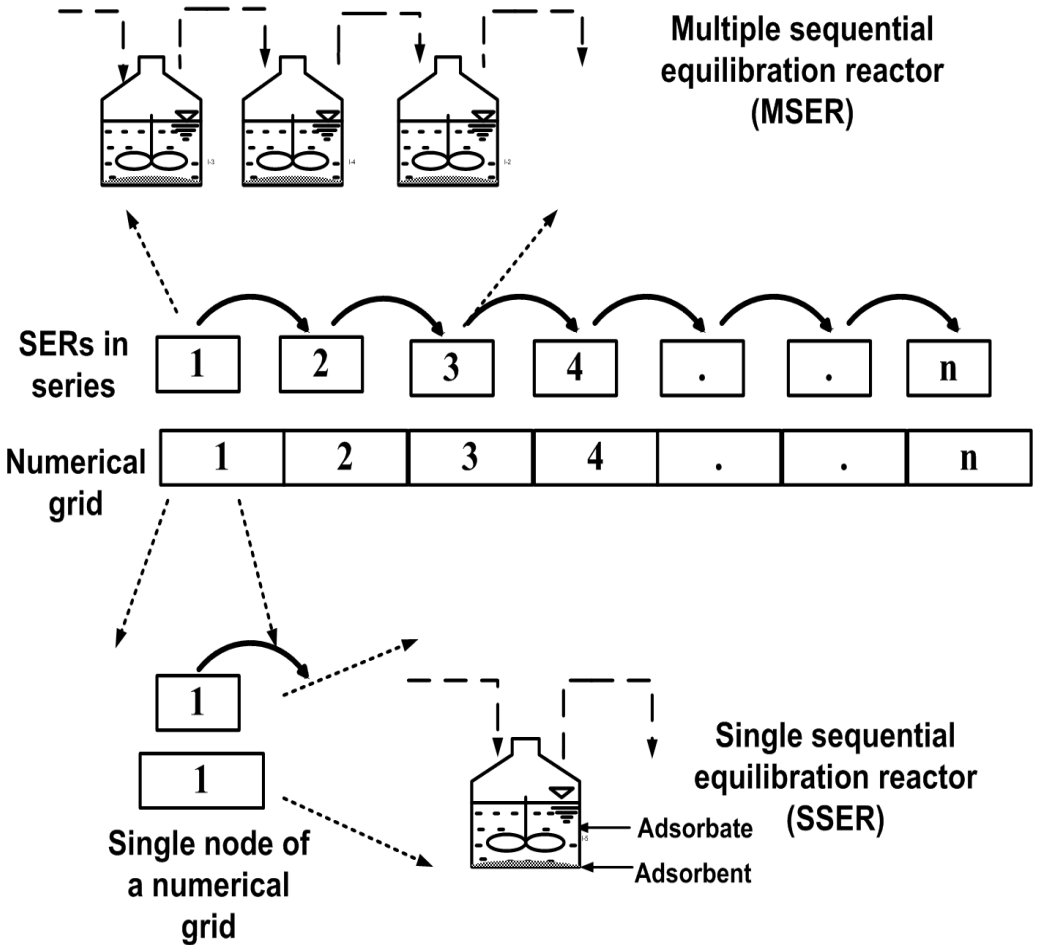

Figure 4-1 : Conceptual diagram of a numerical grid compared to a sequential equilibration reactors (SER) system. A MSER system is shown in the top and a SSER system is shown in the bottom.

The objective of this chapter is to demonstrate the use of sequential equilibration reactor experimental setups for conducting equilibrium geochemical transport

experiments. Both the single and multiple sequential equilibration reactor setups are used to generate equilibrium transport data for arsenic adsorption on synthetic iron-coated sand. The generated experimental datasets are then used to test whether a surface complexation model developed from batch experimental setup can be used to model equilibrium transport observed in sequential equilibration reactor systems under a wide range of pH, solid/solution ratio and concentration conditions.

4.2 Materials and methods

4.2.1 Experimental methods

We used iron (goethite) coated sand (ICS), designated as Sand-A in Chapter three, as the adsorbent. The procedure used for synthesizing the iron-coated sand is described in our earlier publications (Cheng *et al.*, 2004; Loganathan *et al.*, 2009). Scanning electron microscopy (SEM) images showed that the iron coating mainly consisted of goethite (Loganathan *et al.*, 2009). The characteristics of the iron-coated sand such as iron content and surface area are summarized in Table 4-1.

Table 4-1: Characteristics of Sand-A

Iron content (mg Fe/ g sand)	3.48 ±0.1
Surface area (m^2/ g sand)	1.08
Maximum adsorption (mg As(V)/g sand)	0.14
Surface site density (μmoles/m^2)	1.73
Surface site density (sites/nm^2)	1.04

Arsenic solutions were prepared from a 100 ppm stock solution, which was made by dissolving 0.416 grams of reagent grade $Na_2HAsO_4.7H_2O$ in one liter of deionized water. The ionic strengths of all the solutions were adjusted to 0.01 M using sodium nitrate ($NaNO_3$). The pHs of the solutions were adjusted using NaOH or HNO_3 and the value was measured using an Orion (model 250A) pH meter, which was calibrated using commercial pH 4.0, 7.0, and 10 buffers. The average temperature was maintained at $25^0C \pm 2^0C$ for all experiments. 500 ml polypropylene plastic bottles were used as experimental reactors. Our initial kinetic experiments indicated that near equilibrium conditions were reached in less than ten hours. Similar results have also been observed in previous studies (Manning and Goldberg, 1996; Wilkie and Hering, 1996). All the sequential equilibration reactor experiments were done by equilibrating 100 ml (defined as one reactor volume or RV) of arsenate solution with iron-coated sand in a tumbling shaker. The supernatant solution was centrifuged and filtered through 0.45 μm membrane filter (Millipore), which was fitted to a disposable syringe. The solutions were analyzed for total arsenic using a graphite furnace atomic absorption spectrophotometer (GFAAS; Perkin-Elmer 5100 PC) which has a detection limit of 5 $\mu g\ L^{-1}$ (5 ppb) of total arsenic.

4.2.2 Design of SSER and MSER experiments

The single sequential equilibration reactor (SSER) experimental setup consists of a single batch reactor operated in a sequential fashion as shown in Figure 4-1. A known mass of iron-coated sand was loaded into the reactor. Each "sequential-equilibration-cycle" consisted of introducing new influent solution into the reactor, equilibrating for 24

hours in a tumbling shaker and removing the aqueous phase for analysis. The aqueous phase was centrifuged, filtered and analyzed for arsenic at the end of each sequential-equilibration-cycle. During the entire experiment, the immobile phase (sand) was retained in the reactor. For the next sequential-equilibration-cycle, new arsenate solution was introduced into the same reactor, allowed to equilibrate, and the aqueous phase was removed and analyzed. This process was repeated several times. A SSER system is conceptually a numerical grid with a single node and can help simulate breakthrough from the first node for multiple reactor volumes.

Our multiple sequential equilibration reactor (MSER) experimental setup consisted of three sequentially-linked reactors as shown in Figure 4-1. Initially the influent solution was introduced to the first reactor. After equilibration in the first reactor, the aqueous solution phase from the first reactor was transferred to the second reactor, allowed to equilibrate, and later transferred to the third reactor. The solution from the last reactor was removed, centrifuged, filtered and analyzed for arsenic. During the entire experiment, the immobile phase (sand) was retained within the reactors.

Due to their conceptual similarity with one-dimensional numerical models, both SSER and MSER experiments can be used to produce datasets for testing transport codes that are coupled to batch equilibrium-geochemical models using the operator split procedure [e.g., PHT3D (Prommer *et al.*, 2003a)]. The sequential equilibration reactor systems offer a simple alternative to conduct well-constrained experiments for generating datasets to test equilibrium-geochemical transport codes. Although the modeling part of geochemical transport is well established, the experimental design perhaps reflects one of

the first attempts to test the modeling methods. Previous studies have either used batch or column experiments and compared the results against equilibrium transport models. Whereas, sequential equilibration experiments physically implement the actual algorithm of the numerical equilibrium transport models.

4.2.3 Surface complexation modeling methods

In Chapter 3, we presented an approach for scaling surface complexation models for goethite and goethite coated sands. The scaling approach can greatly reduce model development time for different iron coated sands and iron-oxides. We used the model from Chapter 3 (Jeppu *et al.*, 2010) to describe arsenate adsorption onto Sand-A. The surface complexation reactions and the model parameters for Sand-A were previously summarized in Table 3-2. These reaction equations and constants were incorporated in PHREEQCI to make predictions for our experiments. The advection block available within PHREEQCI allowed us to simulate the geochemistry-coupled advective transport on a numerical grid as shown in Figure 4-1. The difference between model predictions and experimental data was quantified using R^2 value of predictions which is defined by the equation:

$$R^2 = 1 - \left[\frac{\sum_{i=1,n} (C_i - f_i)^2}{\sum_{i=1,n} (C_i - C_m)^2} \right] \qquad (4\text{-}1)$$

Where, C_i is the measured aqueous concentration, f_i is the model predicted aqueous concentration, and C_m is the mean of observed aqueous concentration data.

4.3 Results

Adsorption of arsenic on goethite may depend on a wide range of geochemical parameters such as pH, dissolved organic matter, solid/solution ratio, competing-ions, redox conditions and adsorbate concentrations (Smedley and Kinniburgh, 2002; Hartzog *et al.*, 2009; Nath *et al.*, 2009). Solid/solution ratio, pH and adsorbate concentration determine the adsorption breakthrough time for arsenate adsorption on irons under laboratory conditions. We conducted sequential equilibration reactor experiments at various pH, solid/solution ratio, and initial arsenic concentration conditions to check if the surface complexation models are able to predict the experimental data during variations of these different conditions. Since SSER experiments require considerably less time and effort than MSER experiments, we conducted a total of seven SSER experiments. Only one MSER experiment was conducted and the results are reported in the last section.

4.3.1 Studying the effect of variations in solid/solution ratio on arsenate transport

First, we conducted single sequential equilibration reactor experiments to study equilibrium transport at different solid/solution ratios. Three experiments were conducted with different solid/solution ratios of 30 g/L, 60 g/L and 120 g/L and the results are as shown in Figure 4-2.

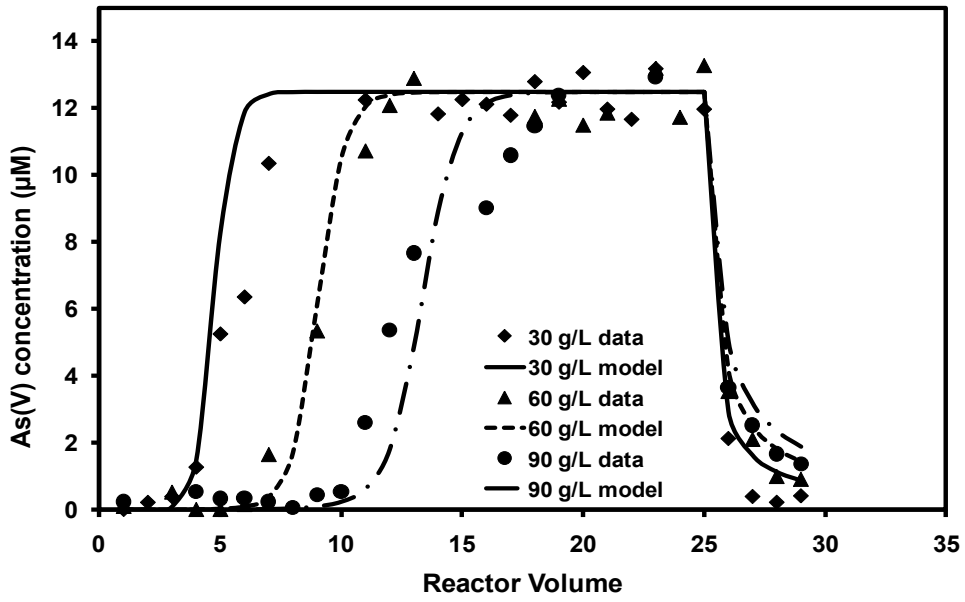

Figure 4-2: Comparison of PHREEQCI predictions and SSER experimental data at different solid/solution ratio for 12.5 µM As(V) solution (pH = 4,I = 0.01 M).

The initial influent solution had an initial concentration of 12.5 µM As(V). The pHs of all solutions were 4 and ionic strengths of solutions were 0.01M. In each sequential-equilibration-cycle, the sand was equilibrated with 100 ml (defined as one reactor volume or RV) of arsenate solution for 24 hours and then the liquid phase was removed and analyzed. In the whole experiment, the sand was treated with twenty-five sequential-equilibration-cycles (25 RVs) of new As(V) solution, and then flushed with four sequential-equilibration-cycles (4 RVs) of deionized water. We tested the PHREEQCI code with the SCM model for Sand-A from Chapter 3, by using it to make predictions for this experimental system at different solid/solution ratios and the results are also shown in Figure 4-2. It can be seen that the model predictions closely matched the breakthroughs and overall trend observed in the experimental system for all the three

solid/solution ratios. The R^2 values were 0.89, 0.90 and 0.88 for the 30 g/L, 60 g/L and 120 g/L experiments, respectively. The transport of arsenate was retarded by adsorption, which is proportional to the solid/solution ratio. When the system was flushed with deionized water, the data show a sharp decline in the effluent arsenic concentrations. This can be expected since goethite has high affinity for As(V) at lower pH values and hence it is difficult to desorb the adsorbed arsenate at pH 4 (Manning and Goldberg, 1996; Dixit and Hering, 2003).

4.3.2 Studying the effects of variations in pH on arsenate transport

Next, to study equilibrium transport of arsenate at different pHs, we conducted single sequential equilibration reactor experiments at the following three pH values: 4, 7 and 10. The concentration of As(V) in the influent was 12.5 μM and ionic strength was 0.01M. In each sequential-equilibration-cycle, the sorbent (30 g/L of IOCS) was equilibrated with 100 ml (one RV) of arsenate solution and then the equilibrated solution was removed and analyzed. The entire experiment consisted of 17 sequential-equilibration-cycles of equilibrating with new As(V) solution, followed by three sequential-equilibration-cycles of flushing with deionized water at the same pH and ionic strength. Figure 4-3 shows the effluent As(V) concentration from this SSER system. The PHREEQCI code with the SCM model for Sand-A was tested by using it to make predictions for these experiments at different pHs and the results are also shown in Figure 4-3.

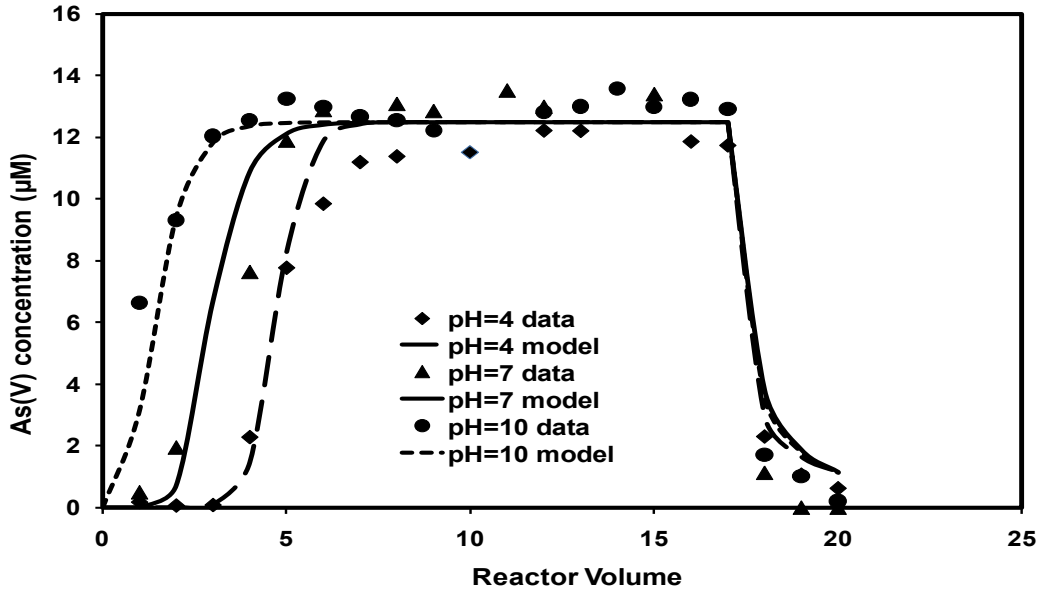

Figure 4-3 : Comparison of PHREEQCI predictions and SSER experimental data for effect of varying pH for 12.5 µM As(V) solution using 30 g/L of the ICS (I =0.01 M).

It can be seen from the Figure that the model predictions closely matched the experimental breakthroughs and overall trends for all the three pH values. The R^2 values are 0.96, 0.91 and 0.94 for pH 4, 7 and 10 data, respectively. Arsenate transport was found to be highly dependent on pH. At pH 10 the breakthrough occurs at 1 reactor volume, which indicates that there is very low adsorption. At pH 7, breakthrough occurs after 2 pore volumes. Whereas at pH 4, breakthrough occurs after 4 pore volumes. Since arsenate adsorption is strong at low pH values, the pH-4 system treated the maximum number of reactor volumes of arsenate, followed by pH-7 and pH-10 systems, respectively.

4.3.3 Studying the effect of variations in the concentration on arsenate transport

Next, we wanted to study equilibrium geochemical transport at different arsenate concentrations using single sequential equilibration reactor (SSER) experiments. To accomplish this, we conducted two experiments using the following initial arsenate concentrations: 12.5 μM and 25 μM. (Note that the 12.5 μM dataset is repeated in Figure 4-3 and 4-4). The pH was fixed at 4 and the ionic strength was 0.01M for all solutions. In each sequential-equilibration-cycle, the sorbent (ICS at a concentration of 30 g/L) was equilibrated with 100 ml (one RV) of new arsenate solution and then the equilibrated solution was removed and analyzed. The whole experimental consisted of treating the sand with 17 sequential-equilibration-cycles of new As(V) solution, followed by 3 sequential-equilibration-cycles of flushing with deionized water, which is at the same pH and ionic strength. Figure 4-4 shows the output As(V) breakthrough data profile for this SSER system. The PHREEQCI code with the SCM model for Sand-A was tested by using it to make predictions for this experimental system and the results are also shown in Figure 4-4.

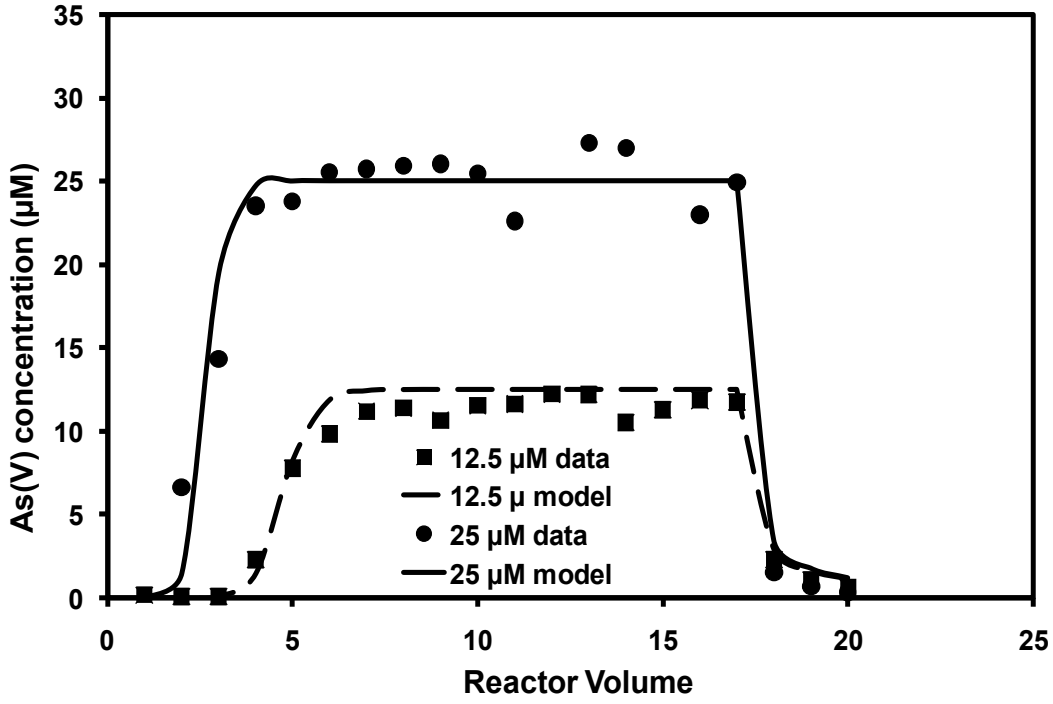

Figure 4-4: Comparison of PHREEQCI predictions and SSER experimental data for effect of varying initial arsenate concentration for As(V) = 12.5 µM and 25 µM (pH = 4, I = 0.01 M).

It can be seen from the Figure that the model predictions closely matched the experimental breakthroughs and overall trends for both concentration values. The R^2 values were 0.96 and 0.88 for 12.5 µM and 25 µM data, respectively. Surface complexation models fail to give good predictions when the concentration is at or above surface saturation (Dzombak and Morel, 1990). The SCM model for Sand-A gave good predictions since model development was done using measured site densities.

4.3.4 Studying arsenate transport in a multiple sequential equilibration reactor

Finally, we conducted a sequential equilibration reactor experiment using three batch reactors in series to study equilibrium transport in a multiple sequential equilibration reactor (MSER). The concentration of As(V) in the influent was 1.25 μM and pH was 7. The solid/solution ratio was 1g iron-coated sand/L and ionic strength was 0.01M. Each sequential-equilibration-cycle consisted of equilibrating the sand with 100 ml (one RV) of arsenate solution and transferring the equilibrated adsorbate to next reactor. We first introduced fresh arsenate stock solution into the first reactor. The system was allowed to equilibrate; then, the effluent from first reactor was transferred to the second reactor and the second reactor effluent was transferred to the third reactor, after equilibration. After equilibration, the effluent from the third reactor was analyzed for arsenic concentration. During first phase of this experiment, a total of fourteen sequential-equilibration-cycles (14 RVs) of arsenic-contaminated water were passed through the system. Later, during the second phase of the experiment, four sequential-equilibration-cycles (4 RVs) of clean DI water (at pH 7 and I=0.01M) were flushed through the system. The observed breakthrough data (arsenic levels measured in the effluent from the third reactor) are shown in Figure 4-5 below. We used the SCM model for Sand-A incorporated within PHREEQCI code to make predictions for this multiple sequential equilibration reactor (MSER) system and the model results are also shown in the Figure. It can be seen from Figure 3-5 that the model was able to predict the breakthrough profiles and overall trends well for MSER experiment. The R^2 value was 0.89, indicating good match between the experimental data and model predictions.

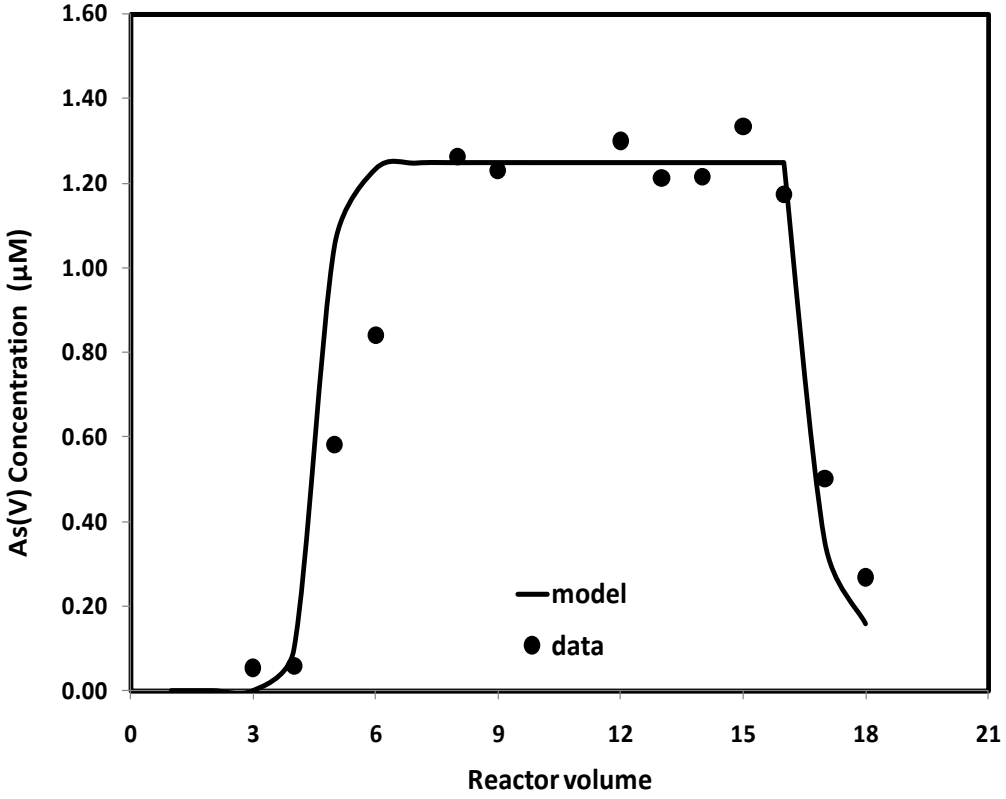

Figure 4-5 : Comparison of PHREEQCI predictions and experimental data for multiple sequential equilibration reactor (MSER) experiment data with three reactors in series using 1g/L of the Sand-A and 1.25 µM As(V) solution (pH = 7, I = 0.01 M).

4.4 Discussion

Overall, the surface complexation model implemented within PHREEQCI advection block was able to provide good predictions for the wide range of experiments conducted under different solid/solution ratios, pHs and arsenate concentrations. The SCM-coupled transport code was able to simulate both SSER and MSER experiments.

We attribute the robustness of the model to predict under a range of conditions, to the use of actual measured site density, without assuming an arbitrary theoretical site density value. Goldberg (1991) noted that site density is the most important and sensitive parameter in surface complexation models. Average of R^2 values of predictions, over of all our experiments, was 0.91. As expected, the predicted (and observed) breakthrough time in the experiments was proportional to the solid/solution ratio. When the solid/solution ratio was doubled, the breakthrough time nearly doubled. Also, when the pH increased, the breakthrough time decreased. This is because arsenate adsorption is strongest around pH4 and reduces with increase in pH (Dixit and Hering, 2003) .

When we use computer models for simulating column experiments involving equilibrium geochemical reactions, there is an inherent uncertainty whether the results were influenced by kinetic effects or not. This is because column experiments usually do not provide sufficient residence time for geochemical reactions to reach equilibrium. For example, a typical column with characteristic dimensions of 1 cm diameter and 10 cm length, porosity of 0.3, and supporting a relatively low flow rate of 0.5 ml/ min would have a residence time of 5 minutes. To obtain a residence time of 24 hours, we need to pump the influent at an extremely low flow rate of 0.00164 ml/ min, which will be difficult to achieve and control. Whereas, most adsorption reactions on metal oxides have equilibration time ranging from hours to days (Manning and Goldberg, 1996; Raven *et al.*, 1998; Khaodhiar *et al.*, 2000; Dixit and Hering, 2003). The proposed sequential equilibration reactor experiments (both MSER and SSER systems) offer a practical, cost-effective method to study such equilibrium-controlled reactive transport systems. This

methodology also offers the flexibility to vary experimental conditions such as solid/solution ratio, which cannot be varied in column experiments.

The sequential equilibration reactor experimental setup has the characteristics of a batch experimental setup and provides complete control over the reaction time. Sequential equilibration reactors also resemble column experiments since they provide transport information. The proposed sequential equilibration reactor experimental system can hence be considered as an intermediate-scale experimental setup between batch and column experiments. When there are serious discrepancies between batch and column experiments [for example: (Barnett *et al.*, 2000)] , Sequential Equilibrium Reactor experiments can be used to isolate and investigate the underlying causes of the differences.

Sequential equilibration reactors can also be used to conduct feasibility studies to investigate the effectiveness of remediation strategies that use sorbents and/or liquid amendments that involve geochemical reactions. Currently, there are no suitable laboratory-scale testing procedures available for evaluating the feasibility of remediation strategies that employ chemical processes involving geochemical equilibrium reactions. The SSER and MSER experimental setups can be used to test such remediation strategies and the results from these studies can be used to calibrate reactive transport codes, which can then be used to simulate large-scale remediation of the plumes at the field scale. Both SSER and MSER experiments also allow us to easily vary the solid/solution ratio and

other treatment variables and hence can be used to design optimized remediation strategies.

One of the disadvantages of the proposed sequential equilibration reactor system is that dispersion is not accounted for in these experiments. However, dispersion can be measured independently from tracer experiments. The measured dispersion can then be integrated into reactive transport models to account for the dispersive mixing.

4.5 Conclusions

In this study we have demonstrated the use of a novel sequential equilibration reactor experimental setup to study equilibrium geochemical transport. The experimental system uses multiple batch reactors in series, operated in a sequential fashion, which directly mimic one-dimensional numerical grids used by geochemical equilibrium transport codes. Seven SSER experiments and one MSER experiment (using three reactors) were conducted to generate datasets for equilibrium-controlled transport of arsenate on iron-coated sand at different pH, solid/solution ratio, and initial arsenate concentration levels. A previously developed surface complexation model was integrated within PHREEQCI and it was able to make good predictions (average R^2 =0.91) without any parameter adjustment.

The proposed sequential equilibration reactor system is an alternative, cost-effective approach for studying equilibrium-controlled reactive transport problems. The experimental system can be used for validating numerical equilibrium reactive transport codes for a specific contaminant of interest. It can also be used for conducting laboratory

feasibility studies of remediation systems involving equilibrium geochemical conditions. Future studies in this area also have the potential to bridge the gap between batch and column experiments and could help shed some light on the significant scaling issues associated with reactive transport problems.

CHAPTER 5

A SEMI-ANALYTICAL SOLUTION FOR REACTIVE TRANSPORT IN SEQUENTIAL EQUILIBRATION REACTORS USING A NOVEL UNIFIED LANGMUIR-FREUNDLICH ISOTHERM

5.1 Introduction

Equilibrium geochemical reactions play a major role in determining the fate and transport of groundwater contaminants. Typical column experiments fail to capture equilibrium geochemical reactive transport behavior due to low residence times (typically in minutes), presence of preferential flow paths, and influence of non-linear reaction kinetics (Barnett *et al.*, 2000; Jeppu *et al.*, 2011). In Chapter 3, we proposed a novel sequential equilibration reactor (SER) experimental system which can be used to study equilibrium geochemical reactive transport using a series of batch reactors. The experimental setup conceptually mimics a one-dimensional numerical grid commonly assumed in reactive transport codes such as PHT3D and PHREEQCI (Clarlton and Parkhurst, 2002). A conceptual diagram of two types of sequential equilibration reactor systems used in this study are given in Figure 4-1 in Chapter 4. As shown in the top part of the figure, a multiple sequential equilibration reactor (MSER) system consists of a

number of batch reactors equilibrating in series. A single sequential equilibration reactor (SSER) consists of a single reactor treating fresh batch of influent several times. In Chapter 4, we used a transport coupled surface complexation models incorporated in PHREEQCI to simulate SER experiments. However, this approach is more complex and time consuming. Mathematical solutions can be derived from mass balance for SER systems. Currently there are no mathematical solutions for SER systems available in literature. Such mathematical solutions have are less complex and easier to use compared to surface complexation coupled transport codes. These semi-analytical models can also be used to validate SER experiments and surface complexation coupled transport codes. In this Chapter we develop a semi-analytical solution to model the transport in SER experiments.

In this Chapter we also developed a novel Unified Langmuir-Freundlich adsorption isotherm to describe adsorption at different pH values and used it in the semi-analytical solution. The most widely used isotherms for modeling adsorption of geochemical species on iron-oxides and iron-oxyhydroxides are Langmuir isotherm (Hingston, 1970; Raven *et al.*, 1998; Thirunavukkarasu *et al.*, 2001; Thirunavukkarasu *et al.*, 2003; Kundu and Gupta, 2006) and Freundlich isotherm (Raven *et al.*, 1998; Lin and Wu, 2001; Badruzzaman *et al.*, 2004). Other isotherms that are occasionally used include Radke-Praunitz isotherm, Dubinin–Radushkevich (D–R) isotherm, Toth isotherm, and Temkin isotherm (Rau *et al.*, 2003; Kundu and Gupta, 2006).

The Langmuir-Freundlich isotherm, also known as the Sips's equation, is another versatile adsorption isotherm that has the potential to simulate both Langmuir and

Freundlich behaviors (Sips, 1948; Sips, 1950; Nahm *et al.*, 1977). Rau et al. (2003) studied arsenate adsorption on metal-oxides using different types of adsorption isotherms and concluded that Langmuir-Freundlich isotherms best described the data. The Langmuir-Freundlich isotherm has also been successfully used to model adsorption by molecularly-imprinted polymers (Umpleby *et al.*, 2001; Turiel *et al.*, 2003)

Adsorption isotherm datasets are typically developed for a single pH value. Hence, most adsorption isotherm models are valid only at the pH it was developed and hence it cannot be used to predict transport scenarios involving pH variations. A few researchers have attempted to use adsorption isotherm equations to model adsorption at different pH values. Anderson et al. (1976) used the Langmuir isotherm to predict arsenate adsorption at different pH values. Hingston et al. (1971) used a modified Langmuir isotherm to model competitive adsorption of arsenate in presence of phosphate at different pH values. However, both these studies fitted different maximum adsorption capacities and Langmuir constants at different pH values. They have not presented a unified model for all pH values. Yu et al. (1999) used a modified Langmuir isotherm to describe pH-dependent bio-sorption of heavy metals on marine algae. A similar modified Langmuir isotherm has been used to model arsenic adsorption on amorphous iron oxide (Hsia *et al.*, 1992). However, these studies involve graphical estimation of reaction equilibrium constant and assumed different adsorption capacities at different pH. Hence, such Langmuir isotherms have not been widely used.

Currently, the effect of pH variation on sorption behavior of inorganic contaminants onto metal-oxides is primarily being modeled using surface complexation

models (Westall and Hohl, 1980; Davis and Kent, 1990; Dzombak and Morel, 1990). This numerical approach is intricate and time consuming compared to simpler analytical isotherm models such as Langmuir isotherm and Freundlich isotherm. However, isotherm models are typically restricted to a single pH value. Hence, there is a need for a unified approach which can help develop isotherm models that describe the pH effects on adsorption. Such an isotherm could be easily incorporated into large-scale groundwater contaminant transport codes such as MT3DMS (Zheng and Wang, 1999) and RT3D (Clement *et al.*, 1998) to predict pH dependent adsorption effects.

The objectives of this chapter are (i) to develop a semi-analytical solution to model equilibrium transport in sequential equilibration reactor systems, (ii) to develop an unified adsorption isotherm, which can predict adsorption at different pH values, and use the unified adsorption isotherm in the semi-analytical solution, and (iii) to compare the semi-analytical-model based predictions against experimental datasets for arsenic(V) adsorption on iron-coated sands under a wide range of pH, solid/solution ratio and initial concentrations levels.

5.2 Materials and methods

5.2.1 Experimental methods

The procedure used for synthesizing the iron (goethite) coated sands is described in detail in Chapter 3 and our earlier publications (Cheng *et al.*, 2004; Loganathan *et al.*, 2009; Jeppu *et al.*, 2010). Iron-coated sand, identified as Sand-D in Chapter 3 was used

for experiments in this study. The characteristics of Sand-D are summarized in Table 5-1.

Table 5-2: Characteristics of Sand-D

Parameter	Value
Iron content (mg Fe/ g sand)	3.15
Surface area (m^2/ g sand)	0.57
Surface site density (sites/nm^2)	1.38

Arsenic solutions were prepared from a 100 ppm stock solution, which was made by dissolving 0.416 grams of reagent grade $Na_2HAsO_4.7H_2O$ in 1 liter of deionized water. The ionic strengths of all the solutions were adjusted using sodium nitrate to 0.01 M. The pH of the solution was adjusted using either NaOH or HNO_3 and the value was measured using an Orion (model 250A) pH meter which was calibrated using commercial pH 4.0, 7.0, and 10 buffers. The average temperature was set at $25^0C \pm 2^0C$ for all experiments. All the sequential equilibration reactor experiments were done by equilibrating 100 ml (defined as one reactor volume or RV) of arsenate solution with iron-coated sand in a tumbling shaker. The supernatant solution was centrifuged and filtered through 0.45 μm Teflon membrane filter (Millipore), which was fitted to a disposable syringe. The solutions were analyzed for total arsenic using a graphite furnace atomic absorption spectrophotometer (GFAAS; Perkin-Elmer 5100 PC) which has a detection limit of 5 $\mu g\ L^{-1}$ total arsenic.

5.2.2 The Langmuir-Freundlich isotherm

In this study, the Langmuir-Freundlich (LF) isotherm equation (Sips, 1948; Sips, 1950; Nahm *et al.*, 1977) was used to model arsenic(V) adsorption on iron-coated sand in batch adsorption isotherm experiments. The LF isotherm can written as:

$$q = K_{max} \frac{(K_1 C)^n}{(K_1 C)^n + 1} \tag{5-1}$$

where,

q is the amount of As(V) adsorbed on the sand at equilibrium (mg As(V)/ g sand)

K_{max} is the maximum adsorption capacity (mg As(V)/ g sand)

C is the aqueous phase concentration at equilibrium (μmoles/ L)

K_1 is the affinity constant for adsorption

n is the heterogeneity index

When *n* is between 0 and 1, the sorbant is assumed to be heterogeneous (Umpleby *et al.*, 2001; Turiel *et al.*, 2003). For a homogeneous material, *n* is set to 1, and the Langmuir-Freundlich isotherm reduces to the standard Langmuir isotherm below:

$$q = K_{max} \frac{C}{K_S + C} \tag{5-2}$$

where,

$K_S = 1/K_1$

Also, when C or K_1 approaches 0, the value of denominator in the LF isotherm (see Equation 5-1), approaches 1, and the LF isotherm approaches the Freundlich isotherm (Umpleby *et al.*, 2001; Turiel *et al.*, 2003):

$$q = KC^n \tag{5-3}$$

Where,

$K = (K_{max}K_1^n)$.

When both n = 1 and K_1 is very small, the denominator in Equation-1 approaches unity and the LF isotherm reduces to the linear adsorption isotherm:

$$q = K_d\ C \tag{5-4}$$

Where, $K_d = K_{max}K_1$. Thus, the LF isotherm is a versatile model that can simulate all Langmuir, Freundlich and Linear isotherm behaviors that are commonly observed in groundwater systems.

5.2.3 Design of sequential equilibration reactor experiments

The design of sequential equilibration reactor experiments has been discussed in detail in the previous chapter (Section 4.3.2). A conceptual representation of the single sequential equilibration reactors and multiple sequential equilibration reactors is shown in Figure 4-1. Single sequential equilibration reactor (SSER) experiments required less time and effort; hence we conducted several SSER experiments to produce experimental data to validate the adsorption models under equilibrium reactive transport conditions. The SSER experiments were similar to experiments conducted in Chapter 4, but were

conducted using a different sand, Sand-D. Also, a synthetic MSER experimental dataset, which employed five reactors in series, was simulated using PHREEQCI and the results were compared against the new analytical solution validate the analytical solution.

5.2.4 Development of a semi-analytical solution for modeling one-dimensional advection-dominated equilibrium transport data

A mathematical method to calculate the concentration of the effluent concentration from an advection-dominated grid cell (or a reactor) can be derived using a mass balance analysis. Consider a grid cell or a single sequential equilibration reactor, as shown in Figure 5-1.

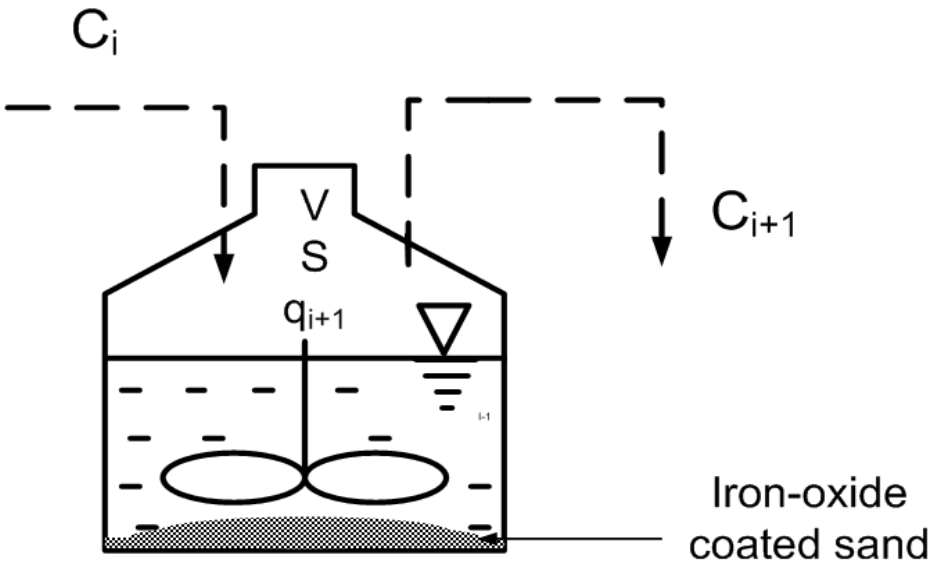

Figure 5-1 : Conceptual representation of a single sequential equilibration reactor (SSER)

The figure uses the following notations**:**

C_{inf} is the influent sorbate [arsenic(V)] concentration before equilibrium at step "i" (mg/L)

C_{i+1} is the equilibrated concentration of the sorbate in the reactor at step "i+1" (mg/L)

q_i is the initial solid phase (iron-coated sand) concentration of arsenic in the reactor (mg/g) at step "i"

q_{i+1} is the final equilibrium solid phase concentration in the reactor (mg/g) at setp "i+1"

V as the reactor volume (L), and

S is the sorbent (sand) concentration (g/L).

A mass balance analysis of the sorbate in the reactor before and after equilibrium can be written as:

$$C_i V + q_i SV = C_{i+1} V + q_{i+1} SV \tag{5-5}$$

Which can be simplified as,

$$C_{i+1} = C_{inf} - S(q_{i+1} - q_i) \tag{5-6}$$

Using the Langmuir-Freundlich equation (Eqn 5-1) in the above expression, C_{i+1} can be found by numerically solving the following equation:

$$C_{i+1} = C_{inf} - SK_{max}\left[\frac{(K_1 C_{i+1})^n}{(K_1 C_{i+1})^n + 1} - \frac{(K_1 C_i)^n}{(K_1 C_i)^n + 1}\right] \tag{5-7}$$

The above equation can be represented as a nonlinear function:

$$f(C_{i+1}) = C_{i+1} - C_{inf} + SK_{max}\left[\frac{(K_1 C_{i+1})^n}{(K_1 C_{i+1})^n + 1} - \frac{(K_1 C_i)^n}{(K_1 C_i)^n + 1}\right] = 0 \qquad (5\text{-}8)$$

We can use the Newton-Raphson method to obtain the roots of the non-linear equation (5-8). For a k^{th} iteration, the general Newton-Raphson formula can be written as :

$$C_{k+1} = C_k - \frac{f(C_k)}{f'(C_k)} \qquad (5\text{-}9)$$

where,

$$f'(C_k) = 1 + SK_{max}\frac{(K_1 C_k)^n C_k n}{\left[(K_1 C_k)^n + 1\right]^2} \qquad (5\text{-}10)$$

By solving for C_{i+1} using the above Newton-Raphson equation, we can evaluate the concentration of the equilibrated effluent. The above procedure can be repeated sequentially to get the effluent concentration after each equilibration step in a given reactor or a node. When there are n nodes linked in series, the effluent from one node can be used as the influent to the next node, and the mathematical calculations can be repeated in a sequential fashion to obtain the effluent breakthrough concentrations from the last node.

5.2.5 Geochemical equilibrium transport modeling using PHREEQCI

A scalable surface complexation modeling (SCM) framework, discussed in Chapter 3, was used to simulate the arsenic surface complexation reactions. Reaction equations and the model parameters used are summarized in Table 5-2. These reaction equations and constants were incorporated into PHREEQCI to make predictions. The advection block available in PHREEQCI was used to simulate the geochemistry-coupled advective transport. The difference between model predictions and experimental data was quantified using the R^2 value for our predictions defined by the equation:

$$R^2 = 1 - \left[\frac{\sum_{i=1,n} (C_i - f_i)^2}{\sum_{i=1,n} (C_i - C_m)^2} \right] \qquad (5\text{-}11)$$

Where, C_i is the measured aqueous concentration, f_i is the model predicted aqueous concentration, and C_m is the mean of the observed aqueous concentration data.

Table 5-3: Aqueous protonation constants and intrinsic surface complexation constants used for the goethite-coated sand, Sand-D, at a surface site density of 1.38 sites/nm^2 and at zero ionic-strength

Reactions			**Log K** (I=0 and Γ=1.38 sites/ nm^2)	
Protonation reactions for As(V)				
H_3AsO_4		= $H_2AsO_4^- + H^+$	-2.24	(1)
H_3AsO_4		= $HAsO_4^{2-} + 2H^+$	-9.20	(2)
H_3AsO_4		= $AsO_4^{3-} + 3H^+$	-20.70	(3)
Surface hydrolysis reactions of the iron-oxide coated				
>FeOH	$+ H^+$	= > $FeOH_2^+$	7.32	(4)
>FeOH		= > $FeO^- + H^+$	-9.42	(5)
Surface complexation reactions				
>FeOH	+	= >FeH_2AsO_4 + H_2O	11.25	(6)
>FeOH	+	= >$FeHAsO_4^-$ + H_2O + H^+	5.86	(7)
>FeOH	+	= >$FeAsO_4^{2-}$ + H_2O + $2H^+$	-0.45	(8)
Surface site density =1.38 sites/nm^2, Surface area=0.57 m^2/ g				

5.3 Results

5.3.1 Development of a Unified Langmuir-Freundlich isotherm to model pH dependent adsorption

We first used the previously developed surface complexation model, summarized in Table 5-2, to simulate a series of adsorption isotherms datasets at different pH as shown in Figure 5-2. We then fitted the simulated adsorption isotherm datasets at pH values 4, 5.5, 7, 8.5 and 10, using the LF isotherm equation. The fitted adsorption isotherms are shown in Figure 5-2 along with experimental adsorption isotherm at pH 4 from our earlier study (Chapter 3, Figure 3-3)

The LF model parameters were fitted using the generalized reduced gradient algorithm available within the EXCEL solver. The LF constants were solved for by simultaneously minimizing the SQE (sum of squared errors) of the fits at five different pHs. We hypothesized that the maximum adsorption capacity and the heterogeneity index are independent of pH. So the values of K_{max} (maximum adsorption capacity, which corresponds to total number of sites) and n (heterogeneity index) are assumed to be constant irrespective of the pH value. So the value of K_{max} and n were optimized as constant for the entire pH range. Only the affinity constant (K_1) was allowed to change with pH, and K_1 value was separately fitted to each isotherm. The fitted values of the LF isotherm parameters are given in Table 5-3. The R^2 values of the fitted curves were 0.994, 0.940, 0.813, 0.974, 0.974 and 0.894 at pH 4, 5.5, 7, 8.5 and 10, respectively. The results suggest that the LF isotherm can be used to fit adsorption isotherm data observed at different pH values.

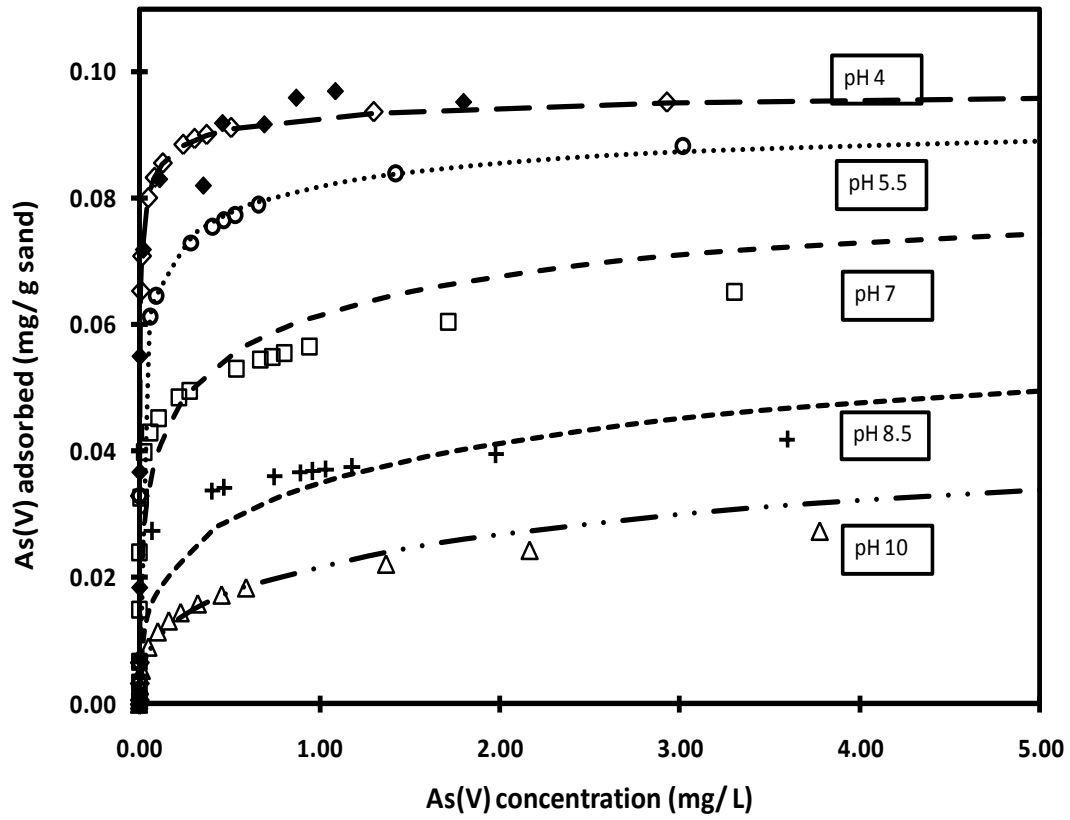

Figure 5-2 : Adsorption isotherms from surface complexation model at different pH values and corresponding LF model fits. Also shown is experimental data at pH 4. Closed symbols represent experimental data. Open symbols represent surface complexation model generated data. Lines represent LF model predictions.

Table 5-4: Values of the fitted Langmuir-Freundlich parameters

pH	K_{max}(mg/g)	N	K_s (μM)
4	0.1	0.387	769
5.5	0.1	0.387	50.9
7	0.1	0.387	3.35
8.5	0.1	0.387	0.200
10	0.1	0.387	0.0371

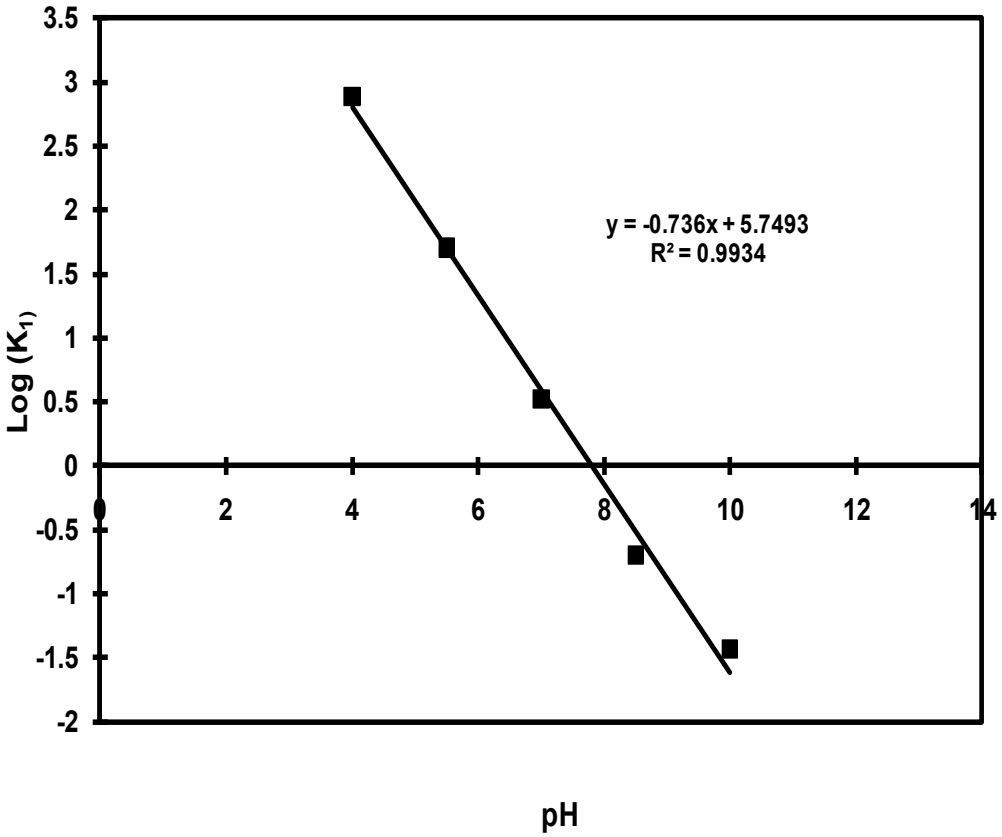

Figure 5-3: Plot of pH Vs LF model parameter K_1

Since adsorption affinity changes with pH in a logarithmical relationship, as seen in Figure 5-2, the affinity constant K_1 can be expressed as a function of pH as $K_1(pH)$. We can then write the Langmuir-Freundlich equation 5-1 in its general form as:

$$q = K_{max} \frac{[CK_1(pH)]^n}{[CK_1(pH)]^n + 1} \tag{5-12}$$

The above equation is identified hereafter as the Unified Langmuir-Freundlich (ULF) model, and will be used to describe variations in adsorption at different pH values using a single set of isotherm-model constants.

We plotted Log K_1 Vs pH to determine the relationship between K_1 and pH as shown in Figure 5-3. The data indicated that Log K_1 varies linearly with pH. The R^2 value of the linear fit was 0.996 and the equation is:

$$K_1 = 10^{5.705 - 0.722pH} \tag{5-13}$$

Inserting the above expression (5-13) for affinity constant K_1 into the ULF model equation (5-12) allowed us to develop an expression that can model pH effects.

The ULF model for arsenate adsorption on iron-coated sand system can be written as:

$$q = K_{max} \frac{(C10^{5.705-0.722pH})^n}{(C10^{5.705-0.722pH})^n + 1} \quad (5\text{-}14)$$

Which is of the form:

$$q = K_{max} \frac{(C10^{b-apH})^n}{(C10^{b-apH})^n + 1} \quad (5\text{-}15)$$

The constants a and b can be obtained from Log K_1 Vs pH plot as shown in Figure 5-3. The ULF model in equation (5-14) was incorporated in the semi-analytical solution (Equation 5-7) to solve for the equilibrium arsenate concentrations in our sequential equilibration reactor experiments explained in later sections. The predictions from the ULF equation based semi-analytical solution were compared with experimental data.

5.3.2 Modeling transport in single sequential equilibration reactor experiments using the semi-analytical solution coupled with the ULF model

In order to test the proposed semi-analytical solution under different transport simulations involving a wide range of pH, solid/solution ratio and concentrations conditions, we conducted multiple SSER experiments. The data from the SSER experiments were used to further test the predictive capability of our model under equilibrium transport conditions.

5.3.2.1 Modeling the effect of variations in solid/solution ratios

To test the ULF-model based semi-analytical solution at different solid/solution ratios, we conducted SSER experiments at three different solid/solution ratios of 50 g/L, 100 g/L and 150 g/L. The concentration of As (V) in the influent was fixed at 12.5 μM at a pH value of 4 and ionic strength 0.01M. In each sequential-equilibration-cycle the sand was equilibrated with 100 ml (one RV) of arsenate solution for 24 hours. The total experiment consisted of equilibration with of the iron-coated sand with 25 RVs of fresh 12.5 μM As(V) solution, followed by flushing with 4 RVs of deionized water of pH 4 and ionic strength 0.01M. The ULF-mode based semi-analytical solution was used to make predictions for the experimental system. The model parameters for the Unified Langmuir-Freundlich model at pH 4 are given in Table 5-3. The semi-analytical model results along with experimental data are shown in Figure 5-4. The breakthroughs were at 5, 10 and 15 pore volumes as predicted by the models. It can be seen from the figure that the model predicted the overall trend observed in the experimental system. The R^2 values were 0.9690, 0.9357, 0.9214 for the semi-analytical models at 50 g/L, 100 g/L and 150 g/L, respectively, which indicates a good fit. Arsenate concentration in the effluent decreased rapidly when the system was flushed with deionized water as predicted by the models.

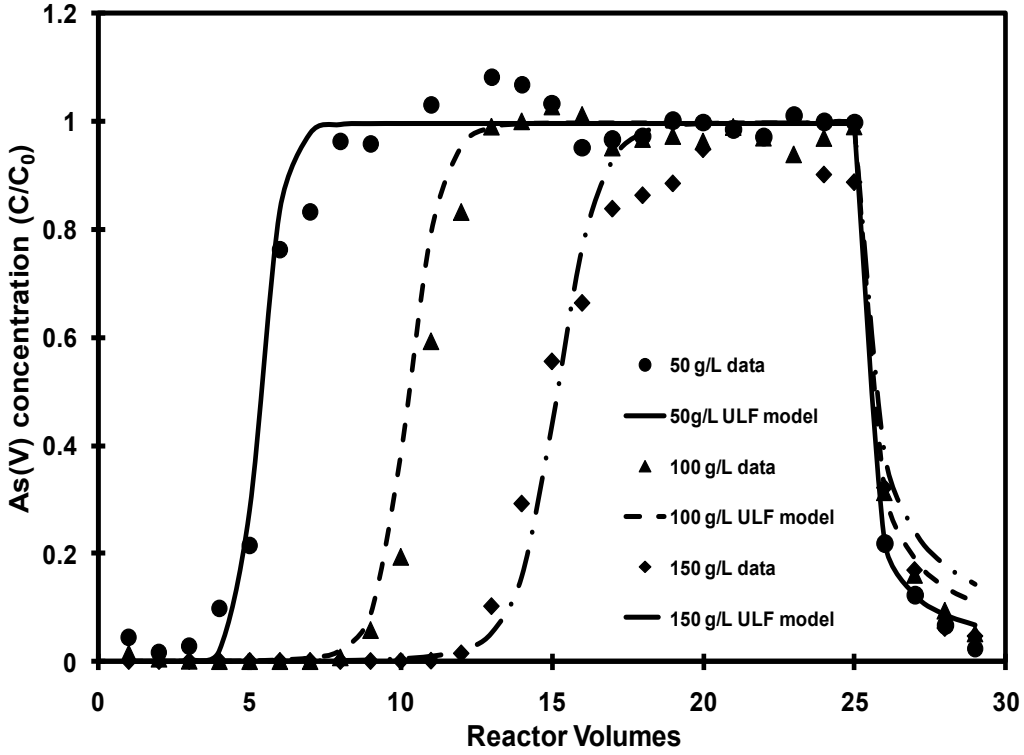

Figure 5-4: Comparison of ULF model predictions with SSER experimental data for effect of varying solid/solution ratio at 12.5 μM As(V) (pH = 4, I = 0.01 M)

5.3.2.2 Modeling the effect of variations in pH

To test the semi-analytical solution based on the ULF model under different pH conditions, we conducted SSER experiments at following three pH values: 4, 7 and 10. The concentration of As (V) in the influent was 12.5 μM with ionic strength 0.01M. In each sequential-equilibration-cycle, the sorbent (50 g/L of Sand-D) was equilibrated with 100 ml (one RV) of arsenate solution for 24 hours in a tumbling shaker. The total experiment consisted of equilibrating the iron-coated sand with 17 RVs of fresh 12.5 μM As(V) solution, followed by flushing with 3 RVs of deionized water at the same pH. Figure 5-5 show the output As(V) concentration from this SSER system. The ULF

model based semi-analytical model was used to make predictions for this experimental system and the results are also shown in the figure. The Unified Langmuir-Freundlich model parameters are given in Table 5-3 for the different pH values used. It can be seen from the figure that at different pH values the model predictions closely matched the breakthroughs and overall trend. The R^2 values were 0.9125, 0.9441, 0.8211 for the semi-analytical models at pH 4, 7 and 10, respectively. Since arsenate adsorption is strong at low pH values, the pH 4 system treated the maximum number of RVs, followed by pH-7 and pH-4 systems, respectively.

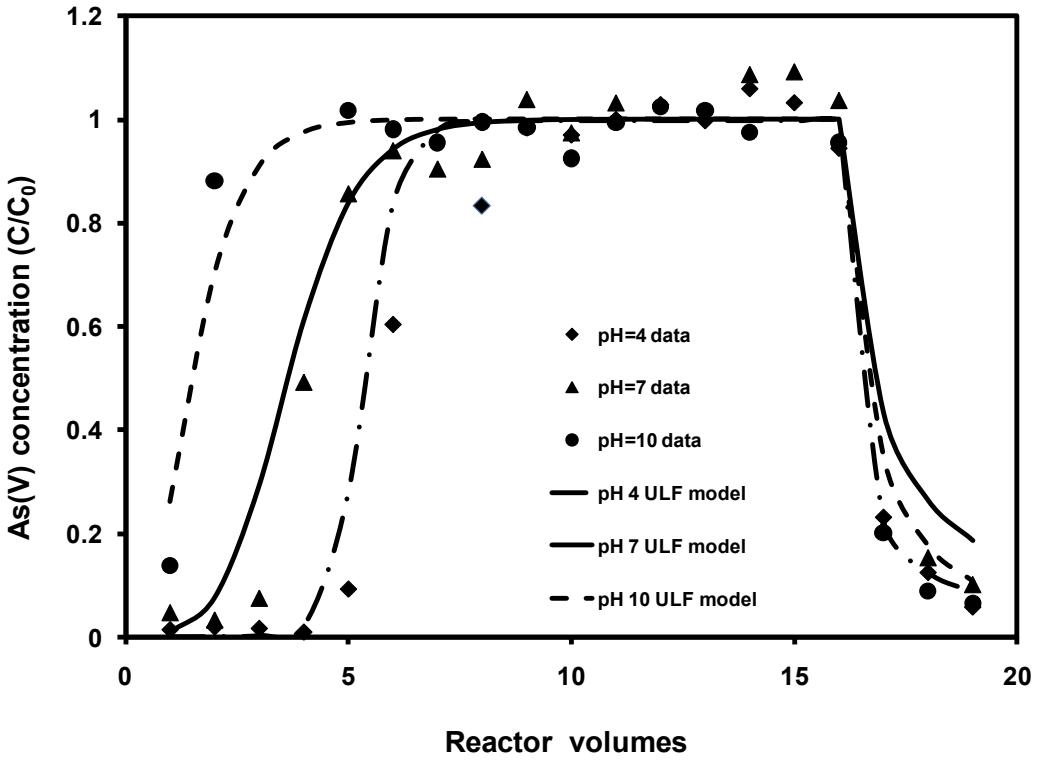

Figure 5-5: Comparison of ULF model predictions with experimental data for effect of pH for As(V) =12.5 uM ppm (I=0.01M)

5.3.2.3 Modeling the effect of variations in initial arsenate concentration

Further, we wanted to test the semi-analytical solution based on the ULF model at different initial arsenate concentrations. We conducted sorption experiments using 6.6 μM, 12.5 μM and 25 μM as initial arsenate concentration. The pH was fixed at 4 and ionic strength at 0.01M. In each sequential-equilibration-cycle cycle, the sorbent (50 g/L of Sand-D) was equilibrated with 100 ml (one RV) of arsenate solution for 24 hours. The experimental steps included equilibration of 17 RVs of fresh As(V) solution with the sand, followed by flushing with 3 RVs of deionized water at the same pH and ionic strength. Figure 5-6 shows the output As(V) breakthrough data profile for this SSER system. The arsenate concentrations in the figure are normalized to 12.5 μM arsenate concentration. The ULF model based semi-analytical model was used to make predictions and the results are also shown in the figure. It can be seen from the figure that the model predictions closely matched the experimental breakthroughs and overall trends in the data. The R^2 values were 0.8716, 0.8914, 0.9650 for the semi-analytical model at 6.6 μM, 12.5 μM and 25 μM of initial arsenate concentrations respectively.

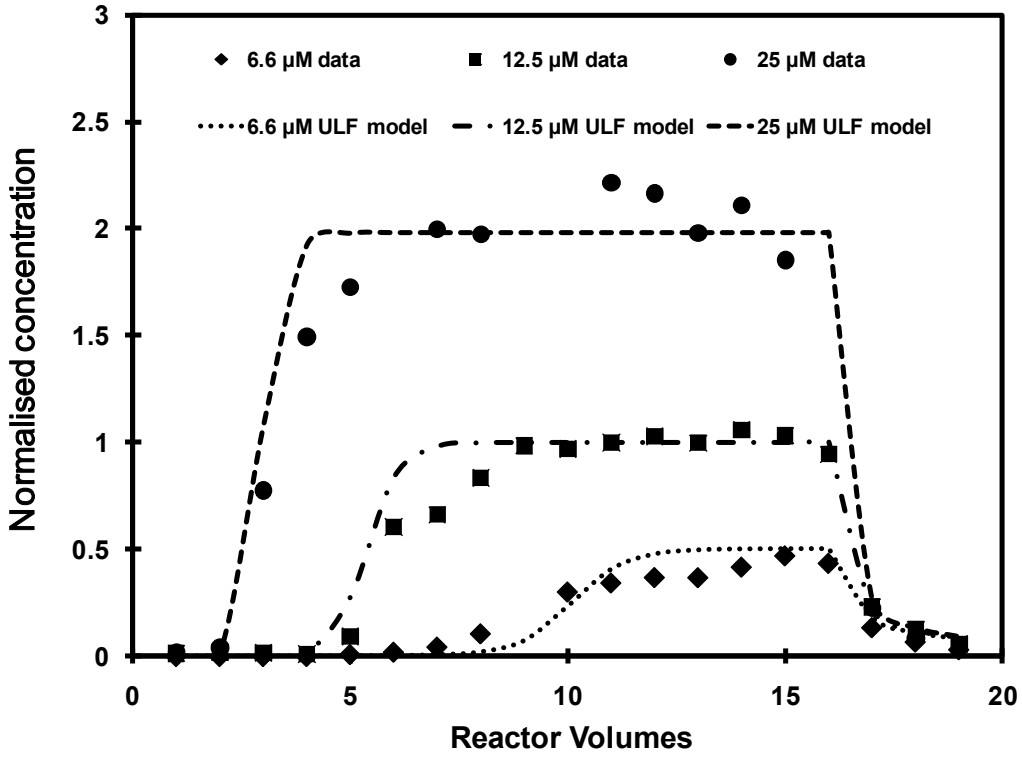

Figure 5-6 : Comparison of ULF model predictions and ScBR experimental data for effect of varying initial arsenate concentration of As(V) = 6.6 µM, 12.5 µM and 25 µM (pH = 4, I = 0.01 M). Arsenate concentration values are normalized to 12.5 µM.

5.3.3 Comparison of the predictions from the semi-analytical model with PREEQCI model predictions

We compared the predictions from the semi-analytical solution with the predictions from PHREEQCI at different pH values to evaluate whether the semi-analytical model could match predictions from a detailed surface-complexation model based predictions. The predictions from the semi-analytical model and the PHREEQCI

model at different pH are compared in Figure 5-7. Both models were able to predict the breakthrough at different pH values satisfactorily.

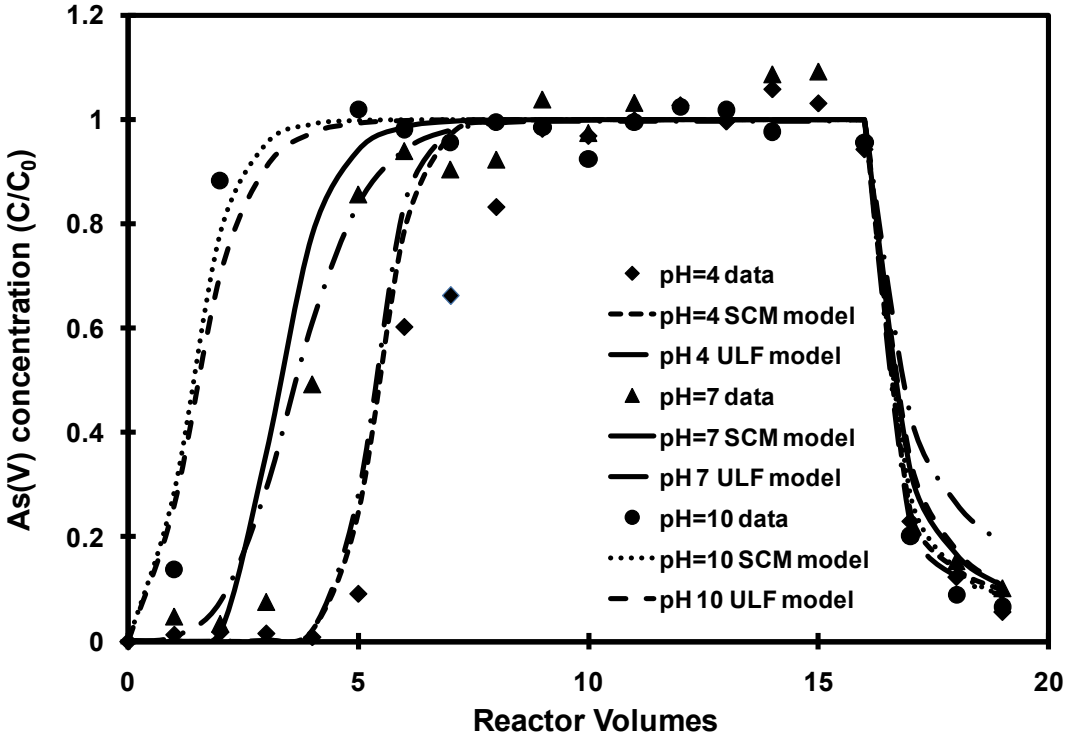

Figure 5-7 : Comparison of ULF model predictions with PHREEQCI predictions and experimental data at different pHs (As(V) =12.5 uM ppm, I = 0.01 M)

The R^2 values were 0.947, 0.930, 0.938 for the PHREEQCI model and 0.944, 0.947 and 0.932 for the semi-analytical models. This indicates that the proposed ULF model based semi-analytical solution could give predictions as good as surface complexation model based PHREEQCI predictions.

The mechanistic surface complexation models are much more complex than the proposed ULF model. The surface complexation models are also highly system dependent (Goldberg, 1991). The surface complexation model uses 10 parameters (see

Table 5-2), which are: 8 equilibrium constants, site density and surface area. Whereas, the ULF model required only three parameters and provided equally good predictions, as indicated by R^2 values. Also, due to the large number of parameters and complexity, the surface complexation models are difficult to incorporate into standard reactive transport codes such as RT3D(Clement, 1997) and MT3DMS (Zheng and Wang, 1999). The Unified Langmuir-Freundlich model presented here however can be easily incorporated into transport codes to predict adsorption under varying pH values.

5.3.4 Comparison of the semi-analytical model with PHREEQCI models for a synthetic five reactor sequential equilibration reactor experiment

Finally, we tested whether the semi-analytical solution based on the ULF model could provide good predictions for a one-dimensional equilibrium transport system represented by a MSER experiment. We conducted a synthetic numerical experiment using five reactors in series. The initial arsenate concentration was 12.5 μM. The pH was fixed at 4 and ionic strength at 0.01M. Solid/solution ratio was 10 g/L of sand-A. The experimental steps included 20 sequential-equilibration-cycles of treatment with new As(V) solution, followed by flushing with 10 sequential-equilibration-cycles of deionized water at the same pH and ionic strength. Figure 5-8 compares the output As(V) breakthrough predictions profile for this MSER system from semi-analytical model and PHREEQCI. It can be seen from the figure that the semi-analytical model closely matches PHREEQCI in its predictions. The R^2 value of fitting was 0.99 and indicates an excellent match. This shows that the semi-analytical model combined with Unified

Langmuir-Freundlich model can be used for modeling multiple sequential batch reactors using the proposed method.

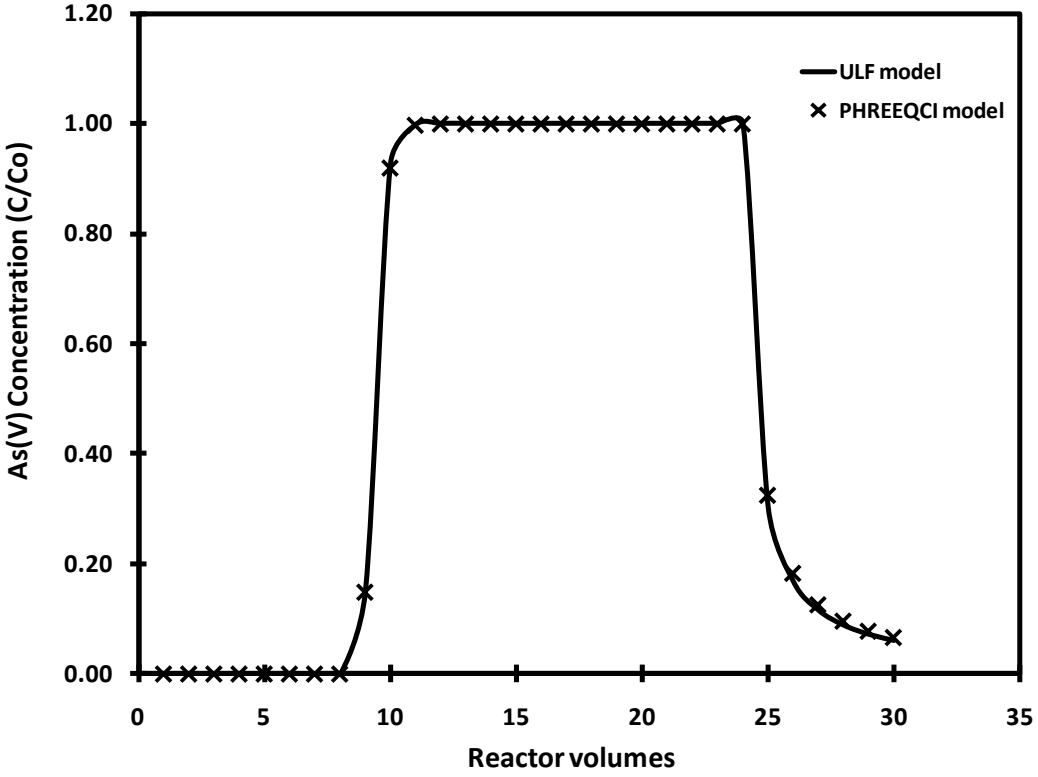

Figure 5-8 : Comparison of ULF model with PHREEQCI model for a five reactor experiment (10 g/L sand in each reactor, pH =4, As(V) =12.5 uM ppm, I = 0.01 M)

5.3.5 Verifying the model predictions using theoretical estimates

The experimental breakthrough curves at pH 4 can also be approximately predicted by calculations using the knowledge of value of maximum adsorption capacity at pH 4. The iron-coated sand can adsorb 0.097 mg arsenate/ g sand and 1000 ml of 12.5 µM As(V) contains 0.94 mg As(V). So, for example, in Figure 5-4, theoretically breakthroughs can be expected to occur approximately at approximately 5, 10, and 15

pore volumes for 50 g/L, 100 g/L and 150 g/L sand, respectively. Also in Figure 5-6 breakthrough can be expected to occur at approximately 2.5, 5 and 10 pore volumes for 6.6, 12.5 μM and 25 μM As(V) solutions, respectively. This is because, 1000 ml of 6.6 μM, 12.5 μM and 25 μM As(V) contain 0.47 mg, 0.94 mg and 1.88 mg As(V), respectively. Thus theoretical calculations confirm the validity of our model predictions.

5.3.6 Using the ULF model for predicting arsenate transport in a column

We designed a hypothetical column experiment to test the predictive capacity of the Unified Langmuir-Freundlich model in column experimental setup. A column of 7 cm length and 1 cm diameter is assumed. The column is filled with Sand-D of bulk density 1600 g/L and porosity of 0.365 as given in Table 5-4. Ionic strength is maintained at 0.01 M during the entire experiment. The hypothetical experiment consisted of three stages. In the first stage, arsenate solution of 13.3 μM (1mg/L) concentration at pH 4 is introduced for 500 pore volumes. In the second stage of the experiment, the influent is switched to an arsenate solution at pH 5 and concentration of 6.67 μM/L for the next 200 pore volumes. Finally, in the third stage of the experiment, the column is flushed with DI water at pH 6 from 300 pore volumes to 1000 pore volumes.

Table 5-5: Column Parameters

Parameter	Value	Units
Bulk density	1600	g/L
Porosity	0.365	–
Flow rate	0.2	ml/min

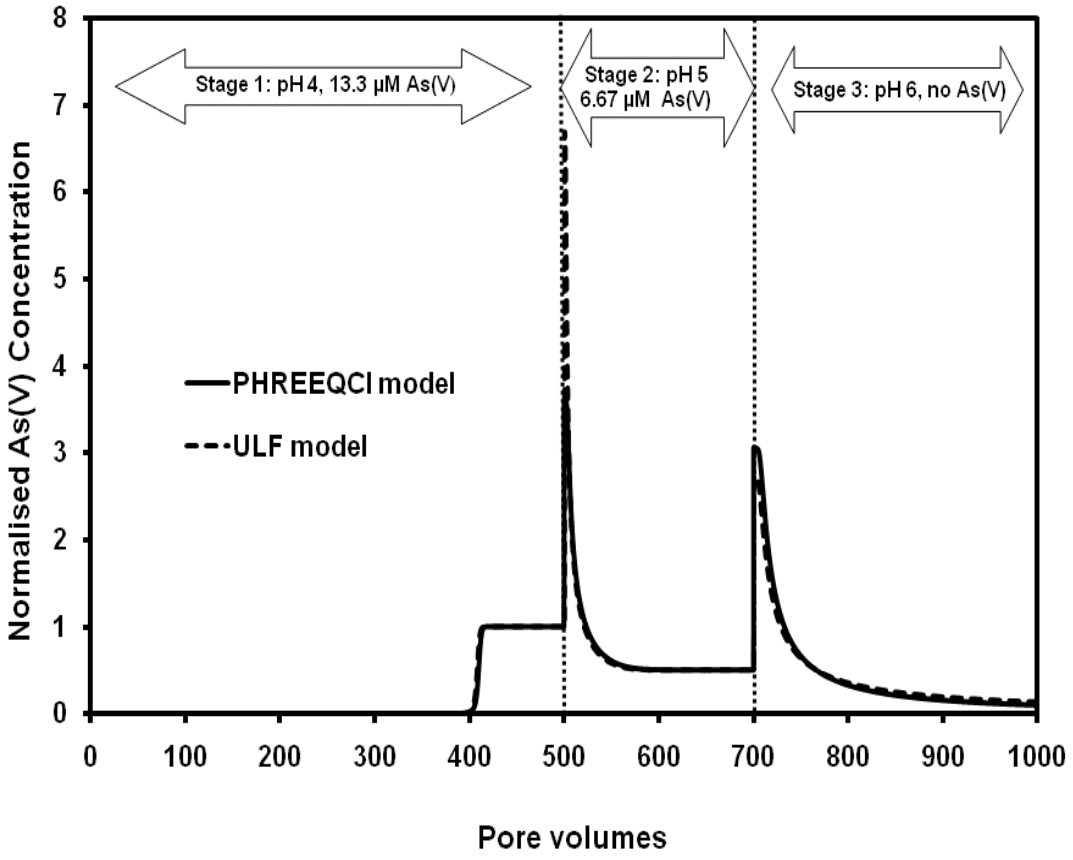

Figure 5-9 : Comparison of ULF model predictions with surface complexation model based PHREEQCI predictions for the iron-coated sand column experiment.

Predictions of the above experiment were conducted using the ULF model and the surface complexation model given in Table 5-2. The ULF model was incorporated in a

one-dimensional transport code (given in Aappendix A), which uses finite difference method for solving the advection-dispersion equation. In a second model, the surface complexation was incorporated in the PHREEQCI code (given in Appendix B). Both these models were used to predict the arsenate transport in the column experiment and the results are compared in Figure 5-9.

The Figure indicates that the ULF isotherm based transport code was able to match the predictions from PHREEQCI code for all the three stages of the column experiment. The model predictions shows high retardation (R~400), which indicates that adsorption by iron-oxides and iron-oxyhydroxides can greatly retard arsenic transport at low pH values. When the pH is changed to 5, there is a sudden release of high concentration of arsenate in the effluent, which suggests that if the pH of influent increases the metal-oxides in subsurface may release high levels of arsenic to groundwater. Similarly, when the pH is changed to 6, there is a sudden release of adsorbed arsenic. This further indicates that even small changes in pH can cause major change in arsenate concentration levels.

Typically, the use of geochemistry-coupled transport codes would take considerable effort and resources than lumped parameter models. For example, the the PHREEQCI code took 407 seconds (6 minutes 47 seconds) to complete, whereas the Unified Langmuir-Freundlich model took only 8 seconds to run. A Dell Inspiron 6000 laptop with Intel Pentium 4 processor of 1.6 GHz speed and a memory of 1 GB RAM was used in the simulation. In another simulation, where a surface-complexation code MICROQL2 (Westall, 1979a) was coupled to a transport routine, the ULF-based code

was around ten times faster. This result shows that using a ULF model can significantly decrease computational time required. This also suggests that computational time for three dimensional reactive transport models could be greatly reduced by using the ULF models.

5.3.7 Use of the ULF model to simulate an existing benchmark problem

The Cederberg problem (Cederberg *et al.*, 1985) is one of the key benchmark problems available in the published literature for validating surface-complexation coupled transport models. We wanted to validate our approach using this benchmark data. First, we developed a Unified Langmuir-Freundlich isotherm to model the isotherms at different pH values as shown in Figure 5-10. The ULF model parameters were obtained by fitting the constants to the surface-complexation model generated data. The fitted Unified Langmuir-Freundlich parameters are given in Table 5-5.

The Unified Langmuir-Freundlich models were able to model the isotherms which were linear in nature. When n =1 and K_1 is very small the Unified Langmuir-Freundlich equation becomes linear isotherms. We fixed the value of n as 1 the K_1 and K_{max} values. As in the case of arsenate, the Log of K_1values varied linearly with pH as indicated by the Figure 5-11**.**

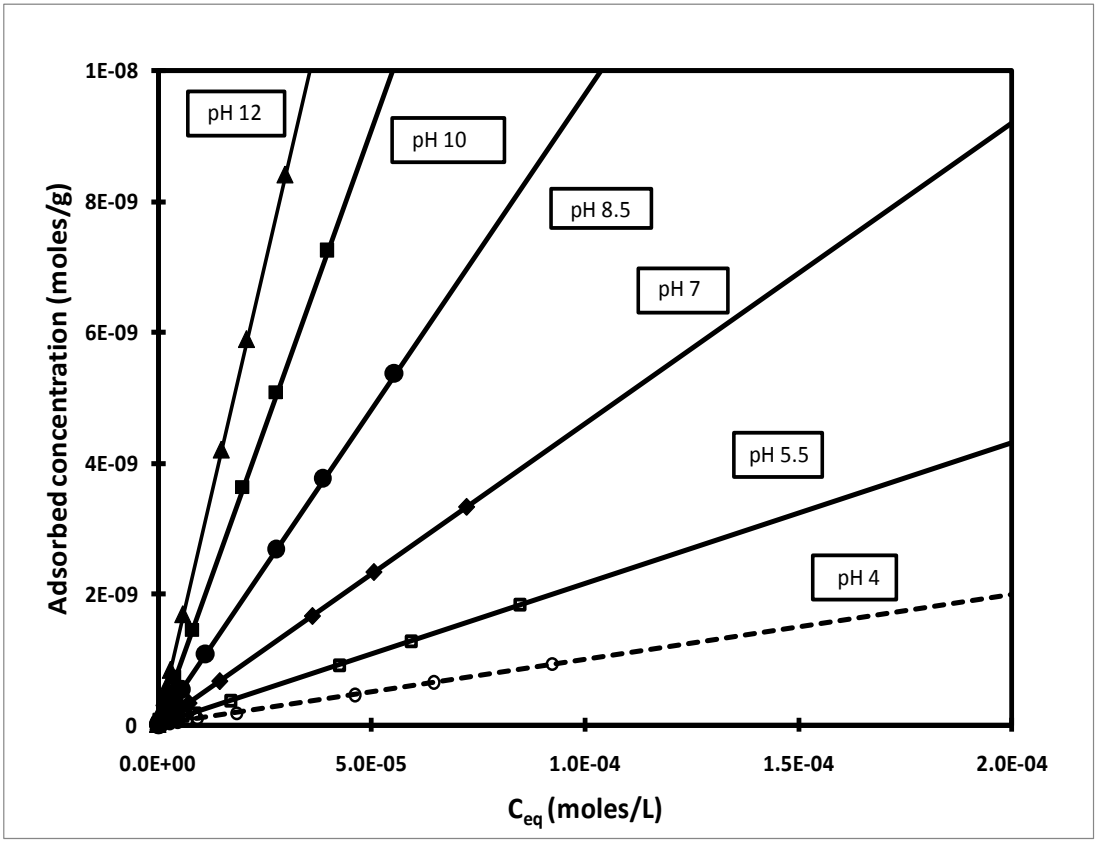

Figure 5-10 : Adsorption isotherms from surface complexation model at different pH values and corresponding Unified Langmuir-Freundlich model fits. Covered and open symbols represent surface complexation model generated data. Lines represent Unified Langmuir-Freundlich model predictions.

Table 5-6: Values of the fitted ULF model parameters for Cadmium adsorption by (Cederberg *et al.*, 1985)

pH	K_{max}(mg/g)	n	K_s (μM)
4	0.00195	1	0.0051
5.5	0.00195	1	0.0110
7	0.00195	1	0.0236
8.5	0.00195	1	0.0495
10	0.00195	1	0.0934
12	0.00195	1	0.1440

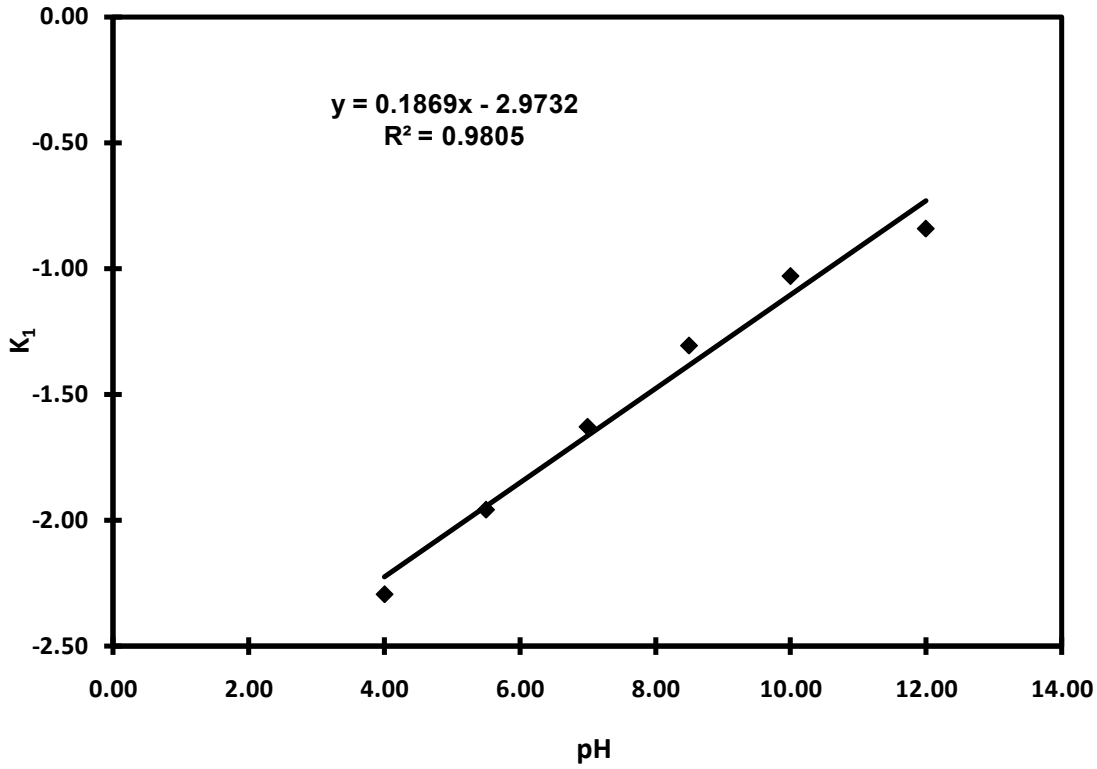

Figure 5-11 : Plot of pH Vs ULF model parameter K_1 for Cadmium

The ULF parameters were used in a one-dimensional transport code to model the cadmium transport problem given by (Cederberg *et al.*, 1985). The results are shown in Figure 5-12**.** The ULF models are able to predict transport and matched the predictions by the surface-complexation coupled transport code TRANQL. These results are significant because they suggest that a pH dependent ULF isotherm is able to predict transport as good as a mechanistic geochemical-coupled transport code. This also indicates that our approach can be applied for a wide range of other contaminants.

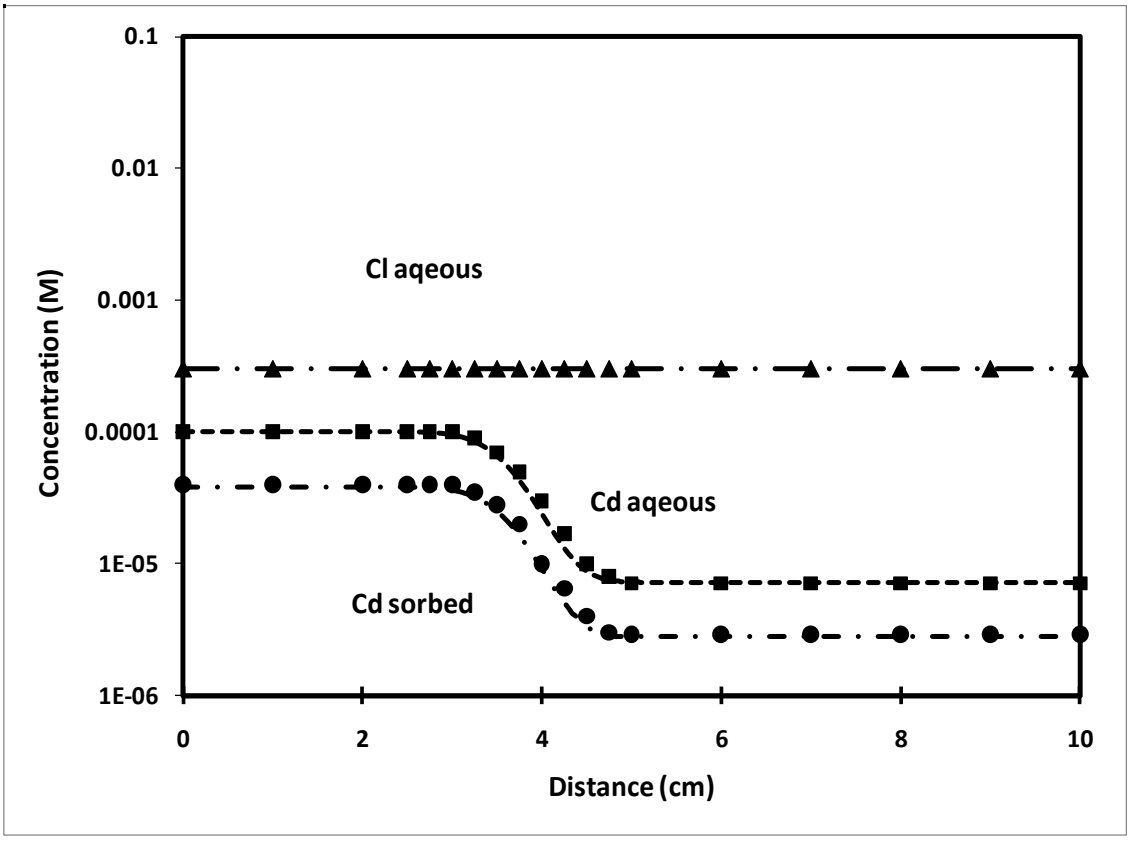

Figure 5-12 : Comparison of ULF model predictions (dotted lines) and data from (Cederberg *et al.*, 1985) (open symbols).

5.5 Conclusions

Arsenate adsorption on iron-coated sand was investigated over a wide range of pH, solid-to-solution ratio, and initial concentration levels using adsorption isotherms and sequential equilibration reactor experiments. A ULF isotherm model was developed that could predict adsorption at different pH values. A mathematical method was also derived for modeling transport in sequential batch reactors. The mathematical model was used to predict adsorption in sequential batch reactor experiments and was found to provide good predictions.

The ULF model was integrated within a transport code to test the usability of the model for simulating column transport scenarios. The ULF model was able to successfully predict arsenate adsorption in column scale simulations. We further validated our approach by comparing against an existing benchmark problem available in literature (Cederberg *et al.*, 1985). The successful use of the ULF model in batch, sequential-batch and column experiments indicate that the model could be used to make predictions over a wide range of experimental conditions. The ULF model helped reduce the computational time by more than an order of magnitude. These results suggest that the ULF model is a useful alternative for modeling adsorption under variable pH conditions.

CHAPTER 6

SUMMARY, IMPLICATIONS AND RECOMMENDATIONS

6.1 Summary

In this dissertation we have investigated the interaction of arsenate with synthetic iron-coated sands. This dissertation has helped develop a better understanding of arsenic adsorption on goethite and has made the following contributions:

(i) We developed a scaling procedure for surface complexation models that can greatly reduce model development time and effort. The scaled models can be used to predict adsorption on goethite-coated sands with different solid/solution ratio and surface saturation. The scaled models can also be used to predict adsorption on different forms of goethite including pure (uncoated) goethite and goethite coated on sands.

(ii) We proposed a novel sequential equilibration reactor experimental setup for studying equilibrium-controlled, advection-dominated reactive transport problems. The experimental results were used to validate predictions generated using reactive transport model, which consisted of a batch surface complexation model incorporated in PHREEQCI advection routine.

(iii) We have developed a unified Langmuir-Freundlich isotherm, which was able to model pH-dependent adsorption involving surface complexation reactions. We also derived a semi-analytical solution for modeling equilibrium controlled, advection-dominated one-dimensional reactive transport problems. The unified Langmuir-Freundlich model and the semi-analytical solution were validated by using experimental datasets and literature-derived benchmark problems that use surface complexation reactions.

6.2 Implications and recommendations

We have investigated adsorption of arsenic on iron-coated sands using both experimental and modeling approaches. Results of this dissertation are expected to have strong implications on predicting the fate and transport of inorganic contaminants in subsurface systems.

The scaling methods developed allow surface complexation models developed for one sorbent to be used for other similar sorbents by employing the scaling procedure. We have demonstrated that the site density is the most important parameter in surface complexation models. Site density can vary even for sorbents prepared by same chemical procedure. Hence it is recommended that site density be measured and not assumed. Future work in this area could be to test the scaling procedure for other anions such as phosphate and other metal-oxide and metal-oxyhydroxide sorbents.

The sequential equilibration reactor experimental setup can be used to rapidly generate datasets to validate equilibrium geochemical transport models. Future research should employ this experimental setup to conduct feasibility studies for remediation systems, and to generate datasets to validate the transport codes used to model such remediation systems.

The Unified Langmuir-Freundlich isotherm we developed is a powerful framework that can be used for modeling pH dependent adsorption. This model can be easily integrated into groundwater transport codes unlike surface complexation models. The ULF isotherm-based transport codes can decrease computational time significantly (more than 10 times) when compared to surface-complexation-coupled transport codes. Further work can be done to extend the Langmuir-Freundlich model to model competitive adsorption and kinetic-limited adsorption reactions.

REFERENCES

Ahamed, S.,Sengupta, M.K.,Mukherjee, A.,Hossain, M.A.,Das, B.,Nayak, B.,Pal, A.,Mukhejee, S.C.,Pati, S.,Dutta, R.N.,Chattejee, G.,Mukhejee, A.,Srivastava, R., Chakraborti, D., (2006). Arsenic groundwater contamination and its health effects in the state of Uttar Pradesh (UP) in upper and middle Ganga plain, India: A severe danger. *Science of the Total Environment*, **370**, 310-322.

Allison, J.D.,Brown, D.S., Novagradac, K.J., (1990). MINTEQA2/PRODEFA2, A geochemical assessment model for environmental systems: Version 3.0.

Allison, J.D., (2003). *MINTEQA2 for Windows, Equilibrium Speciation Model - Version 1.50*. In.

Anawar, H.M.,Akai, J.,Komaki, K.,Terao, H.,Yoshioka, T.,Ishizuka, T.,Safiullah, S., Kato, K., (2003). Geochemical occurrence of arsenic in groundwater of Bangladesh: sources and mobilization processes. *Journal of Geochemical Exploration*, **77**, 109-131.

Anderson, M.A.,Ferguson, J.F., Gavis, J., (1976). Arsenate adsorption on amorphous aluminum hydroxide. *Journal of Colloid and Interface Science*, **54**, 391-399.

Azcue, J.M.,Nriagu, J.O., Schiff, S., (1994). Role of Sediment Porewater in the Cycling of Arsenic in a Mine-Polluted Lake. *Environment International*, **20**, 517-527.

Badruzzaman, M.,Westerhoff, P., Knappe, D.R.U., (2004). Intraparticle diffusion and adsorption of arsenate onto granular ferric hydroxide (GFH). *Water research*, **38**, 4002-4012.

Bale, A.J., Morris, A.W., (1981). Laboratory simulation of chemical processes induced by estuarine mixing: The behaviour of iron and phosphate in estuaries. *Estuarine, Coastal and Shelf Science*, **13**, 1-10.

Ball, J.W.,Jenne, E.A., Cantrell, M.W., (1981). WATEQ3 A geochemical model with uranium added.

Barnett, M.O.,Jardine, P.M.,Brooks, S.C., Selim, H.M., (2000). Adsorption and transport of uranium (VI) in subsurface media. *Soil Science Society of America Journal*, **64**, 908.

Beauchemin, S., Kwong, Y.T.J., (2006). Impact of redox conditions on arsenic mobilization from tailings in a wetland with neutral drainage. *Environ. Sci. Technol.*, **40**, 6297-6303.

Boreysza, K.,Fabritius, B., Laures, C., (2006). *Arsenic pollution of ground water in Bangladesh*. In: University of Stuttgart, Stuttgart

Brendler, V.,Vahle, A.,Arnold, T.,Bernhard, G., Fanghanel, T., (2002). RES³T - Rossendorf Expert System for surface and sorption thermodynamics. *Journal of Contaminant Hydrology*, **61**, 281-291.

Brendler, V.,Arnold, T.,Richter, A., Bernhard, G., (2004). Capability of surface complexation models and databases for predicting radionuclide sorption. *Conference Proceedings Waste Management 2004*, **February 29- March 4**.

British Geological Survey, Mott MacDonald Ltd, (1999). *Groundwater Studies for Arsenic Contamination in Bangladesh. Final Report*. In: British Geological Survey, London:UK

Cederberg, G.A.,Street, R.L., Leckie, J.O., (1985). A Groundwater Mass Transport and Equilibrium Chemistry Model for Multicomponent Systems. *Water Resour. Res.*, **21**, 1095-1104.

Chapman, D.L., (1913). A contribution to the theory of electrocapillarity. *Philosophical Magazine Series 6*, **25**, 475-481.

Cheng, T.,Barnett, M.O.,Roden, E.E., Zhuang, J.L., (2004). Effects of phosphate on uranium(VI) adsorption to goethite-coated sand. *Environ. Sci. Technol.*, **38**, 6059-6065.

Cheng, T.,Barnett, M.O.,Roden, E.E., Zhuang, J.L., (2006). Effects of solid-to-solution ratio on uranium(VI) adsorption and its implications. *Environ. Sci. Technol.*, **40**, 3243-3247.

Clarlton, S.R., Parkhurst, D.L., (2002). *PHREEQCI - A graphical user interface to the geochemical model PHREEQC: U.S. Geological Survey Fact Sheet FS-031-02, April 2002, 2p*. U.S. Geological Survey Denver, Colorado.

Clement, T.P., (1997). RT3D - A modular computer code for simulating reactive multi-species transport in 3-Dimensional groundwater aquifers, Battelle Pacific Northwest National Laboratory Research Report, PNNL-SA-28967. Available at: http://bioprocess.pnl.gov/rt3d.htm.

Clement, T.P.,Sun, Y.,Hooker, B.S., Petersen, J.N., (1998). Modeling Multi-species Reactive Transport in Groundwater Aquifers. *Groundwater Monitoring & Remediation Journal*, **18**, 79-92.

Coston, J.A.,Fuller, C.C., Davis, J.A., (1995). Pb^{2+} and Zn^{2+} adsorption by a natural aluminum-bearing and iron-bearing surface coating on an aquifer sand. *Geochimica Et Cosmochimica Acta*, **59**, 3535-3547.

Dadwhal, M.,Ostwal, M.M.,Liu, P.K.T.,Sahimi, M., Tsotsis, T.T., (2009). Adsorption of Arsenic on Conditioned Layered Double Hydroxides: Column Experiments and Modeling. *Industrial & Engineering Chemistry Research*, **48**, 2076-2084.

Davis, J.A., (1977). *Adsorption of trace metals and complexing ligands at oxide/water interface*. In: Stanford University, Stanford, Calif.

Davis, J.A., Leckie, J.O., (1978a). Surface ionization and complexation at oxide-water interface .2. Surface properties of amorphous iron oxyhydroxide and adsorption of metal-ions. *Journal of Colloid and Interface Science*, **67**, 90-107.

Davis, J.A., Leckie, J.O., (1978b). Effects of adsorbed complexing ligands on trace metal uptake by hydrous oxides. *Environ. Sci. Technol.*, **12**, 1309–1315.

Davis, J.A., Kent, D.B., (1990). Surface complexation modeling in aqueous geochemistry. *Reviews in Mineralogy*, **23**, 177-260.

Davis, J.A.,Coston, J.A.,Kent, D.B., Fuller, C.C., (1998). Application of the surface complexation concept to complex mineral assemblages. *Environ. Sci. Technol.*, **32**, 2820-2828.

Davis, J.A.,Ochs, M.,Olin, M.,Payne, T.E., Tweed, C.J., (2005). *NEA Sorption Project Phase II: Interpretation and Prediction of Radionuclide Sorption Onto Substrates Relevant for Radioactive Waste Disposal Using Thermodynamic Sorption Models: a Report Produced for the Management Board of the NEA Sorption Project*. In: OECD.

Dhar, R.K.,Biswas, B.K.,Samanta, G.,Mandal, B.K.,Chakraborti, D.,Roy, S.,Jafar, A.,Islam, A.,Ara, G., Kabir, S., (1997). Groundwater arsenic calamity in Bangladesh. *Current Science*, **73**, 48-59.

Dixit, S., Hering, J.G., (2003). Comparison of arsenic(V) and arsenic(III) sorption onto iron oxide minerals: Implications for arsenic mobility. *Environ. Sci. Technol.*, **37**, 4182-4189.

Dixit, S., Hering, G.J., (2006). Sorption of Fe(II) and As(III) on goethite in single- and dual-sorbate systems. *Chemical geology*, **228**, 6-15.

Drever, J.I., (1982). Geochemistry of natural waters. *Prentice-Hall, Inc., Englewood Cliffs New Jersey. 1982. 388*.

Dugger, D.L.,Stanton, J.H.,Irby, B.N.,McConnell, B.L.,Cummings, W.W., Maatman, R.W., (1964). The exchange of twenty metal ions with weakly acidic silanol group of silica gel. *Journal of physical chemistry*, **68**, 757-760.

Dzombak, D.A., Morel, F.M.M., (1987). Development of a database for modeling adsorption of inorganics on iron and alliminum-oxides. *Environmental Progress*, **6**, 133-137.

Dzombak, D.A., Morel, F.M.M., (1990). *Surface Complexation Modeling - Hydrous ferric oxide*. John Wiley and Sons, New York.

Ekberg, C., Emrén, A.T., (2001). Uncertainties in Solubility Calculations. *Monatshefte für Chemie / Chemical Monthly*, **132**, 1171-1179.

Engesgaard, P., Kipp, K.L., (1992). A geochemical transport model for redox-controlled movement of mineral fronts in groundwater flow systems: A case of nitrate removal by oxidation of pyrite. *Water Resour. Res.*, **28**, 2829-2843.

Felmy, A.R.,Girvin, D.C., Jenne, E.A., (1983). MINTEQ: A computer program for calculating aqueous geochemical equilibria, report, 62 pp, USEPA, Washington, D.C.

Fendorf, S.,Eick, J.M.,Grossl, P., Sparks., L.D., (1997). Arsenate and chromate retention mechanisms on goethite. 1. Surface structure. *environmental science and technology*, **31**, 315-320.

Ferguson, J.F., Gavis, J., (1972). Review of arsenic cycle in natural waters. *Water Research*, **6**, 1259-1267.

Friedly, J.C.,Kent, D.B., Davis, J.A., (2002). Simulation of the mobility of metal-EDTA complexes in groundwater: The influence of contaminant metals. *Environ. Sci. Technol.*, **36**, 355-363.

Fuller, C.C.,Davis, J.A.,Coston, J.A., Dixon, E., (1996). Characterization of metal adsorption variability in a sand and gravel aquifer, Cape Cod, Massachusetts, USA. *Journal of Contaminant Hydrology*, **22**, 165-187.

Gao, H.,Butler, A.,Wheater, H., Vesovic, V., (2001). Chemically reactive multicomponent transport simulation in soil and groundwater: 1. Model development and evaluation. *Environmental Geology*, **41**, 274-279.

García-Luque, E.,Forja Pajares, J.M., Gómez-Parra, A., (2006). Assessing the geochemical reactivity of inorganic phosphorus along estuaries by means of laboratory simulation experiments. *Hydrological Processes*, **20**, 3555-3566.

Giammar, D.,DeCapio, V., Moore, C., (2004). Lead adsorption to goethite-coated quartz sand. *American Chemical Society Conference Proceedings*, **March 28, 2004**.

Goldberg, S., (1985). Chemical modeling of anion competition on goethite using the constant capacitance model. *Soil Science Society of America Journal*, **49**, 851-856.

Goldberg, S., (1986). Chemical modeling of arsenate adsorption on aluminum and iron-oxide minerals. *Soil Science Society of America Journal*, **50**, 1154-1157.

Goldberg, S., (1991). Sensitivity of surface complexation modeling to the surface site density parameter. *Journal of Colloid and Interface Science*, **145**, 1-9.

Goldberg, S., (1992). Use of surface complexation models in soil chemical systems., *Advances Agronomy*, **47**, 233-239.

Goldberg, S., Johnston, C.T., (2001). Mechanisms of arsenic adsorption on amorphous oxides evaluated using macroscopic measurements, vibrational spectroscopy, and surface complexation modeling. *Journal of Colloid and Interface Science*, **234**, 204-216.

Gouy, G., (1910). *Journal of physics-Paris*, **9**.

Goyer, R.A., (1996). *Casarett and Doull's toxicology: the basic science of poisons*. In: McGraw-Hill New York, NY, USA.

Grossl, P.R., Sparks, D.L., (1995). Evaluation for Contaminant Ion Adsorption-Desorption on Goethite Using Pressure-Jump Relaxation Kinetics. *Geoderma*, **67**, 87-101.

Gustafsson, J.P., (2006). *Visual MINTEQ*. In: Department of land and water resources engineering, KTH, Stockholm, Sweden.

Harter, R.D., Naidu, R., (2001). An assessment of environmental and solution parameter impact on trace-metal sorption by soils. *Soil Science Society of America Journal*, **65**, 597-612.

Hartzog, O.K.,Kanel, S.K.,Loganathan, V.A.,Jeppu, G.P.,Barnett, M.O., Clement, T.P., (2009). Normalization, Comparison, and Scaling of Adsorption Data: Arsenate and Goethite. *Journal of Colloid and Interface Science*, **333**, 6-13.

Herbelin, A., Westall, J.C., (1999). *FITEQL: A Computer program for determination of chemical equilibrium constants from experimental data, Version 4.0*. Department of Chemistry, Oregon State University, Corvallis.

Hingston, F.J., (1970). Specific adsorption of anions on goethite and gibbsite., *PhD thesis. University of W. Australia, Nederlands*.

Hingston, F.J.,Posner, A.M., Quirk, J.P., (1971). Competitive adsorption of negatively charged ligands on oxide surfaces. *Faraday Society*, **52**, 334-342.

Hsia, T.H.,Lo, S.L., Lin, C.F., (1992). As (V) adsorption on amorphous iron oxide: Triple layer modelling. *Chemosphere*, **25**, 1825-1837.

Huang, C.P., Stumm, W., (1973). Specific adsorption of cations on hydrous γ-Al2O3. *J. Colloid Interface Sci.* , **43**, 409-420.

Huber, N.K., Garrels, R.M., (1953). Relation of pH and oxidation potential to sedimentary iron mineral formation. *Economic Geology*, **48**, 337-357.

Inch, K.J., Killey, R.W.D., (1987). Surface area and radionuclide sorption in contaminated aquifers. *Water Pollution Research Journal of Canada*, **22: 85-98.**

Jain, A.,Raven, K.P., Loeppert, R.H., (1999). Arsenite and Arsenate Adsorption on Ferrihydrite: Surface Charge Reduction and Net OH- Release Stoichiometry. *Environ. Sci. Technol.*, **33**, 1179-1184.

Jeppu, G.,Clement, T.P.,Barnett, M.O., Lee, K.K., (2010). A scalable surface complexation modeling framework for predicting arsenate adsorption on goethite-coated sands. *Journal of environmental engineering and science*, **27**, 147-158.

Jeppu, G.,Clement, T.P., Barnett, M.O., (2011). A novel experimental system to study equilibrium-reactive transport problems. **Manuscript to be submitted**.

Kenneth, L.K., Jr, (1997). *Guide to the revised heat and solute transport simulator: HST3D- Version 2. Water resources investigations report 97-4157*. U.S. Geological survey, Denver, Colorado.

Kersten, M., Kulik, D.A., (2005). Competitive scavenging of trace metals by HFO annd HMO during redox-driven early diagenesis of ferromanganese nodules. *Journal of soils and sediments*, **5**, 7-47.

Khaodhiar, S.,Azizian, M.F.,Osathaphan, K., Nelson, P.O., (2000). Copper, Chromium, and Arsenic Adsorption and Equilibrium Modeling in An Iron-Oxide-Coated Sand, Background Electrolyte System. *Water, Air, & Soil Pollution*, **119**, 105-120.

Kirby, C.S., Brady, J.A.E., (1998). Field determination of Fe2+ oxidation rates in acid mine drainage using a continuously-stirred tank reactor. *Applied Geochemistry*, **13**, 509-520.

Kosnett, M.J., (1994). *Arsenic*. In: Olson, K.K. (Ed.), Poisoning and Drug Overdose. Appleton & Lange, Norwalk, Connecticut, pp. 87-89.

Kuhlmeier, P.D., (1997). Sorption and desorption of arsenic from sandy soils: Column studies. *Journal of Soil Contamination*, **6**, 21-36.

Kulik, D.A., (2002). Sorption modeling by Gibbs energy minimization: Towards a uniform thermodynamic database for surface complexes of radionuclides. *Radiochim. Acta*, **90**, 815-832.

Kulik, D.A.,Berner, U., Curti, E., (2003). *Modeling chemical equilibrium partitioning with the GEMS-PSI code*. In: Smith, B., Gschwend, B. (Eds.), Nuclear Energy and Safety, PSI Scientific Report. Paul Scherrer institute, Villigen, Switzerland, pp. 109-122.

Kulik, D.A., (2006). Classic adsorption isotherms incorporated in modern surface complexation models: Implications for sorption of actinides. *Radiochim. Acta*, **94**, 765-778.

Kundu, S., Gupta, A.K., (2006). Arsenic adsorption onto iron oxide-coated cement (IOCC): regression analysis of equilibrium data with several isotherm models and their optimization. *Chemical Engineering Journal*, **122**, 93-106.

Kurbatov, M.H.,Wood, G.B., Kurbatov, J.D., (1951). Isothermal adsorption of Cobalt from Dilute solutions. *journal of physical chemistry*, **55**, 1170-1182.

La Force, M.J.,Hansel, C.M., Fendorf, S., (2000). Arsenic speciation, seasonal transformations, and co-distribution with iron in a mine waste-influenced palustrine emergent wetland. *Environmental Science and Technology*, **34**, 3937-3943.

Levenspiel, O., (1991). *Chemical reaction engineering*. Wiley Eastern Limited.

Lin, T.F., Wu, J.K., (2001). Adsorption of arsenite and arsenate within activated alumina grains: equilibrium and kinetics. *Water research*, **35**, 2049-2057.

Lion, W.L.,Altmann, S.R., Leckie, J.O., (1982). Trace-metal adsorption characteristics of estuarine particulate matter: evaluation of contributions of iron/manganese oxide and organic surface coatings. *Environ. Sci. Technol*, **16**, 660-666.

Loganathan, V.A.,Barnett, M.O.,Clement, T.P., Kanel, S.R., (2009). Scaling of adsorption reactions: U(VI) experiments and modeling. *Applied geochemistry.*, **24**, 2051-2060.

Luoma, S.N., Davis, J.A., (1983). Requirements for modeling trace metal partitioning in oxidized estuarine sediments. *Marine chemistry*, **12**.

Macur, R.E.,Wheeler, J.T.,McDermott, T.R., Inskeep, W.P., (2001). Microbial populations associated with the reduction and enhanced mobilization of arsenic in mine tailings. *Environ. Sci. Technol*, **35**, 3676-3682.

Mandal, B.K., Suzuki, K.T., (2002). Arsenic round the world: a review. *Talanta*, **58**, 201-235.

Manning, B.A., Goldberg, S., (1996). Modeling competitive adsorption of arsenate with phosphate and molybdate on oxide minerals. *Soil Science Society of America Journal*, **60**, 121-131.

Mathur, S.S., Dzombak, D.A., (2006). *Surface complexation Modeling; Goethite*. In: Lutzenkirchen, J. (Ed.), Elsevier, pp. 443-468.

McDuff, R.E., Morel, F.M.M., (1972). REDEQL, a general program for the computation of chemical equilibrium in aqueous systems. Keck Laboratory of Environmental Engineering Science, California Institute of Technology, Pasadena, CA.

Mead, M.N., (2005). Arsenic: in search of an antidote to a global poison. *Environmental health perspectives*, **113**, A378-386.

Meng, X.,Bang, S., Korfiatis, G.P., (2000). Effects of silicate, sulfate, and carbonate on arsenic removal by ferric chloride. *Water Research* **34**, 1255-1261.

Mohan, D., Pittman, C.U., (2007). Arsenic removal from water/wastewater using adsorbents - A critical review. *Journal of Hazardous Materials*, **142**, 1-53.

Nahm, M.H.,Herzenberg, L.A.,Little, K., Little, J.R., (1977). A new method of applying the Sips equation. *The Journal of Immunology*, **119**, 301.

Narasimhan, T.N.,White, A.F., Tokunaga, T., (1986). Groundwater Contamination from an Inactive Uranium Mill Tailings Pile .2. Application of a Dynamic Mixing Model. *Water Resources Research*, **22**, 1820-1834.

Nath, B.,Chakraborty, S.,Burnol, A.,Stuben, D.,Chatterjee, D., Charlet, L., (2009). Mobility of arsenic in the sub-surface environment: An integrated hydrogeochemical study and sorption model of the sandy aquifer materials. *Journal of Hydrology*, **364**, 236-248.

Nickson, R.T.,McArthur, J.M.,Ravenscroft, P.,Burgess, W.G., Ahmed, K.M., (2000). Mechanism of arsenic release to groundwater, Bangladesh and West Bengal. *Applied Geochemistry*, **15**, 403-413.

Noorishad, J.,Carnahan, C.L., Benson, L.V., (1987). Development of the nonequilibrium reactive chemical transport code CHMTRNS, Rep. LBL-22361, Lawrence Berkeley Lab., Univ. of Calif., Berkeley.

Ochs, M.,Davis, J.A.,Olin, M.,Payne, T.E.,Tweed, C.J.,Askarieh, M.M., Altmann, S., (2006). Use of thermodynamic sorption models to derive radionuclide K-d values for performance assessment: selected results and recommendations of the NEA sorption project. *Radiochimica Acta*, **94**, 779-785.

Parkhurst, D.L.,Thorstenson, D.C., Plummer, L.N., (1980). PHREEQE - A computer program for geochemical calculations. *U.S. Geol. Surv. Water Resour. Invest. Rep., 80-96, 195 pp.*

Parkhurst, D.L., (1995). User's guide to PHREEQC, A computer model for speciation, reaction-path, advective-dispersive transport and inverse geochemical calculations U.S. Geol. Surv. Water Resour. Invest. Rep. 95-4227.

Parkhurst, D.L., Appelo, C.A.J., (1999). User's guide to PHREEQC (version 2) - A computer program for speciation, batch-reaction, one-dimensional transport, reaction path, and inverse geochemical calculations. *U.S. Geol. Surv. Water Resour. Invest. Rep., 99, 4259, 312 pp*.

Parkhurst, D.L.,Kipp, K.L.,Engesgaard, P., Charlton, S.R., (2004). PHAST–A program for simulating ground-water flow, solute transport, and multicomponent geochemical reactions. *USGS Techniques and Methods*, **6**.

Parkhurst, D.L., and C. A. J. Appelo, (1999). User's guide to PHREEQC (version 2) - A computer program for speciation, batch-reaction, one-dimensional transport, reaction path, and inverse geochemical calculations. *U.S. Geol. Surv. Water Resour. Invest. Rep., 99, 4259, 312 pp*.

Parks, G.A., DeBruyn, P.L., (1962). The zero point of charge of oxides. *Journal of physical chemistry*, **66**, 967-973.

Parlange, J.Y.,Starr, J.L.,Barry, D.A., Braddock, R.D., (1984). Some approximate solutions of the transport equation with irreversible reactions. *Soil Science Society of America Journal*, **137**, 434-442.

Phanikumar, M.S., McGuire, J.T., (2004). A 3D partial-equilibrium model to simulate coupled hydrogeological, microbiological, and geochemical processes in subsurface systems. *Geophysical Research Letters*, **31**.

Prommer, H.,Barry, D.A., Zheng, C., (2003a). MODFLOW/MT3DMS-Based Reactive Multicomponent Transport Modeling. *Ground Water*, **41**, 247-257.

Prommer, H.,Barry, D.A., Zheng, C., (2003b). MODFLOW/MT3DMS-based Reactive Multicomponent Transport Modeling. *Groundwater*, **41**, 247-257.

Radu, T.,Hilliard, J.C.,Yang, J.K., Barnett, M.O., (2005a). Transport of As(III) and As(V) in experimental subsurface systems. *Advances in Arsenic Research*, **915**, 91-103.

Radu, T.,Subacz, J.L.,Phillippi, J.M., Barnett, M.O., (2005b). Effects of dissolved carbonate on arsenic adsorption and mobility. *Environmental Science and Technology*, **39**, 7875-7882.

Radu, T.,Kumar, A.,Clement, T.P.,Jeppu, G., Barnett, M.O., (2007). Development of a scalable model for predicting arsenic transport coupled with oxidation and adsorption reactions. *Contaminant Hydrology*.

Rahman, M.,Tondel, M.,Ahmad, S.A.,Chowdhury, I.A.,Faruquee, M.H., Axelson, O., (1999). Hypertension and arsenic exposure in Bangladesh. *Hypertension*, **33**, 74-78.

Rau, I.,Meghea, A.,Peleanu, I.,Gonzalo, A.,Valiente, M., Zaharescu, M., (2003). Modelling the arsenic (V) and (III) adsorption. *Czechoslovak Journal of Physics*, **53**, 549-556.

Raven, K.P.,Jain, A., Loeppert, R.H., (1998). Arsenite and arsenate adsorption on ferrihydrite: kinetics, equilibrium, and adsorption envelopes. *Environ. Sci. Technol*, **32**, 344-349.

Richter, A.,Brendler, V., Bernhard, G., (2003). The mineral-specific sorption database REST^{3}T: Concept description, implementation and application towards contiminated systems. *Geochimica Et Cosmochimica Acta*, **67**, 397.

Richter, A.,Brendler, V., Nebelung, C., (2005a). The effect of parameter uncertainty on blind prediction of Np(V) sorption onto hematite using the Diffuse Double Layer Model. *Radiochim. Acta*, **93**, 527-531.

Richter, A.,Brendler, V., Nebelung, C., (2005b). Blind prediction of Cu(II) sorption onto goethite: Current capabilities of diffuse double layer model. *Geochimica Et Cosmochimica Acta*, **69**, 2725-2734.

Richter, A., Brendler, V., (2006). Sparse and uncertain SCM parameter sets: What are the consequences?, *Abstr. Pap. Am. Chem. Soc.*, **231**, 1.

Rimstidt, J.D., Dove, P.M., (1986). Mineral/solution reaction rates in a mixed flow reactor: Wollastonite hydrolysis. *Geochimica et Cosmochimica Acta*, **50**, 2509-2516.

Romero-Gonzalez, M.R.,Cheng, T.,Barnett, M.O., Roden, E.E., (2007). Surface complexation modeling of the effects of phosphate on uranium(VI) adsorption. *Radiochimica Acta*, **95**, 251-259.

Rubin, J., (1983). Transport of Reacting Solutes in Porous-Media - Relation between Mathematical Nature of Problem Formulation and Chemical Nature of Reactions. *Water Resources Research*, **19**, 1231-1252.

Saunders, J.A.,Lee, M.K.,Shamsudduha, M.,Dhakal, P.,Uddin, A.,Chowdury, M.T., Ahmed, K.M., (2008). Geochemistry and mineralogy of arsenic in (natural) anaerobic groundwaters. *Applied Geochemistry*, **23**, 3205-3214.

Schecher, W.D., Driscoll, C.T., (1987). An evaluation of uncertainty associated with aluminum equilibrium calculations. *Water Resour. Res.*, **23**, 525-534.

Schecher, W.D., McAvoy, D.C., (1998). MINEQL+: A Chemical Equilibrium Modeling System, User's Manual, Version 4.0. *Environmental Research Software, Hallowell, ME 04347*.

Scheidegger, A.,Borkovec, M., Sticher, H., (1993). Coating of silica sand with goethite - preparation and analytical identification. *Geoderma*, **58**, 43-65.

Schertmann, U., Cornell, R.M., (2000). *Iron oxides in the laboratory: preparation and characterization*. Wiley-VCH, Weinheim.

Schindler, P., Kamber, H., (1968). Die Acidität von Silanolgruppen. Vorläufige Mitteillung. *Helvetica Chimica Acta*, **51**, 1781-1786.

Schindler, P.W., Gamsjager, H., (1972). Acid-base reactions of the TiO2 (Anatase)-water interaface and the point of zero charge of TiO2 suspensions. *Kolloi Z. Z. Pollymere*, **250**, 759-763.

Schnoor, J.L., (1996). *Environmental modeling. Fate and transport of pollutants in water, air, and soil*. John Wiley & Sons, New York, NY.

Shamsudduha, M.,Marzen, L.J.,Uddin, A.,Lee, M.K., Saunders, J.A., (2009). Spatial relationship of groundwater arsenic distribution with regional topography and water-table fluctuations in the shallow aquifers in Bangladesh. *Environmental Geology*, **57**, 1521-1535.

Sips, R., (1948). Combined form of Langmuir and Freundlich equations. *J. Chem. Phys*, **16**, 490–495.

Sips, R., (1950). On the structure of a catalyst surface. II. *The Journal of Chemical Physics*, **18**, 1024.

Smedley, P.L., Kinniburgh, D.G., (2002). A review of the source, behavior and distribution of arsenic in natural waters. *Applied Geochemistry* **17**, 517–568.

Smith, A.H.,Lingas, E.O., Rahman, M., (2000). Contamination of drinking-water by arsenic in Bangladesh: a public health emergency. *Bulletin of the World Health Organization*, **78**, 1093-1103.

Sposito, G., Mattigod, S.V., (1980). *GEOCHEM: A computer program for the calculation of chemical equilibria in soil. Keamey Foundation, Soil Science*. In: University of California, Riverside.

Stanton, J., Maatman, R.W., (1963). The reaction betwen aqueous uranyl ion and the surface of silica gel. *journal of Colloid and Interface Science*, **18**, 132-146.

Stollenwerk, K.G., (1995). Modeling the Effects of Variable Groundwater Chemistry on Adsorption of Molybdate. *Water Resources Research*, **31**, 347-357.

Stumm, W.,Huang, C.P., Jenkins, S.R., (1970). Specific Chemical Interaction Affecting Stability of Dispersed Systems. *Croatica Chemica Acta*, **42**, 223-245.

Sun, X.H., Doner, H.E., (1996). An investigation of arsenate and arsenite bonding structures on goethite by FTIR. *Soil Science*, **161**, 865-872.

Sun, Y.,Petersen, J.N.,Clement, T.P., Skeen, R.S., (1999). Development of analytical solutions for multispecies transport with serial and parallel reactions. *Water Resources Research*, **35**, 185-190.

Sverjensky, A.D., (2003). Standard states for the activities of mineral surface sites and species. *Geochimica Et Cosmochimica Acta*, **67**, 17-28.

Tchounwou, P.B.,Patlolla, A.K., Centeno, J.A., (2003). Carcinogenic and systemic health effects associated with arsenic exposure - A critical review. *Toxicologic Pathology*, **31**, 575-588.

Thirunavukkarasu, O.S.,Viraraghavan, T., Subramanian, K.S., (2001). Removal of arsenic in drinking water by iron oxide-coated sand and ferrihydrite-Batch studies. *Water Quality Research Journal of Canada*, **36**, 55-70.

Thirunavukkarasu, O.S.,Viraraghavan, T., Subramanian, K.S., (2003). Arsenic removal from drinking water using iron oxide-coated sand. *Water, Air, & Soil Pollution*, **142**, 95-111.

Truesdell, A.H., Jones, B.F., (1974). WATEQ, A computer program for calculating chemical equilibria of natural water. *U.S. Geol. Surv. J. Res.*, **2**, 233-248.

Tsai, S.M.,Wang, T.N., Ko, Y.C., (1999). Mortality for certain diseases in areas with high levels of arsenic in drinking water. *Archives of Environmental Health*, **54**, 186-193.

Turiel, E.,Perez-Conde, C., Martin-Esteban, A., (2003). Assessment of the cross-reactivity and binding sites characterisation of a propazine-imprinted polymer using the Langmuir-Freundlich isotherm. *The Analyst*, **128**, 137-141.

Umpleby, R.J.,Baxter, S.C.,Chen, Y.,Shah, R.N., Shimizu, K.D., (2001). Characterization of Molecularly Imprinted Polymers with the Langmuir- Freundlich Isotherm. *Anal. Chem*, **73**, 4584-4591.

Valocchi, A.J.,Street, R.L., Roberts, P.V., (1981). Transport of ion-exchanging solutes in groundwater: Chromatographic theory and fiels simulations. *Water Resources Research*, **17**, 1517-1527.

Walter, A.L.,Frind, E.O.,Blowes, D.W.,Ptacek, C.J., Molson, J.W., (1994). Modeling of Multicomponent Reactive Transport in Groundwater .1. Model Development and Evaluation. *Water Resources Research*, **30**, 3137-3148.

Walvekar, R.R.,Kane, S.V.,Nadkarni, M.S.,Bagwan, I.N.,Chaukar, D.A., D'Cruz, A.K., (2007). Chronic arsenic poisoning: a global health issue - a report of multiple primary cancers. *Journal of Cutaneous Pathology*, **34**, 203-206.

Wang, H.D.,White, G.N.,Turner, F.T., Dixon, J.B., (1993). Ferrihydrite, Lepidocrocite, and Goethite in Coatings from East Texas Vertic Soils. *Soil Science Society of America Journal*, **57**, 1381-1386.

Wang, S.-W.,Liu, C.-W., Jang, C.-S., (2007). Factors responsible for high arsenic concentrations in two groundwater catchments in Taiwan. *Applied Geochemistry*, **22**, 460-476.

Waychunas, G.A.,Rea, B.A.,Fuller, C.C., Davis, J.A., (1993). Surface chemistry of ferrihydrite: Part 1. EXAFS studies of the geometry of coprecipitated and adsorbed arsenate. *Geochimica et Cosmochimica Acta*, **57**, 2251-2269.

Wernberg, T., (1998). Multicomponent groundwater transport with chemical equilibrium and kinetics: model development and evaluation. *Hydrological Sciences - Journal -des Sciences Hydrologiques*, **43**, 299-317.

Westall, J., Hohl, H., (1980). Comparison of electrostatic models for the oxide-solution interface. *Advances in Colloid and Interface Science*, **12**, 265-294.

Westall J. C.,Zachary, J.L., Morel, M.F., (1976). MINEQL: A computer program for the calculation of the chemical equilibrium composition of aqueous system. *Tech Note 18, 91 pp, Dept. of Civ. Eng., Mass. Inst. of Technol., Cambridge*.

Westall, J.C., (1979a). "MICROQL. II. Computation of Adsorption Equilibria in BASIC," Technical Report, Swiss Federal Institute of Technology, EAWAG, Dubendorf, Switzerland.

Westall, J.C., (1979b). "MICROQL. I. A Chemical Equilibrium Program in BASIC," Technical Report, Swiss Federal Institute of Technology, EAWAG, Dubendorf, Switzerland.

WHO, (2003). *United nations synthesis report on arsenic in drinking water-Chapter 1. Source and behaviour of arsenic in natural waters*. In.

Wilkie, A.J., Hering, G.J., (1996). Adsorption of arsenic onto hydrous ferric oxide: effects of adsorbate/adsorbent ratios and co-occurring solutes. *Colloids and Surfaces A: Physicochemical and Engineering Aspects*, **107**, 97-110.

Williams, L.E.,Barnett, M.O.,Kramer, T.A., Melville, J.G., (2003). Adsorption and transport of arsenic(V) in experimental subsurface systems. *Journal of Environmental Quality*, **32**, 841-850.

Yu, Q., Kaewsarn, P., (1999). A model for pH dependent equilibrium of heavy metal biosorption. *Korean Journal of Chemical Engineering*, **16**, 753-757.

Zhang, H., Selim, H.M., (2006). Modeling the transport and retention of arsenic (V) in soils. *Soil Science Society of America Journal*, **70**, 1677-1687.

Zheng, C., Wang, P.P., (1999). *MT3DMS: A modular three-dimensional multispecies model for simulation of advection, dispersion and chemical reactions of contaminants in groundwater systems; Documentation and user's guide, contract report SERDP-99-1*. U.S. Army engineer research and development center, Vicksburg, MS.

APPENDICES

Computer codes

APPENDIX A: FORTRAN CODE FOR ULF ISOTHERM BASED REACTIVE TRANSPORT

```
c**********************************************************************
c**********************************************************************
                        PROGRAM ULFTRANSPORT
c       Program to model arsenate transport in the hypothetical column
c       experiment given in Fig 5-9 using Fortran finite difference code
c**********************************************************************
c**********************************************************************
c       Definition of important variables
c       NC          Number ofo components
c       l           Length of column (cm)
c       Time        No of time steps
c       Nnode       Number of nodes
c       delx        Size of grid in x axis (cm)
c       Co          Courant number
c       Delt        Size of time step (min)
c       Ctx         Array for concentration of components (mg/L)
c       pct         Concentration array at previous time step (mg/L)
c       vv          Velocity (cm/min)
c       Finaltime   Final time at which simulation ends
c       Numsteps    Total number of time steps
c       Dis         Dispersivity (cm2/min) Assume a negligible low value

c----------------------Declaration of variables-------------------------
        Implicit none
        Integer i,nc, time, ncmp,nxcount,nx,k,j,nnode
        Double precision dct(1050), pdct(100), pct(30,2000)
        Double precision ctx(30,2000),nxtotal, l
        Double precision ct(1050), delx,vv
        Double precision delt, numsteps
        Double precision timer,finaltime,dis
        Double precision a(1050), b(1050), c(1050), d(1050),con(1050)
        Double precision alpha, beta,c0

c----------------------Initialization of variables----------------------
```

```
        l = 7.0 !cm
        delx = 0.7 ! .02 !cm
        delt = 1 ! min
        finaltime = 10000 !15. ! '200
        numsteps = finaltime / delt
        timer = 0.0
        vv = 0.7 !cm/day
        Dis = 1E-5 !cm2/min
        nnode = l / delx + 1
        nnode =11
        Alpha =dis*delt/(delx*delx)
        Aeta=(vv*delt/delx)
        Write(*,*) "alpha, beta", alpha, beta
        Print*, "co", vv*delt/delx
        Nc= 4 !aqeous arsenic, solid-phase arsenic, ph, poh
        Ncmp=4

c----------------------Background concentration-----------------------------------

        do nx=2,nnode
                ctx(1, nx) = 1.0e-30 !mg/ l of as(v)
                ctx (2, nx) = 1.0e-30 ! as adsorbed in solid phase
                ctx (3, nx) = 1.0e-4 ! ph not concentration
                ctx (4, nx) = 1.0e-10 ! poh
        end do



c----------------------Source concentration-----------------------------------
                ctx(1, 1) = 1 ! mg/ l of as(v)
                ctx(2, 1) = 1.0e-30 ! as adsorbed in solid phase
                ctx(3, 1) = 1.0e-4 ! ph
                ctx(4, 1) = 1.0e-10      ! poh


                Do nx=1,nnode
                        Do j =1,ncmp
                                pct(j,nx) = ctx(j, nx)
                        End do
                End do
```

```
C---------------------MAIN TIME LOOP-------------------------------------------

        Do Time =1, numsteps

                Print*, "Time = :", Time

c       Stage 1 is 0 to 5000 time steps

        if (time > 5000) then  !stage 2
                ctx(1, 1) = 0.5 ! mg/ l of as(v)
                ctx(3, 1) = 1e-5
                ctx(4, 1) = 1.0e-9

                pct(1, 1) = 0.5 ! mg/ l of as(v)
                pct(3, 1) = 1e-5
                pct(4, 1) = 1.0e-9
        end if

        if (time > 7000) then   !stage 2
                ctx(1, 1) = 1e-10 ! mg/ l of as(v)
                ctx(3, 1) = 1e-6
                ctx(4, 1) = 1.0e-8

                pct(1, 1) = 1e-10 ! mg/ l of as(v)
                pct(3, 1) = 1.0e-6
                pct(4, 1) = 1.0e-8
        end if

                do j = 1,ncmp
                        do k=2, nnode
                                pct(j, k) = ctx(j,k)
                        end do ! end of nx loop
                end do ! end of ncmp loop

!       Loop for one step advancement only for checking purposes

!               do nx=2,nxcount
!                       do j =1,3
!                               ctx(j,nx) = pct(j, nx-1)
!                       end do
!               end do

!       Loop for one step advancement only ends
```

```
c       ~~~~~~~~~~~~~~~~~~~Assembling the a,b,c, d matrix~~~~~~~~~~~~~~~~~
            do j=1,ncmp

                a(1)=0.0
                b(1)=1.0
                c(1)=0.0
                d(1)=pct(j,1)

                a(nnode)=0.0
                b(nnode)=1.0
                c(nnode)=0.0
                d(nnode)=pct(j,nnode-1)

                do k=2, nnode-1
                    a(k)=alpha
                    b(k)= -2*alpha-1.0
                    c(k)=alpha
                    d(k)=-pct(j,k-1)
                end do
c       ~~~~~~~~~~~~~~~~~~~End Assembling the a,b,c, d matrix~~~~~~~~~~~~~~

c       ~~~~~~~~~~~~~~~~~~~Calling Tridiagonal soolver subroutine~~~~~~~~~~~~

                call tridia(nnode, a,b,c,d,con)
c       ~~~~~~~~~~~~~~~~~~~Calling Tridiagonal soolver subroutine~~~~~~~~~~~~

                if (j ==2) then
                go to 11
                end if

                do nx=1,nnode

                    ctx(j,nx)=con(nx)
                end do

11          continue
            end do

            do nx=1,nnode !reaction calling loop

                do j =1,ncmp
                    dct(j) = ctx(j,nx)
                end do
```

```
                        if (time == 5991) then
                                if (nx== 10) then
                                continue
                                end if
                        end if

c           ~~~~~~~~~~~~~~Calling ULF isotherm subroutine~~~~~~~~~~~~~~~~~~
                                        call ULF(nc,dct)
c           ~~~~~~~~~~~~~~Calling ULF isotherm subroutine~~~~~~~~~~~~~~~~~~
                        do j = 1,ncmp
                                ctx(j, nx) = dct(j)
                        end do

                        end do

        write(11,1003), time, ctx(1,nnode),ctx(2,nnode),
    &   ctx(3,nnode), ctx(4,nnode),
    & -log10(ctx(3,nnode)) + -log10(ctx(4,nnode))

1003    format(i6, 5f 20.7)

1209    format(4f 10.4)
        end do ! end of loop for time

write(*,*) "component concentrations for time = ", time
        do nx=1,nnode
                write(*,*) (nx-1)*delx,
    &           ctx(1,nx), ctx(2,nx)

                write(10,1002), (nx-1)*delx, ctx(1,nx), ctx(2,nx)

1002    format(4f 20.7)
10033   format(5f 12.6)
                end do

!----------------------end of main time loop-------------------------------------
        write(*,*) "end of main program"

        stop
        end

c**********************************************************************
C       Subroutine to calculate adsorption using ULF isotherm
c**********************************************************************
```

```
      subroutine ULF (NC,CT)

      integer i,j
      double precision ct1(1050),ct2(1050),ct3(1050),ct4(1050), ct(1050)
      double precision caq, kd , caqi,caqiplus, kmax, nn, ks, ctot,aa
      double precision rho, por, h, oh
      nn = 0.3865
      Kmax = 0.100013
      Ks = 768
      Kd = 0.096771875
      Rho =1600
      Por =0.365
      H = CT(3)
      OH = CT(4)

      pH = -log10(H)
      Ks = 10**(-0.738*pH+5.7493)

      If (ph <= 4) Then
      Ks=768
      END IF

      alpha = Kmax*Rho/Por
      Ctot = CT(1) + CT(2)

      Caqi =0.0000000000001

c-------------Loop for newton raphson method------------------
c                          same as VB code
      Do i = 1,100
      a = (Ks * caqi) ** nn
      fx = caqi - Ctot + alpha * a / (1 + a)
      dfx = 1 + alpha *( a / (1 + a) ** 2 )* nn / caqi
      Csolid  =alpha * a / (1 + a)

      caqiplus = caqi - fx / dfx


      If (Caqiplus < 0) then
            Caqiplus =1e-10
      end if

      caqi = caqiplus
      END DO
```

```
c-------------End loop for newton raphson method-----------------
12              ct(1) = Caqi
                ct(2) = Ctot - Caqi !Csolid
        if (ct(2) < 0) then
        ct(2) =0
        end if

        return
        end

c*********************************************************************
c               Subroutine to solve matrix system using tridiagonal solver
c*********************************************************************
        subroutine tridia(n,a,b,c,d,v)
        implicit none

        double precision a,b,c,d,u,v,ff,dummy,ac
        dimension a(1001),b(1001),c(1001),d(1001),v(1001)
        integer i,j,n
        do i=2,n

                ff=a(i)/b(i-1)
                b(i)=b(i)-c(i-1)*ff
                d(i)=d(i)-d(i-1)*ff
        end do

        v(n)=d(n)/b(n)
        do i=1,n-1

                j=n-i
                v(j)=(d(j)-c(j)*v(j+1))/b(j)

        end do
        return
        end
c*********************************************************************
c******************end of program*********************************
```

APPENDIX B: SURFACE COMPLEXATION MODEL BASED PHREQCI TRANSPORT CODE

```
#************************************************************************
#************************************************************************
#         PHREEQCI PROGRAM FOR TRANSPORT PROBLEM IN FIGURE 5-9
#************************************************************************
#************************************************************************
#This program is to model arsenate transport in a hypothetical column experiment using
#surface complexation model given in Table 5-2 for Sand-D. Note that we have to
#appropriately convert log K values, since master species is AsO4-3 in PHREEQCI
#database compared to MINTEQA2 where master specie is H3AsO4

SURFACE_MASTER_SPECIES 1-9 #DEFINING THE SURFACE COMPLEXATION
REACTIONS
      Surf    SurfOH
SURFACE_SPECIES 1-9
      SurfOH = SurfOH
            log_k   0.0
      SurfOH  + H+ = SurfOH2+
           log_k   7.32
      SurfOH = SurfO- + H+
            log_k   -9.42
      SurfOH + AsO4-3 + 3H+ = SurfH2AsO4 + H2O
            log_k   31.95 #32.67
      SurfOH + AsO4-3 + 2H+ = SurfHAsO4- + H2O
            log_k   26.56
      SurfOH + AsO4-3 + H+ = SurfAsO4-2 + H2O
            log_k   20.25
SOLUTION_MASTER_SPECIES 1-9
      As      H3AsO4       -1.0     74.9216    74.9216
SOLUTION_SPECIES 1-9
#H3AsO4  primary master species
      H3AsO4 = H3AsO4
      log_k          0.0
#H2AsO4-
      H3AsO4 = AsO4-3 + 3H+
      log_k   -20.7
```

```
#HAsO4-2
      H+ + AsO4-3 = HAsO4-2
      log_k   11.50
#AsO4-3
      2H+ + AsO4-3 = H2AsO4-
      log_k          18.465
PHASES
Fix_H+
H+ = H+
log_k 0

#***********Initial and Background concentration****************
SOLUTION 1-10 #10 cells =11 nodes
   temp      25
   pH        4
   units     mmol/kgw
   density   1
   Na        10
   Cl        10
   -water    1 # kg

SURFACE 1-10 Goethite
   -sites DENSITY
   SurfOH  1.38   0.57   4384
end

EQUILIBRIUM_PHASES 1-10
Fix_H+          -4.0 HCl
END

#**********Output formatting (optional)*************************
USER_PUNCH
-headings Total_sorbed_As
-start
10 Astot = MOL("SurfH2AsO4")+ MOL("SurfHAsO4-") + MOL("SurfAsO4-2")
20 PUNCH Astot
30 END
-end

SELECTED_OUTPUT
   -file              s7.sel
   -totals             As
   -molalities         SurfH2AsO4  SurfHAsO4-  SurfAsO4-2
#***********Transport part for stage 1*****************************
```

```
SOLUTION 0
   temp      25
   pH        4
   units     mmol/kgw
   density   1
   Na        10
   As        0.013333
   Cl        10
   -water    1 # kg

EQUILIBRIUM_PHASES 1-10
Fix_H+           -4.00 HCl 1

TRANSPORT
   -cells               10
   -shifts              5000
   -time_step           60 # seconds
   -flow_direction      forward
   -boundary_conditions   constant flux
   -lengths             10*0.007
   -dispersivities      10*1.67E-11 #m2/s, which is same ias 1E-5cm2/min
   -diffusion_coefficient 3e-018
   -print_cells         10
   -punch_cells         10
   -warnings            true
SAVE SOLUTION 1-10
SAVE SURFACE 1-10
END
#**********Transport part for stage 2*****************************

SOLUTION 0
   temp      25
   pH        5
   units     mmol/kgw
   density   1
   Na        10
   As        0.00667
   Cl        10
   -water    1 # kg

EQUILIBRIUM_PHASES 1-10
Fix_H+           -5.00 HCl 1

TRANSPORT
```

```
   -cells               10
   -shifts              2000
   -time_step           60 # seconds
   -flow_direction      forward
   -boundary_conditions   constant flux
   -lengths             10*0.007
   -dispersivities      10*1.67E-11 #m2/s, which is same ias 1E-5cm2/min
   -diffusion_coefficient 3e-018
   -print_cells         10
   -punch_cells         10
   -warnings            true

SAVE SOLUTION 1-10
SAVE SURFACE 1-10
END
#***********Transport part for stage 3*********************************

SOLUTION 0
   temp      25
   pH        6
   units     mmol/kgw
   density   1
   Na        10
   As        1E-10
   Cl        10
   -water    1 # kg

EQUILIBRIUM_PHASES 1-10
Fix_H+          -6.00 HCl 1

TRANSPORT
   -cells               10
   -shifts              3000
   -time_step           60 # seconds
   -flow_direction      forward
   -boundary_conditions   constant flux
   -lengths             10*0.007
   -dispersivities      10*1.67E-11
   -diffusion_coefficient 3e-018
   -print_cells         10
   -punch_cells         10
   -warnings            true

SAVE SOLUTION 1-10
```

```
SAVE SURFACE 1-10
END
#************END OF PROGRAM**********************************
```